POWER SYSTEMS DEVELOPMENT FACILITY

FINAL REPORT

REPORTING PERIOD:

SEPTEMBER 14, 1990 – JANUARY 31, 2009

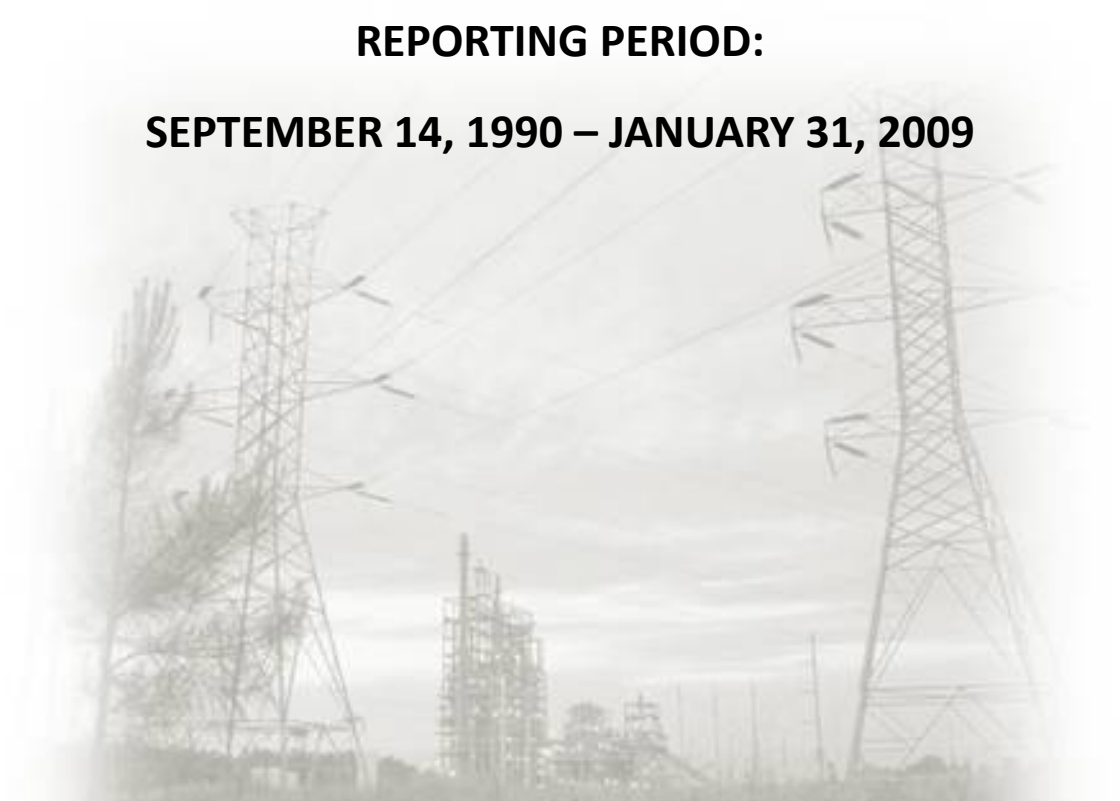

DOE Cooperative Agreement
DE-FC21-90MC25140

Prepared by:
Southern Company Services, Inc.
Power Systems Development Facility
P.O. Box 1069
Wilsonville, AL 35186
Tel: 205-670-5840
Fax: 205-670-5843

April 2009

DISCLAIMER

ABSTRACT

In support of technology development to utilize coal for efficient, affordable, and environmentally clean power generation, the Power Systems Development Facility (PSDF), located in Wilsonville, Alabama, has routinely demonstrated gasification technologies using various types of coals. The PSDF is an engineering scale demonstration of key features of advanced coal-fired power systems, including a Transport Gasifier, a hot gas particulate control device, advanced syngas cleanup systems, and high-pressure solids handling systems.

This final report summarizes the results of the technology development work conducted at the PSDF through January 31, 2009. Twenty-one major gasification test campaigns were completed, for a total of more than 11,000 hours of gasification operation. This operational experience has led to significant advancements in gasification technologies.

ACKNOWLEDGEMENT

The authors wish to acknowledge the contributions and support provided by various project managers, including Morgan “Mike” Mosser of the Department of Energy, Rick Strait of KBR, and John Wheeldon of the Electric Power Research Institute. The project was sponsored by the U.S. Department of Energy National Energy Technology Laboratory under cooperative agreement DE-FC21-90MC25140.

TABLE OF CONTENTS

Section ..... Page

Inside Cover
Disclaimer
Abstract
Acknowledgement

List of Figures v
List of Tables viii

1.0 EXECUTIVE SUMMARY 1-1
1.1 Process Description 1-2
1.2 PSDF Objectives and Accomplishments 1-4
1.3 PSDF Operating History 1-6
1.3.1 Transport Reactor 1-6
1.3.2 Foster Wheeler Advanced Pressurized Fluid Bed Combustor 1-8
1.4 Economic Analyses 1-8
1.5 Project Partner Participation 1-9
1.6 Report Structure 1-10

2.0 COAL PREPARATION AND FEED 2-1
2.1 Coal Preparation 2-1
2.1.1 Coal Mill System Description 2-1
2.1.1.1 Coal Mill Hardware Modifications 2-2
2.1.1.2 Coal Mill Control and Instrumentation Improvements 2-4
2.1.2 Fluid Bed Dryer 2-6
2.2 Coal Feeders 2-13
2.2.1 Original Coal Feeder 2-13
2.2.2 Pressure Decoupled Advanced Coal Feeder 2-16

3.0 TRANSPORT GASIFIER 3-1
3.1 Gasifier Description 3-1
3.2 Gasifier Modifications 3-2
3.2.1 Gas Flow Distribution Modifications 3-2
3.2.2 Gasifier Configuration Modifications 3-3
3.2.2.1 Description of Gasifier Configuration Modifications 3-3
3.2.2.2 Performance Results of Gasifier Configuration Modifications 3-4
3.2.2.3 Refractory Evaluation 3-6
3.3 Gasifier Operations and Performance 3-9

Section ..... Page

3.3.1 Lignite Operations 3-10
3.3.2 Subbituminous Coal Operations 3-13
3.3.3 Bituminous Coal Operations 3-13
3.3.4 Operations Summary 3-14
3.3.5 Parametric Test Results 3-15

4.0 PARTICULATE CONTROL DEVICE 4-1
4.1 Equipment Description 4-1
4.2 Filter Element Testing 4-3
4.2.1 Pall PSS Iron Aluminide Filter Elements 4-4
4.2.1.1 Pall PSS FEAL Corrosion Observations 4-4
4.2.1.2 PSS Filter Element Performance 4-8
4.2.2 Dynalloy Filter Elements 4-9
4.2.2.1 Dynalloy HR-160 Corrosion Observations 4-9
4.2.2.2 Dynalloy Filter Element Performance 4-10
4.2.3 Fecralloy Filter Elements 4-12
4.2.4 Titanium Filter Elements 4-12
4.2.5 Silicon Carbide Filter Elements 4-13
4.3 Failsafe Testing 4-13
4.3.1 On-line Failsafe Testing Methods 4-14
4.3.2 Failsafes Tested 4-15
4.3.2.1 PSDF-Designed Failsafe 4-15
4.3.2.2 Pall FEAL Fuse 4-15
4.3.2.3 Pall Dynalloy HR-160 Fuse 4-15
4.3.2.4 CeraMem Ceramic Failsafe 4-16
4.3.2.5 Specific Surface Ceramic Failsafe 4-16
4.3.3 Failsafe Test Results 4-16
4.4 Gasification Ash Bridging 4-17
4.4.1 Causes of Bridging 4-18
4.4.2 Instrumentation Added to Address Bridging 4-18
4.4.2.1 Filter Element Thermocouples 4-18
4.4.2.2 Resistance Probes 4-20
4.4.2.3 Additional Hopper Thermocouples 4-21
4.4.3 On-line Removal of Ash Bridging 4-21
4.5 Relating Particulate Characteristics to PCD Design Requirements 4-22
4.5.1 Non-Carbonate Carbon versus Particulate Drag 4-22
4.5.2 Particle Size versus Particulate Drag 4-23
4.5.3 Relative PCD Sizing Requirements for Different Fuel Stocks 4-28

5.0 ADVANCED SYNGAS CLEANUP 5-1
5.1 Desulfurization 5-1
5.2 Direct Oxidation of H_2S 5-2
5.3 COS Hydrolysis 5-3
5.4 Ammonia Cracking and Hydrocarbon Reforming 5-4
5.5 Syngas Cooler Fouling Testing 5-5

Section ..... Page

5.6 TDA Research Trace Metals Removal 5-6
5.7 Water-Gas Shift Reaction Testing 5-6
5.7.1 Catalytic Filter Elements 5-6
5.7.2 Fixed Bed Reactor 5-11
5.8 NETL Fuel Cell Module 5-11
5.9 Media Process and Technology Carbon Molecular Sieve Membrane 5-13
5.10 CO_2 Capture 5-14
5.11 Johnson Matthey Mercury Sorbent 5-15

6.0 INSTRUMENTATION, SAMPLING, AND CONTROLS 6-1
6.1 Coal Feed Rate Measurements 6-1
6.1.1 Granucor Coal Rate Measurement 6-1
6.1.2 Nuclear Densitometers 6-2
6.2 Gasifier Pressure Differential Indicators 6-3
6.3 Gasifier Thermocouples 6-4
6.3.1 Configurations 6-5
6.3.2 Thermowell Materials 6-5
6.4 Gasifier Velocity Measurements 6-7
6.5 Real-Time Particulate Monitoring 6-7
6.5.1 PCME DustAlert-90 6-7
6.5.2 Process Metrix Process Particle Counter 6-9
6.6 Solids and Gas Sampling and Analyses 6-12
6.6.1 Solids Sampling 6-13
6.6.2 Gas Sampling 6-15
6.7 Sensor Research and Development Semi-Conducting Metal Oxide Sensors 6-23
6.8 Babcock & Wilcox High Speed Pressure Sensors 6-24
6.9 Process Controls 6-25
6.9.1 Gasifier Temperature Control 6-25
6.9.2 Coal Feed Rate Control 6-27
6.9.3 Standpipe Level Control 6-27
6.9.4 Fluidization Velocity Control 6-28
6.9.5 Safety Interlock System 6-29

7.0 SUPPORT EQUIPMENT 7-1
7.1 Recycle Gas Compressor 7-1
7.2 Piloted Syngas Burner 7-2
7.3 Ash Removal Systems 7-4
7.3.1 Original Ash Removal Systems 7-4
7.3.2 Continuous Ash Depressurization Systems 7-5

8.0 CONCLUSIONS AND LESSONS LEARNED 8-1
8.1 Coal Preparation and Feed 8-1
8.2 Transport Gasifier 8-2
8.3 Particulate Control Device 8-3
8.4 Advanced Syngas Cleanup 8-4

8.5 Instrumentation, Sampling and Process Automation 8-4
8.6 Support Equipment 8-5

9.0 REFERENCES 9-1

APPENDICES
Appendix A Coal Characteristics A-1
Appendix B List of Acronyms and Engineering Units B-1

LIST OF FIGURES

Figure ..... Page

1-1 PSDF Gasification Process Flow Diagram 1-2

2-1 Coal Preparation Process Flow Diagram 2-1
2-2 Pulverized Coal Silo Insert. 2-2
2-3 Coal Sampler 2-3
2-4 Coal Drying Gas Dehumidifier 2-3
2-5 Coal Mill Electric Heater 2-4
2-6 Microwave Solids Flow Switches 2-5
2-7 Dual O_2/CO Analyzers 2-5
2-8 Mill System Human Machine Interface 2-6
2-9 Fluid Bed Dryer System Flow Diagram 2-7
2-10 Fluid Bed Dryer System. 2-8
2-11 Particle Size Distributions of Lignite Processed in Fluid Bed Dryer and of Raw Lignite 2-9
2-12 Product Moisture Content versus Fluid Bed Dryer Outlet Temperature 2-10
2-13 Particle Size Distributions of Pulverized Lignite and of Lignite Processed in Fluid Bed Dryer 2-11
2-14 Particle Sizes of As-Fed Lignite 2-11
2-15 Percentage of Oversize Particles in As-Fed Lignite 2-12
2-16 Percentage of Fine Particles in As-Fed Lignite 2-12
2-17 Moisture Content of As-Fed Lignite before and after Fluid Bed Dryer Installation 2-13
2-18 Original Coal Feed System 2-14
2-19 Vent Valve Replacement on Original Coal Feeder 2-14
2-20 Original Coal Feeder Vent Valve Location 2-15
2-21 Original Coal Feeder Balance Line Location 2-15
2-22 Original Coal Feeder Operating Envelope 2-16

3-1 Schematic of Transport Gasifier 3-1
3-2 Gasifier Refractory Layout 3-6
3-3 Lower Standpipe Refractory after 70 Thermal Cycles. 3-7
3-4 Inspection of Actchem 85VC Refractory following Initial Operation 3-8
3-5 Cracking of Actchem 85VC Refractory after Eleven Thermal Cycles 3-8
3-6 Refractory Loss at the Inlet of the First Solids Separation Device 3-9
3-7 Gasifier Seal Leg Obstruction 3-9
3-8 Kaolin Particle Size Distribution 3-12
3-9 Carbon Conversion as a Function of Gasifier Outlet Temperature 3-16
3-10 Solids Circulation Rate as a Function of Standpipe Level 3-16
3-11 Syngas Heating Value as a Function of Coal Feed Rate 3-17
3-12 Syngas Methane Content as a Function of Pressure 3-17
3-13 Temperature Difference as a Function of Air Flow to LMZ 3-18
3-14 Effect of Transport Air on Syngas Lower Heating Value 3-19
3-15 Effect of Recycle Gas Use for Gasifier Aeration on Syngas Heating Value 3-19
3-16 Sulfur Removal as a Function of Calcium-to-Sulfur Molar Ratio 3-20
3-17 Syngas Hydrogen-to-Carbon Monoxide Ratio versus Steam-to-Coal Ratio 3-20

Figure ..... Page

4-1 Siemens Particulate Control Device 4-1
4-2 Cold Flow PCD Model 4-3
4-3 Micrographs of FEAL Filter Media Showing Progression of Iron Oxide Scale 4-4
4-4 Cleaned FEAL Elements Arranged by Exposure Time 4-5
4-5 Photomicrograph of FEAL Filter Element Section Showing Pitted Areas with Iron Oxide Borders 4-5
4-6 EDX Spectrum from Black Region Indicated in Figure 4-5 4-6
4-7 Photomicrograph of Plugged and Open Areas of FEAL Element 4-6
4-8 EDX Spectra from Plugged and Open Areas Indicated in Figure 4-7 4-7
4-9 Pressure Drop versus Syngas Exposure Time for Pall PSS FEAL Elements 4-8
4-10 Coarse Fiber Dynalloy HR-160 Filter Media with 2,698 Syngas Exposure Hours 4-10
4-11 Fine Fiber HR-160 Filter Media with 979 Syngas Exposure Hours 4-10
4-12 Pressure Drop versus Syngas Exposure Time for Coarse Fiber Dynalloy Elements 4-11
4-13 Pressure Drop versus Syngas Exposure Time for Fine Fiber Dynalloy Elements 4-12
4-14 Section of Damaged Titanium Filter Element 4-13
4-15 Filter Element Thermocouple 4-19
4-16 Filter Element Thermocouple Response during Bridging 4-19
4-17 Filter Element Resistance Probe 4-20
4-18 Filter Element Resistance Probe Response during Bridging 4-20
4-19 PCD Hopper Thermocouple Support Structure 4-21
4-20 Resistance Probe Response during On-Line Bridging Removal 4-22
4-21 PCD Transient Drag versus Carbon Content of In-Situ Samples 4-23
4-22 Laboratory Apparatus for Measuring Drag of Re-suspended Gasification Ash 4-24
4-23 Lab-Measured Drag as a Function of Particle Size with Falkirk Lignite Ash 4-25
4-24 Lab-Measured Drag as a Function of Particle Size with PRB Subbituminous Coal Ash 4-25
4-25 Lab-Measured Drag as a Function of Particle Size with High-Sodium Freedom Lignite Ash 4-26
4-26 SEM Photographs of Low and High Drag Samples from Falkirk Lignite 4-27
4-27 SEM Photographs of Low and High Drag Samples from PRB Coal 4-27
4-28 SEM Photographs of Low and High Drag Samples from Freedom Lignite 4-28
4-29 Graphical Illustration of Terms Used in PCD Sizing 4-30
4-30 Dustcake Development at Points A and B in Figure 4-29 4-30
4-31 Effect of Transient Drag on Required PCD Size at a Given Allowable Pressure Drop 4-32

5-1 Sud-Chemie T-2822 Shift Catalyst Performance 5-7
5-2 Johnson Matthey Katalco K8-11 Shift Catalyst Performance 5-8
5-3 T-2822 and Katalco K8-11 Shift Catalyst Performance Comparison 5-8
5-4 Photomicrographs of Sud-Chemie T-2822 Shift Catalyst before and after Testing 5-9
5-5 Photomicrographs of Johnson Matthey Katalco K8-11 Shift Catalyst before and after Testing 5-9
5-6 Catalytic Filter Element Temperatures during Thermal Upset at Hour 8 5-10
5-7 Catalytic Filter Element Temperatures during Thermal Upset at Hour 39 5-10
5-8 NETL Fuel Cell Module 5-11
5-9 MPT Carbon Molecular Sieve Membrane Installed at PSDF 5-13

Figure ..... Page

6-1 Schematic of Nuclear Densitometer Layout for Developmental Coal Feed System 6-2
6-2 Coal Feed Rate Measurements 6-3
6-3 Schematic of Ceramic Tip for Pressure Differential Indicator 6-3
6-4 Measurements of Ceramic-Tipped Pressure Differential Indicators Compared to Standard Pressure Differential Indicators 6-4
6-5 Ceramic Thermowell Damaged during Removal 6-6
6-6 Post-TC21 and Post-TC23 Inspections of Worn HR-160 Thermowell 6-6
6-7 HR-160 Thermowell Showing Minimal Wear 6-7
6-8 PCME Particulate Monitor Output during Solids Injection Test 6-8
6-9 Comparison of PCME Particulate Monitor Response to Actual Mass Concentration 6-8
6-10 PPC Particulate Monitor Output during Low Particulate Loading 6-10
6-11 PPC Particulate Monitor Output during Solids Injection Test 6-11
6-12 Sampling Locations of the PSDF Gasification Process 6-12
6-13 Solids Sample System at Coal Feeder Surge Bin 6-13
6-14 Gasifier Solids Sampling System 6-14
6-15 In-Situ Particulate Sampling System 6-14
6-16 Bomb Sampler Cylinders 6-16
6-17 Gas Conditioning System 6-17
6-18 Gas Conditioning System with Temperature Control 6-17
6-19 Disassembled Reflux Probe 6-18
6-20 Disassembled Canister Filter 6-18
6-21 On-Line Laboratory GC Unit for PCD Inlet Gas Analysis 6-19
6-22 Continuous Analyzer Cabinet for PCD Inlet Gas Analysis 6-20
6-23 In-Situ Flue Gas Analyzer 6-20
6-24 FTIR Gas Analysis System 6-21
6-25 CO_2 Capture and Water-Gas Shift Reaction Analyzers 6-22
6-26 Syngas Quality Gas Chromatograph 6-22
6-27 Gas Conditioning System. 6-23
6-28 Comparison of Gasifier Temperature Control Schemes 6-26
6-29 Gasifier Temperature Response to Setpoint Change using Pseudo-Fuzzy Control Plane 6-26
6-30 Coal Feed Rate Response to Setpoint Changes 6-27
6-31 Standpipe Level Response to Setpoint Changes 6-28
6-32 Gasifier J-Leg Velocity Control Response to Pressure Change 6-29
6-33 DCS Safety Interlock System 6-30

7-1 Valve Failure on Original Recycle Gas Compressor 7-1
7-2 Schematic and Photograph of Recycle Gas Compressor 7-1
7-3 Flow Schematic of the Piloted Syngas Burner and Combustion Turbine 7-3
7-4 Piloted Syngas Burner Model and Photograph 7-3
7-5 Schematic of Original Ash Cooling and Depressurization Systems 7-4
7-6 CFAD Schematic 7-6
7-7 Particle Size Distributions of Gasification Ash Processed by the CFAD and CCAD Systems 7-7

LIST OF TABLES

Table ..... Page

1-1 Fuels and Sorbents Used during Combustion Mode Testing 1-6
1-2 Summary of PSDF Gasification Testing 1-7
1-3 Comparison of Gasification Process Configurations 1-9

2-1 Performance of Fluid Bed Dryer during Commissioning 2-9

3-1 Gasification Ash Characteristics with PRB Operation before and after Gasifier Modifications 3-5
3-2 Gasifier Performance at Comparable Operating Conditions 3-5
3-3 Transport Gasifier Operations and Performance Summary after Configuration Modifications 3-14
3-4 Gasifier Parametric Tests 3-15

4-1 Nominal PCD Operating Parameters 4-2
4-2 Collection Efficiency Measurements for Dynalloy Elements 4-11
4-3 Cold Flow Model Failsafe Test Results 4-16
4-4 On-Line Failsafe Test Results 4-17

5-1 Sud-Chemie Sulfur Sorbent Properties and Nominal Operating Parameters 5-1
5-2 Synetix Sulfur Sorbent Properties and Nominal Operating Parameters 5-2
5-3 COS Hydrolysis Catalyst Properties and Nominal Operating Parameters 5-4
5-4 Ammonia Cracking and Hydrocarbon Reforming Catalyst Properties 5-4
5-5 Water-Gas Shift Catalyst Properties 5-6
5-6 Water-Gas Shift Catalyst Test Conditions 5-9

6-1 Comparison of PPC and In-Situ Concentrations 6-10
6-2 ASTM Standards Used in Solids Chemical Analyses 6-15

7-1 CFAD and CCAD Operating Conditions 7-6

A-1 As-Fed PRB Subbituminous Coal Characteristics A-1
A-2 As-Fed Mississippi Lignite Coal Characteristics (TC22) A-2
A-3 As-Fed Mississippi Lignite Coal Characteristics (TC25) A-2
A-4 As-Fed Utah Bituminous Coal Characteristics A-3
A-5 As-Fed North Dakota Freedom Mine Low Sodium Lignite Coal Characteristics A-3
A-6 As-Fed North Dakota Freedom Mine High Sodium Lignite Coal Characteristics A-4

1.0 EXECUTIVE SUMMARY

The Power Systems Development Facility (PSDF) is a state-of-the-art test center sponsored by the United States Department of Energy (DOE) and dedicated to the advancement of clean coal technology. Located in Wilsonville, Alabama, the PSDF is a highly flexible test center where researchers can economically demonstrate and evaluate innovative power system components on a semi-commercial scale. The PSDF is operated by Southern Company Services, and other project participants during activity under this cooperative agreement included the Electric Power Research Institute, KBR, the Lignite Energy Council, Siemens Power, Burlington Northern Santa Fe Railway, and Peabody Energy.

Originally, the PSDF was constructed to demonstrate two independent processes: the Transport Reactor process featuring a hot gas particulate control device (PCD); and the Foster Wheeler Advanced Pressurized Fluidized Bed Combustor (APFBC) process. After initial commissioning in 1999 and testing on coal in 2000, testing of the Foster Wheeler process was terminated, and subsequent testing at the PSDF was based on the Transport Reactor process.

Development of advanced power systems at the PSDF focuses specifically on identifying ways to reduce capital cost, enhance equipment reliability, and increase efficiency while meeting strict environmental standards. Testing involves pressurized feed systems, syngas cooling, sensor development, ash cooling and depressurization, and syngas cleanup.

Not only did the PSDF achieve the goal of developing several types of first-of-a-kind technologies (e.g., the Transport Gasifier, continuous ash depressurization systems, a pressure decoupled advanced coal feeder, a piloted syngas burner, etc.), it successfully integrated these components into a reliable gasification process for generating data for scale-up to commercial applications. This successful development and integration required focused process engineering and effective identification of ways to improve operation. To achieve improved operation, over 1,950 management of change (MOC) requests were issued to modify the system over time.

After only eight years from the time of construction and commissioning, the Transport Gasification process was selected for commercial deployment through the DOE Clean Coal Power Initiative. As such, Mississippi Power Company is planning construction of a power plant in Kemper County, Mississippi, based on the Transport Integrated Gasification (TRIG^{TM}) process. The Kemper County facility will use local Mississippi lignite as the fuel and capture and sequester (through enhanced oil recovery) 65 percent of the carbon dioxide produced. It will be one of the cleanest, most energy-efficient coal power plants built to date.

1.1 Process Description

The gasification process as configured at the PSDF, shown in Figure 1-1, features key components of an integrated gasification combined cycle (IGCC) plant. These include high pressure solids feed systems; a Transport Gasifier; syngas coolers; a hot gas filter vessel, the particulate control device (PCD); continuous ash depressurization systems developed at the PSDF for ash cooling and removal; a piloted syngas burner and combustion turbine; a slipstream syngas cleanup unit to test various pollutant control technologies; and a recycle syngas compressor.

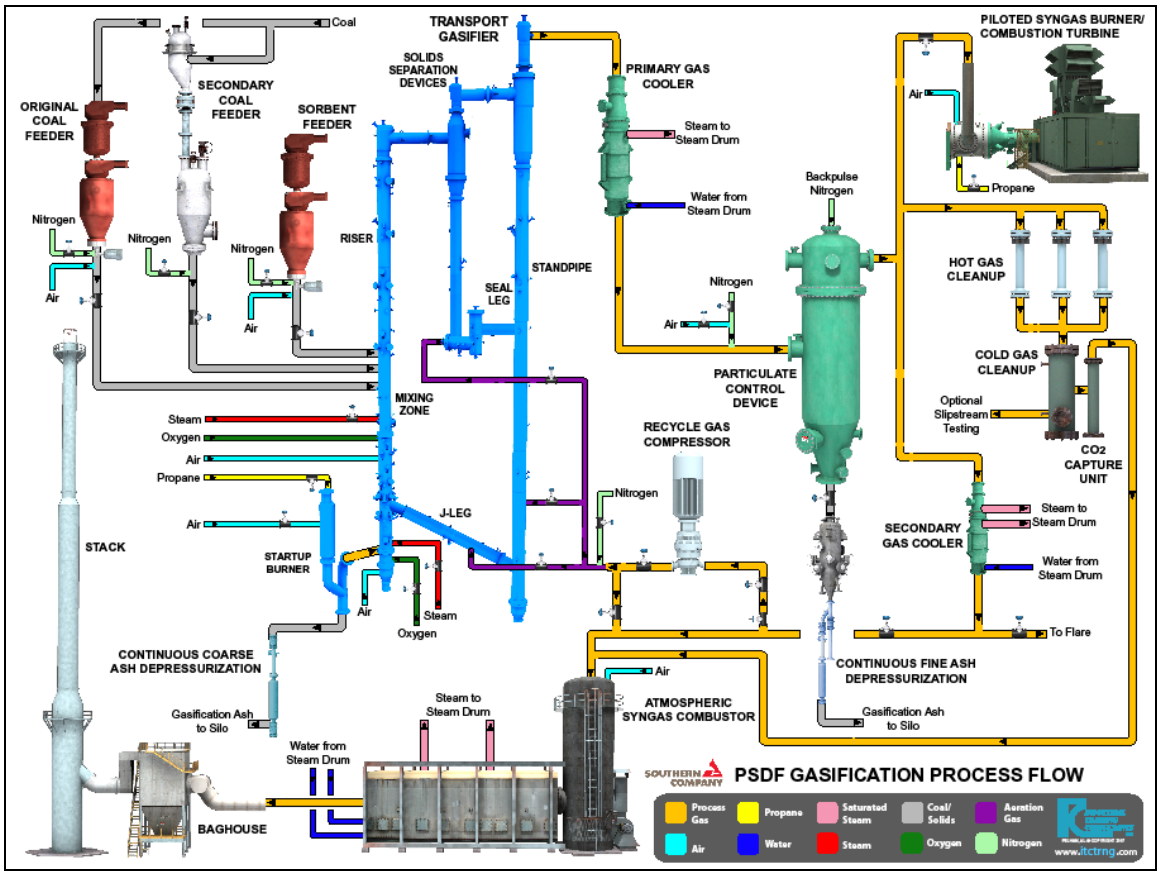

Figure 1-1. PSDF Gasification Process Flow Diagram.

Coal Preparation and Feeding. The coal used as the gasifier feedstock is processed on site. The material is crushed, dried in the fluid bed dryer (high moisture fuels only), and pulverized to a nominal particle diameter between 250 and 400 microns. Coal may be fed to the gasifier using two systems, the original coal feed system and a developmental coal feed system. Coal is fed at a nominal rate of 4,000 lb/hr.

Sorbent Feeding. A sorbent feeder is available to feed material into the gasifier for in-situ sulfur capture or to address ash chemistry issues. For sulfur capture, either limestone or dolomite is fed after being crushed and pulverized to a nominal particle diameter of 10 to

100 microns. The sorbent feeder utilizes the same design as the original coal feeder, but for a lower feed rate of nominally 100 lb/hr.

Start-up Burner. The start-up burner is a direct propane-fired burner operated to heat the gasifier to about 1,200°F. The burner is typically started at a system pressure of 60 psig, and can operate at pressures up to 135 psig.

Transport Gasifier. The Transport Gasifier is a circulating fluidized bed reactor, which was designed based on successful operations of fluid bed catalytic cracking. The gasifier is equally capable of using air or oxygen as the gasification oxidant for producing syngas from coal. The gasifier retains the large majority of the particulate (gasification ash) in the syngas by cyclonic action in a solids separation unit. Gasification ash is removed from the gasifier by a continuous coarse ash depressurization (CCAD) system and sent to an ash silo for temporary storage prior to disposal.

Syngas Filtration. The syngas exits the Transport Gasifier, passes through the primary gas cooler where the gas temperature is reduced to about 750°F, and enters the PCD for final particulate removal. The ash falls to the bottom of the PCD, is cooled and removed through the continuous fine ash depressurization (CFAD) system, and is sent to an ash silo for temporary storage prior to disposal.

Advanced Syngas Cleanup. After exiting the PCD, a small portion of the syngas, up to 100 lb/hr, can be directed to an advanced syngas cleanup system downstream of the PCD. The syngas cleanup system is a specialized, flexible unit, capable of operating at a range of temperatures, pressures, and flow rates. It provides a means to test various pollutant control technologies, including removal of sulfur and mercury compounds, and CO_2 capture. The syngas cleanup slipstream can also be used to test other power technologies such as fuel cells.

Piloted Syngas Burner / Combustion Turbine. A portion of the syngas can also be directed to the piloted syngas burner (PSB), a gas turbine combustor designed to burn coal-derived syngas. After syngas combustion in the burner, the flue gas passes through a 4 MW turbine before exiting the turbine stack. An associated generator can supply power from the turbine to the electric transmission grid.

Syngas Recycle and Final Syngas Processing. The main stream of syngas is then cooled in a secondary gas cooler, which reduces the temperature to about 450°F. Some of this gas may be compressed and recycled back to the gasifier for aeration to aid in solids circulation. The remaining syngas is reduced to near atmospheric pressure through a pressure control valve. The gas is then sent to the atmospheric syngas combustor which burns the syngas components. The flue gas from the atmospheric syngas combustor flows to a heat recovery boiler, through a baghouse, and then is discharged out a stack. A flare is available to combust the syngas in the event of a system trip when the atmospheric syngas combustor is off-line.

1.2 PSDF Objectives and Accomplishments

The PSDF project was established by the DOE to bolster the nation's effort in developing environmentally-acceptable, cost-effective, and reliable coal-based power generation technologies. The objective of the PSDF was to develop advanced coal-fired power generation technologies through the testing of components and advanced power systems under realistic conditions using coal-derived gas streams. Performance of components was also to be demonstrated in an integrated mode of operation and at a component size readily scaleable to commercial systems.

The primary focus of the PSDF project originally centered on two key technologies: hot gas filtration and gasification of low-rank fuels. These two technologies have progressed to the demonstration phase and are incorporated in a Clean Coal Power Initiative Project in Kemper County, Mississippi. Details of these major accomplishments as well as some of the secondary accomplishments achieved at the PSDF are provided below.

Advancement of Hot Gas Filtration to Improve Energy Efficiency. Advanced particulate removal technology and many filter element types have been tested to clean the product gases. Material property testing is continuously conducted to assess suitability for long-term operation. The material requirements have been shared with vendors to aid their filter development programs. To enhance reliability and protect downstream components, failsafe devices that reliably seal off failed filter elements were identified. The filtration system routinely operates with very high collection efficiency, with outlet solids concentrations in the syngas less than 0.1 ppmw. A fundamental understanding of filter cake properties and how they affect operation was developed.

Development of a Gasifier Suitable for Use with Low-Rank Fuels. The Transport Reactor has operated successfully on subbituminous, bituminous, and lignite coals with over 20,000 hours of solids circulation. The Transport Reactor has operated as a pressurized combustor and as a gasifier in both oxygen- and air-blown modes and has exceeded its primary purpose of generating gases for downstream testing. In combustion mode, operation resulted in 99.9 percent coal conversion at low (1,600°F) reactor temperature and over 99 percent sulfur capture at low (1.2 to 1.3) calcium-to-sulfur molar ratios. In gasification mode, operation demonstrated high coal conversions, minimal tar production, and syngas heating values sufficient to fuel a combustion turbine.

The PSDF Transport Gasifier was modified in 2006 to improve the solids collection efficiency, to increase the residence time in the gasifier to increase the carbon conversion and syngas heating value, and to test a solids collection system better suited for commercial scale-up. In subsequent testing with air-blown operations with Powder River Basin (PRB) coal, there was about a 20 percent increase in the raw syngas lower heating value and an improvement in carbon conversion. The TRIG™ technology has progressed to the commercial demonstration phase and is incorporated in a Clean Coal Power Initiative Project in Kemper County, Mississippi.

Recycle Syngas Compressor. To demonstrate gasifier operation in a more commercially viable way, a recycle gas compressor was installed for gasifier aeration, which increased the raw syngas heating value by up to 10 percent.

Vendor Collaboration. The PSDF has developed testing and technology transfer relationships with dozens of vendors to ensure that test results and improvements developed at the PSDF are incorporated into future plants.

Coal Feed and Ash Removal Systems. Reliable operation of the coal feed and ash removal systems is key to successful pressurized gasifier operation. Additional work on the pressurized coal feed systems has increased the understanding and optimization of their performance. Modifications developed at the PSDF and shared with equipment suppliers allow currently offered coal feed equipment to perform in a commercially acceptable manner. An innovative, continuous process was designed and successfully tested that reduces capital and maintenance costs and improves the reliability of fine and course ash removal. The PSDF also hosted scaled-up testing of the Stamet feed pump.

Syngas Cooler: Syngas cooling is of considerable importance to the gasification industry. Devices to inhibit erosion, made from several different materials, were tested at the inlet of the gas cooler, and suitable material was identified.

Sensors and Automation. Significant progress with sensor development and process automation has been achieved. Development of reliable and accurate sensors for the gasification process has concentrated on coal feed, gasifier, and filter systems. PSDF controls specialist implemented effective automatic control of gasifier temperature, standpipe level, and aeration velocity.

Syngas Analysis and Sampling. Advances in syngas sampling and analysis improved the operational reliability of the systems and provided the data needed for technology development and process understanding.

Advanced Syngas Cleanup. A slipstream syngas cleanup unit provided a very flexible test platform for testing numerous syngas contaminant removal technologies. The syngas cleanup unit has been used for testing the removal of compounds such as CO_2, trace metals, sulfur, hydrocarbons, and ammonia. The unit has also been used to test catalytic filter elements that can potentially filter the syngas while simultaneously catalyzing the water-gas shift reaction to enhance CO_2 removal.

Fuel Cells. The first time that a solid oxide fuel cell was operated on coal-derived syngas occurred with a 0.6 kW solid oxide fuel cell manufactured by Delphi using syngas from the Transport Gasifier. The PSDF has also provided syngas for testing of an NETL solid oxide fuel cell.

Patents Pending. Patents were filed and are pending for the solids separation unit incorporated in the 2006 gasifier modifications; the continuous ash depressurization systems; and catalytic filter elements.

1.3 PSDF Operating History

1.3.1 Transport Reactor

System Commissioning. Commissioning activities began in September 1995 and proceeded in parallel with construction activities. Design and construction of the Transport Reactor and associated equipment was completed in early summer of 1996. By mid-year, all separate components and subsystems were fully operational, and commissioning work was focused on integration issues for the entire Transport Reactor train. The first coal feed was achieved on August 18, 1996. A series of characterization tests were completed with the reactor in combustion mode of operation by December 1996 to develop an understanding of reactor system operations. A number of start-up and design problems associated with various pieces of equipment were successfully addressed.

Combustion Mode Testing. During 1997, three characterization tests and one major test campaign were successfully completed. Testing was focused on exposing the PCD filter elements to process gas for 1,000 hours at temperatures from 1,350 to 1,400°F and achieving stable reactor operations. These tests used an Alabama bituminous coal from the Calumet mine and Plum Run dolomite for in-situ sulfur capture.

By May 1999, four additional test campaigns were completed to better quantify the effects of different variables on reactor operation and PCD performance. Several fuels and sorbents (for in-situ sulfur capture) were tested, and are listed in Table 1-1.

Table 1-1. Fuels and Sorbents Used during Combustion Mode Testing.

Fuels Used	Sorbents Used
Eastern Kentucky Bituminous Coal	Florida Gregg Mine Limestone
Petroleum Coke	Ohio Bucyrus Limestone
Illinois #6 Bituminous Coal	Alabama Plum Run Dolomite
Alabama Calumet Bituminous Coal	Alabama Longview Limestone

At the conclusion of combustion mode testing, the reactor had operated for 6,470 hours of solids circulation and 4,985 hours of coal feed.

Gasification Testing. The system was transitioned to gasification operation in late 1999. Four gasification commissioning tests (GCTs), each lasting nominally 250 hours, were completed by early 2001. At the conclusion of this reporting period, 20 gasification test campaigns (TCs) were completed, each nominally 250 to 1,500 hours in duration, for a total of about 11,500 hours of coal gasification operation. Table 1-2 summarizes the gasification testing completed, listing the start date, number of hours on coal, fuel type, and major objectives of each test. More information about the individual test campaigns may be found in the test campaign reports.

Table 1-2. Summary of PSDF Gasification Testing.

Test	Start Date	Duration (hrs)	Fuel Type*	Accomplishments
GCT1	Sep 1999	233	PRB, Illinois #6, Alabama	First gasification testing
GCT2	Apr 2000	218	PRB	Stable operations
GCT3	Feb 2001	184	PRB	Loop seal commissioning
GCT4	Mar 2001	242	PRB	Final gasification commissioning test
TC06	Jul 2001	1,025	PRB	First long duration test campaign
TC07	Apr 2002	442	PRB, Alabama	Lower mixing zone commissioning
TC08	Jun 2002	365	PRB	First oxygen-blown testing
TC09	Sep 2002	309	Hiawatha	New mixing zone steam system
TC10	Oct 2002	416	PRB	Developmental coal feeder commissioning
TC11	Apr 2003	192	Falkirk Lignite	First lignite testing
TC12	May 2003	733	PRB	First solid oxide fuel cell testing ever with coal-derived syngas
TC13	Sep 2003	501	PRB, Freedom Lignite	First operation of combustion turbine on syngas
TC14	Feb 2004	214	PRB	CFAD commissioning
TC15	Apr 2004	200	PRB	Improved oxygen feed distribution
TC16	Jul 2004	835	PRB, Freedom Lignite	High pressure oxygen-blown operation
TC17	Oct 2004	313	PRB, Illinois Basin	Bituminous coal testing
TC18	Jun 2005	1,342	PRB	Recycle gas compressor commissioning
TC19	Nov 2005	518	PRB	CCAD commissioning
TC20	Aug 2006	870	PRB	Gasifier configuration modifications
TC21	Nov 2006	388	Freedom Lignite	Post-modifications lignite testing
TC22	Mar 2007	543	Mississippi Lignite	High moisture lignite testing
TC23	Aug 2007	481	PRB, Freedom Lignite	High sodium lignite testing
TC24	Feb 2008	237	Utah	Post-modifications bituminous coal testing
TC25	Jul 2008	742	Mississippi Lignite	Fluid bed dryer commissioning

*Note: PRB is a subbituminous coal; Illinois #6, Alabama, Hiawatha, Utah, and Illinois Basin coals are bituminous coals.

The first two gasification tests, GCT1 and GCT2, achieved the commissioning of the Transport Gasifier, characterized the limits of operating parameter variations, and identified needed gasifier modifications. To improve the gasifier solids collection efficiency, a loop seal was installed below the primary cyclone to act as a pressure seal. Subsequent tests (GCT3 and GCT4) showed that the improved collection efficiency of the cyclone resulted in significantly lower solids loading to the PCD and higher gasification ash retention in the gasifier, promoting higher carbon conversion.

The first major test campaign in gasification mode commenced in July 2001 (TC06). Due to its long duration and stability of operation, the TC06 test run provided valuable data necessary to analyze long term gasifier operations; identify necessary modifications to improve equipment and process performance; and progress the goal of long-term exposure of PCD filter elements.

In early 2002, a lower mixing zone of specialized construction was added to the gasifier to allow oxygen feed, and this was commissioned in TC07. The first demonstration of oxygen-blown operation occurred in June 2002 (TC08). The transition from different modes of operation was smooth, and it was demonstrated that the full transition from air-blown to oxygen-blown operation could be made within 15 minutes.

Testing over the next four years focused on developing the fuel envelope. While performance was excellent (i.e. with high carbon conversion and gasification efficiency) with highly reactive fuels such as PRB, performance (primarily poor carbon conversion) was limited with lower reactivity fuels and fuels with ash chemistry issues requiring low temperature gasifier operation. These limitations and other issues related to gasifier scale-up for commercial operation prompted major modifications to the gasifier configuration in 2006. Subsequent testing confirmed that the configuration modifications significantly improved gasifier performance and fuel flexibility. These modifications are the basis of the commercial plant design in Kemper County, Mississippi.

1.3.2 Foster Wheeler Advanced Pressurized Fluid Bed Combustor

Commissioning of the APFBC commenced in October 1999, and coal was fed for the first time in October 2000. The unit burned Alabama bituminous coal for 170 hours, operating for 90 hours under fully automatic control while integrated with the combustion turbine. The turbine was driven by the coal-derived flue gas to produce the air for combustion and to generate up to 2.5 MW of power.

Studies conducted by DOE, Southern Company, and the Electric Power Research Institute (EPRI) led to the conclusion that feeding both the syngas and flue gas produced by the APFBC process to the same gas turbine combustor could not be accomplished with available commercial gas turbine designs. When commencing the APFBC development work, Foster Wheeler assumed that the turbine manufacturers would design a turbine suitable for the technology. As such a turbine was not made available, Foster Wheeler suspended its APFBC work. Consequently, Foster Wheeler and DOE National Energy Technology Laboratory (NETL) agreed to discontinue testing of this technology at the PSDF.

1.4 Economic Analyses

To guide future tests and commercialization of the technologies at the PSDF, a series of conceptual commercial plant designs have been completed in partnership with DOE NETL and EPRI.

To allow the most meaningful comparisons between cases, a common design basis was used whenever possible. Major similarities in the recent studies completed include the following:

- Two Transport Gasifiers
- Low-sulfur PRB coal, fed dry

- 2 X 1 combined cycle plant consisting of 2 General Electric 7FA+e gas turbines and an 1,800 psia reheat steam cycle
- Dry ash removal from the syngas at 500 to 700°F by metal filter elements
- Selective catalytic reduction in the heat recovery steam generator to control nitrogen oxides
- Greenfield site in the southeast United States at 114 feet above sea level with average ambient conditions of 65°F and 60 percent relative humidity

Table 1-3 gives the results of case studies run for six different process configurations, including air- and oxygen-blown gasifier operation and three variations of gas cleanup. These studies were published previously (Rogers, et al., 2006).

Table 1-3. Comparison of Gasification Process Configurations.

	Case 1	Case 2	Case 3	Case 4	Case 5	Case 6
Oxidant	Air	Oxygen	Air	Oxygen	Air	Oxygen
Gas Cleanup	Stack Gas	Stack Gas	Syngas	Syngas	CO_2 Capture	CO_2 Capture
Net Power Output, MW	573.9	511.9	594.6	530.9	428.0	361.0
Net Efficiency (HHV), %	42.1	39.9	41.0	40.0	29.0	26.1
Net Efficiency (LHV), %	44.6	42.2	43.4	42.3	30.7	27.6
Heat Rate (HHV), Btu/kWh	8,100	8,560	8,320	8,530	11,800	13,100
Heat Rate (LHV), Btu/kWh	7,650	8,090	7,860	8,060	11,100	12,400
Coal Feed Rate, lb/hr	532,000	502,000	566,000	519,000	577,000	541,000
Gas Turbine Output, MW	394.0	394.0	394.0	394.0	394.0	394.0
Steam Turbine Output, MW	266.1	209.2	287.4	230.1	196.8	132.5
Plant Auxiliary, MW	86.2	91.3	86.8	93.2	162.8	165.5
Total Cost of Electricity, mills/kWh	40.4	46.4	40.0	45.6	63.7	78.3

The results of these studies indicated that for the production of power from low-sulfur PRB coal with currently available technologies, air-blown Transport Gasification is preferable to oxygen-blown Transport Gasification. They also demonstrated that for these project configurations and design assumptions, syngas cleanup is preferable to stack gas cleanup. It was also shown that the costs of carbon capture from either the oxygen blown or air blown systems are significant.

1.5 Project Partner Participation

During operation of the PSDF through its initial cooperative agreement with the DOE, several of the project participants provided personnel support in addition to financial support. On-site technical advisors from industrial participants including KBR and Siemens Power provided support such as:

- Reviewing and commenting on test campaigns and detailed plans for particular tests

- Reviewing test related process operations with technical and operation personnel before commencing on a particular operation or test
- Participating in operations with other technical engineers at the PSDF and provide suggestions to operators for safe operation of the facility meeting test objectives
- Reviewing plans for sampling and laboratory analyses
- Review and suggesting necessary changes and additions to data reduction and analyses performed at the PSDF
- Performing comprehensive data analyses that are consistent with test objectives or goals to improve system operation
- Communicating operational status and data analyses to home offices
- Preparing test reports for the DOE
- Participating in DOE contractor's review meetings
- Participating in preparing technical papers for presentation in meetings and conferences

Participation by EPRI included providing technical staff to participate in the analysis of research activities and economic studies and the reporting of test results.

1.6 Report Structure

This report presents the operational data and results of gasification technology development at the PSDF through January 31, 2009, compiled in the sections listed below.

Section 2 Coal Preparation and Feed — Details numerous modifications made to the coal mill process, including the addition of a fluid bed dryer; discusses operation of the original coal feed system and the developmental feed systems.

Section 3 Transport Gasifier — Discusses the development of the Transport Gasifier, gasifier performance with the variety of coals tested, and results of parametric testing.

Section 4 Particulate Control Device — Details the performance of different filter elements and failsafes, progress with addressing ash bridging, specialized instrumentation, and studies of ash characterization.

Section 5 Advanced Syngas Cleanup — Describes testing of various syngas cleanup technologies, such as water-gas shift and COS hydrolysis reactions, as well as support of outside research including the National Energy Technology Laboratory fuel cell module and the Media and Process Technology hydrogen membrane.

Section 6 Instrumentation, Sampling, and Controls — Details progress made with gasifier instrumentation, coal feed rate measurements, and particulate monitoring; describes the various solids and gas sampling systems;

provides information about the gasifier control systems and safety interlock system.

Section 7 Support Equipment — Describes operations of the recycle gas compressor and piloted syngas burner. Describes the original ash removal systems and the continuous ash removal systems developed on-site for cooling and depressurizing the gasification ash from the gasifier and PCD.

Section 8 Conclusions — Summarizes the major conclusions and lessons learned from PSDF operation.

Section 9 References — Lists the references used in this report.

Appendix A Coal Characteristics — Provides characteristics of the coals tested in recent gasification operation.

Appendix B List of Acronyms and Engineering Units— Presents the acronyms and engineering units used in this report.

2.0 COAL PREPARATION AND FEED

2.1 Coal Preparation

Coal preparation was performed with two Williams Patent Crusher fluid bed roller mill systems designed for bituminous coal with about 10 weight percent moisture. A variety of coals ranging from lignite to bituminous were processed, requiring mill system modifications in order to produce the desired particle size and moisture content for reliable feeding to the gasifier. Instrumentation and control logic were enhanced to improve system control, reliability, and troubleshooting. A fluid bed dryer was also installed and commissioned for operation of higher moisture coals that required longer drying residence times to adequately reduce moisture levels.

2.1.1 Coal Mill System Description

Crushed coal is fed by a feed screw to the roller mill, a pulverizer, where it is mechanically ground and contacted with heated process gas (mainly nitrogen) from an electric heater. By design, the pulverizer functions as a flash dryer with the heated process gas also functioning to convey the pulverized coal from the mill. This results in a very short residence time (approximately 1 to 3 seconds) during which only surface or "free" moisture is evaporated. High moisture coals containing a high relative amount of intrinsically bound moisture, such as lignite, retain much of this bound moisture through this process and require longer residence time for drying.

Figure 2-1 shows the process flow diagram for the basic coal preparation system without the fluid bed dryer operating.

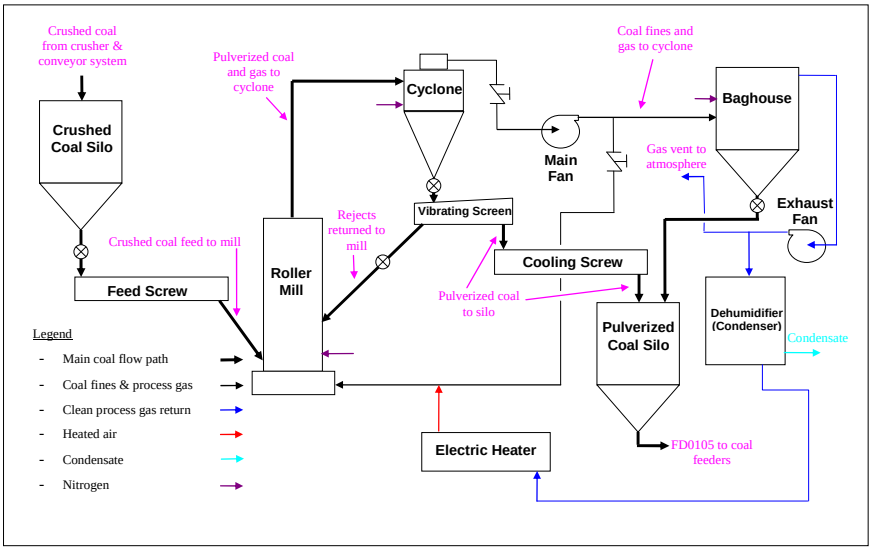

Figure 2-1. Coal Preparation Process Flow Diagram

A cyclone separates the process gas (containing coal fines) from the pulverized coal. The separated process gas is then filtered in a baghouse and is dehumidified, heated in an

electric heater, and recycled back to the pulverizer. The separated coal is screened, and oversize coal returns to the pulverizer for further milling. The pulverized coal product continues through a screw cooler, and is stored in a silo ready for use as gasifier feedstock.

2.1.1.1 Coal Mill Hardware Modifications

Coal Silo Inserts. The two pulverized coal silos were designed based on experience from conventional coal plants. However, the differences in coal particle sizes and moisture contents (and thus flow characteristics) between the coal fed to the Transport Gasifier and coal fed at conventional plants created problems with coal conveying. The silo design promoted funnel flow, causing particle size segregation and coal feeder difficulty.

To adjust the silos to better handle the flow characteristics of the gasification process coal, the silos were fitted with internal cones to prevent a funnel flow and to create a mass flow regime. The new coal silo inserts improved coal feeder operations by preventing particle size segregation in the pulverized silos, which resulted at times in a high percentage of fines in the feed material. A liner made of low-friction Tivar material was also added to the bottom of the silo hoppers to promote flow. Figure 2-2 shows one of these inserts as it was being installed.

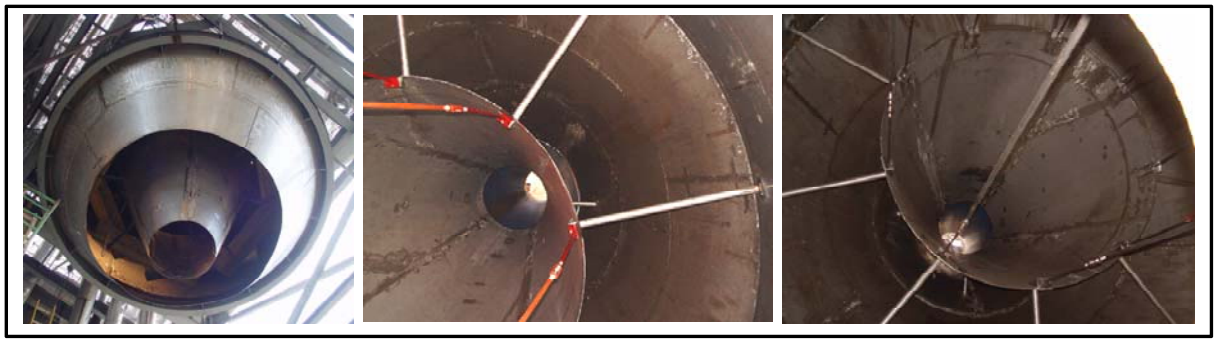

Figure 2-2. Pulverized Coal Silo Insert.

Automatic Coal Samplers. Automatic coal samplers were added to the pulverized coal silos to give real-time data to improve mill operations. Figure 2-3 provides photographs of a coal sampler installed in the coal mill system. The data collected allowed quicker adjustments to the mill controls to address deviations in particle size and moisture content from the desired values and was used to determine when material was unsuitable for feeding.

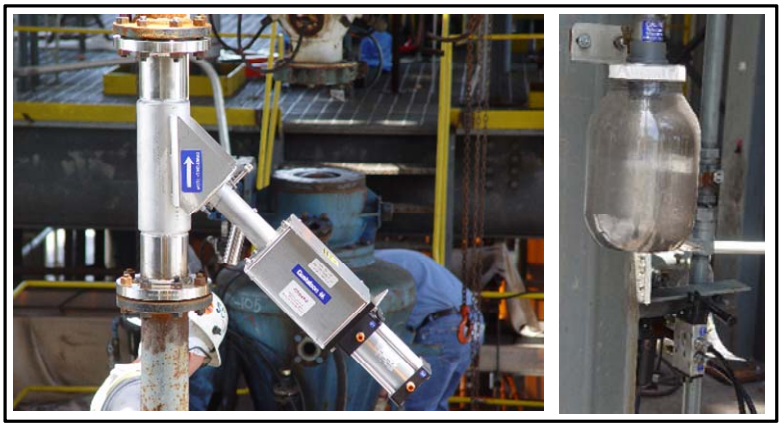

Figure 2-3. Coal Sampler.

Conveying Gas Controls. To improve control of mill conveying gas (vitiated air), a V-cone flow meter and an automatic configuration to adjust flow settings using input from the flow meter were installed. The gas flow had previously been adjusted in the field based on a local flow measurement. The modification allowed real-time flow control so that the particle size distribution (PSD) could be controlled more tightly.

Dehumidifier Installation. Dehumidifiers were installed in April 2005 to remove condensate from the drying gas to avoid moisture saturation of the gas. This also decreased the amount of make-up nitrogen that was required due to reduced exhaust gas requirements. This modification resulted in a lower operating cost due to the lower nitrogen flow. The dehumidifier installed is shown in Figure 2-4. Measurements confirmed that the dehumidifier decreased the moisture content in the gas.

Figure 2-4. Coal Drying Gas Dehumidifier.

Replacement of the Mill Propane Heaters with Electric Heaters. Two electric heaters with 18 heater elements were installed in both coal mills in 2006 to serve as the heat source for drying. Figure 2-5 is a photograph of the electric heater as installed. The electric heater heats recycled gas (about 90 percent nitrogen) after the gas passes through the dehumidifier before in enters the pulverizer. The electric heater improved mill operation

since it replaced the direct-fired propane heater that was contributing to moisture saturation in the recycled gas.

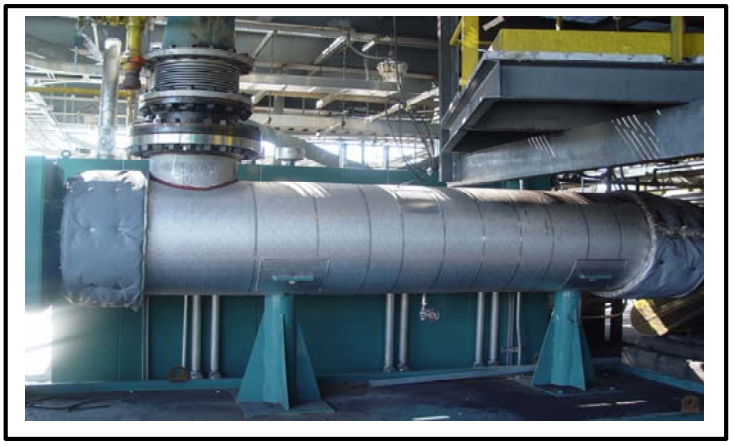

Figure 2-5. Coal Mill Electric Heater.

Condensate Trap. In November 2006, a condensate collection pot was installed to trap and automatically drain condensate carryover from the dehumidifier into the electric heater to prevent damaging the heater elements. This modification was successful in reducing condensate carryover.

Nitrogen Purge on Mill Chute. Nitrogen purges were added to the mill feed chute to improve flowability of material and prevent mill feed interruptions. The purges improved operations providing a more consistent coal feed into the mill.

2.1.1.2 Coal Mill Control and Instrumentation Improvements

On-line Particle Size and Moisture Analyzers. Malvern particle size and moisture analyzers were installed to provide real-time data for improved control of mill operations. However, after extensive trouble shooting, issues with inconsistencies in the samples remained due to problems with the sample delivery system.

Microwave Flow Switch. A microwave flow switch was added beneath each cycle rotary valve on both mill systems. The switches detect a loss of solids flow from the cyclone, which indicates bridging. This allowed for early detection and response to prevent carryover of material into the fan and possible equipment damage and lower system reliability. Figure 2-6 shows the microwave flow switches.

Figure 2-6. Microwave Solids Flow Switches.

Dual Oxygen and Carbon Monoxide Analyzers. Dual oxygen and carbon monoxide analyzers were installed downstream of the baghouse to allow for detection of partial oxidation inside the baghouse. Installation in this area is critical due to the high concentration of coal fines. Figure 2-7 is a photograph of the analyzers installed. The carbon monoxide (CO) readings have been steady during normal operations.

Figure 2-7. Dual O_2/CO Analyzers.

Controls System. Preceding the July 2008 test run the mill control system was replaced. Since the existing Williams control system was no longer going to be supported after 2011 and was limited in its capability, an Allen Bradley programmable logic controller (PLC) was installed. The Allen Bradley PLC added the ability for expansion, diagnostics, advanced control, and communications with the distributed control system (DCS) and the Plant Information (PI) plant historian. The Allen Bradley PLC significantly improved the controls capability and system troubleshooting. Some examples include information on motor status and valve positions, ability to bring additional data points into the DCS and PI, and the capability of setting up and saving system operating conditions for multiple fuel types. Figure 2-8 shows the human machine interface that was created for use with the Allen Bradley PLC.

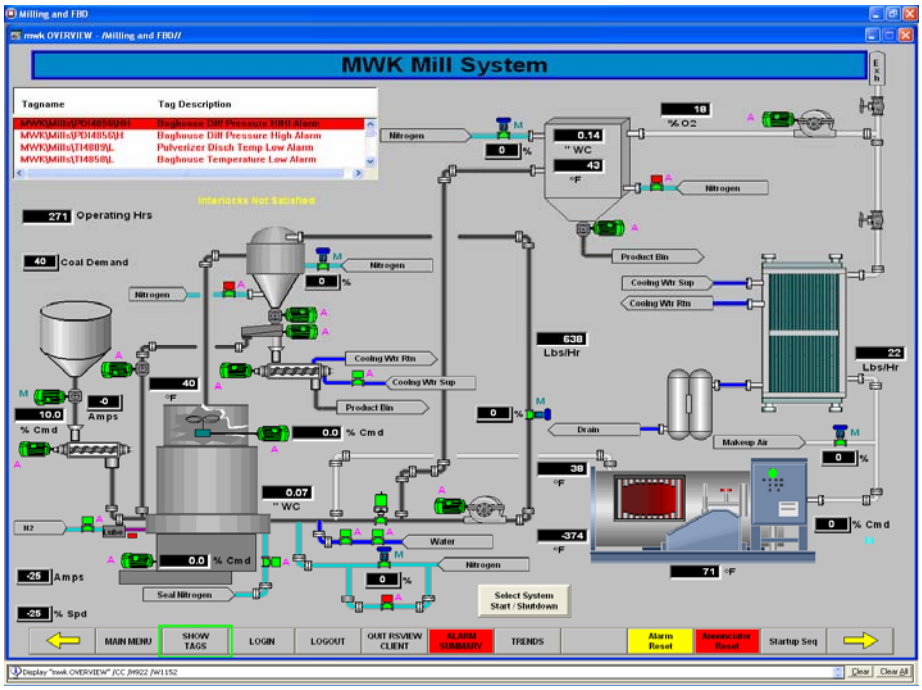

Figure 2-8. Mill System Human Machine Interface.

2.1.2 Fluid Bed Dryer

The coal preparation system originally installed at the PSDF was designed to process bituminous coal, which contains about 10 weight percent moisture. However lower rank fuels were also tested to develop fuel flexibility with the Transport Gasification process. The higher moisture content of the lower rank coals caused operating problems with the coal preparation and feed systems. Previous mill system modifications improved operation and allowed for effective processing of tested subbituminous and lignite coals. However, when the high moisture Mississippi lignite was first tested in TC22 (March 2007), the coal preparation system could not sufficiently dry the coal because of its higher relative amount of intrinsically bound moisture. During TC22, the as-fed coal moisture content averaged 28 weight percent, and this relatively high moisture content caused numerous coal feed operational problems. To improve coal feeding with high moisture coals, additional drying residence time was needed to decrease the moisture content to 20 weight percent or less.

A fluid bed coal dryer was installed and commissioned to improve the drying capacity of the coal preparation system when processing high moisture fuels and thus expand the PSDF process fuel envelope. This system offers economic advantages in a commercial application due to the use of waste heat to increase the process gas temperature. During TC25, the fluid bed dryer successfully reduced the Mississippi lignite moisture content low enough for reliable coal feeding. The lignite was processed first in a crusher, then in the fluid bed dryer, and finally in a pulverizer before being conveyed to the coal feed systems.

Equipment Description. The fluid bed technology employed for the new coal dryer system does not require any internal moving parts, operates with high thermal efficiency, and uses less energy per pound of water removed than conventional drying methods. Figure 2-9 is a flow diagram of the PSDF fluid bed coal dryer system.

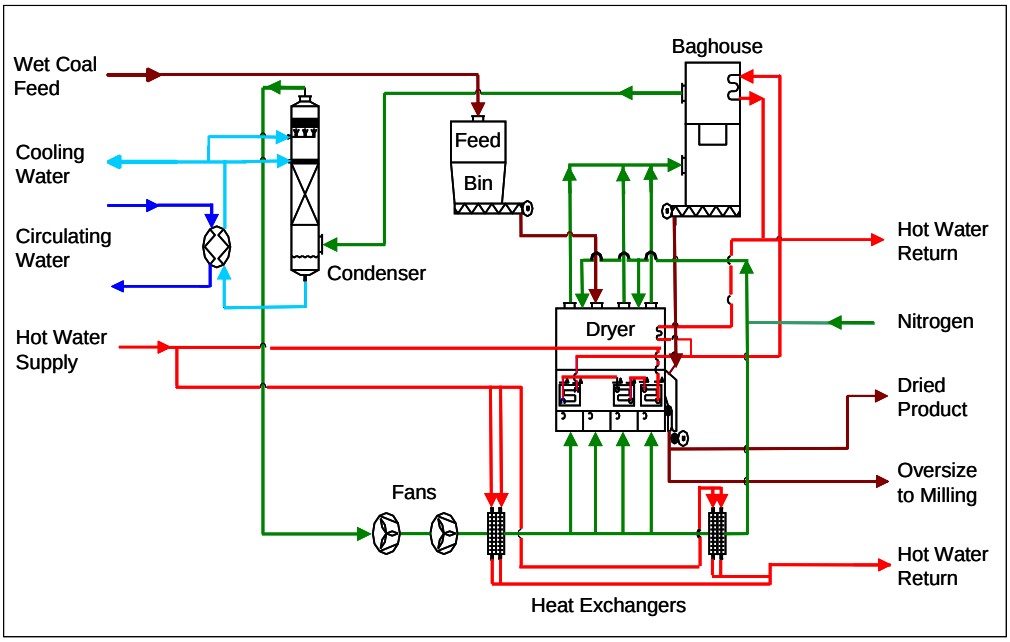

Figure 2-9. Fluid Bed Dryer System Flow Diagram.

After processing through a crusher, the coal is fed into the dryer feed bin and then directly to the dryer by a variable rate feed system. Nitrogen is used for drying and fluidization and is heated in a finned tube heat exchanger prior to entering the dryer. As the nitrogen and moist coal mix, the moisture transfers from the coal to the nitrogen. Three in-bed heat exchangers promote additional drying. The fluidized coal flows around and through the heat exchangers for efficient utilization of this drying energy.

The nitrogen at the top of the dryer is nearly saturated with water vapor. A slipstream of gas that bypasses the dryer is sent through a second finned tube heat exchanger to reheat the exit vapor preventing condensation of the gases in the exhaust duct or the baghouse. The gases pass through a baghouse, where entrained particulate is extracted from the gas stream and is conveyed to the dryer product outlet where it is mixed with the dried coal.

Exhaust gas from the baghouse enters a direct contact spray condenser, where the evaporated moisture from the lignite is condensed and extracted. A quench-water recirculation pump takes water from the condenser basin and discharges it above a packed bed to cool the process gas and condense the evaporated water. This condensed water goes to the process wastewater stream at the PSDF, but could be recycled in a commercial facility.

The water from the condenser basin is circulated through a heat exchanger to maintain a constant cooling water temperature. A cooling tower is used to provide cooling water to the shell and tube heat exchanger. The source of thermal energy for the dryer heat exchangers is a high temperature water heater operating at 300°F. The operating conditions selected emulate waste heat streams at a commercial facility, further enhancing the efficiency of the operation.

The quenched nitrogen stream exits the condenser and passes through primary and secondary process blowers. Some gas may be exhausted to the atmosphere to control system pressure.

Commissioning. The fluid bed dryer system, manufactured by Schwing Bioset, was designed in early 2007. Construction and installation was completed in March 2008, and the initial commissioning was completed off-line in May 2008. Figure 2-10 is a photograph of the fluid bed dryer system installed at the PSDF.

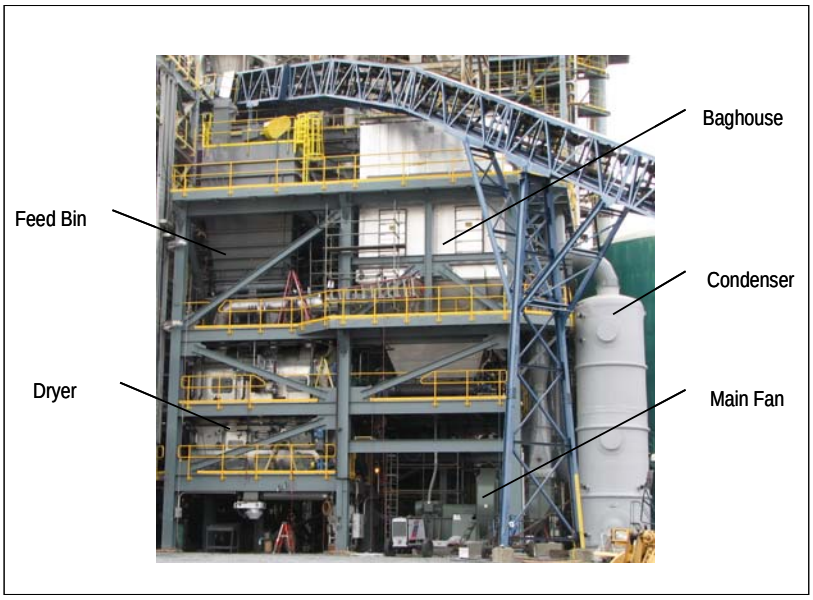

Figure 2-10. Fluid Bed Dryer System.

Several operating challenges, mostly associated with support equipment and with incorrect manufacturers' installation, were resolved, and a number of parametric tests were successfully completed. The dryer operated on high moisture lignite successfully for 150 hours during the initial commissioning phase at the design coal feed rate of 13,600 lb/hr. Samples of the dryer feedstock, product, and oversize were collected during each test to determine the optimal operating conditions for particle size and coal moisture reduction. Heat transfer data was also collected to assess dryer thermal efficiency.

Commissioning Results. The results from commissioning activities were:

- Quantification of coal particle size attrition through dryer
- Quantification of oversize removal rate
- Dryer operation at different hot water supply temperatures
- Minimization of nitrogen consumption
- Confirmation of design mass and energy balances
- Development of programmable logic controls
- Identified steps to stop a CO increase
- Demonstrated that cleanout of the fluidization windbox was unnecessary
- Improved the nitrogen makeup and nitrogen vent control

Performance during Commissioning. Table 2-1 shows the fluid bed dryer operating performance during commissioning with particle sizes represented as mass median diameters (MMDs). Testing revealed that while particle attrition in the dryer reduced the coal particle size significantly, the percentage of oversize particles was higher than desired for coal feed system operation. Thus, the material was sent to the pulverizers for final product sizing. Figure 2-11 shows the particle size distribution curves for the raw lignite and the fluid bed dryer product.

Table 2-1. Performance of Fluid Bed Dryer during Commissioning.

	Average Value
Inlet Coal Moisture Content, wt %	44
Outlet Coal Moisture Content, wt %	21
Moisture Content Reduction, %	56
Inlet Coal MMD, micron	1,100
Outlet Coal MMD, micron	890
Outlet Coal Oversize (>1,180 micron) Content, wt %	40
Outlet Coal Fine (<45 micron) Content, wt %	5

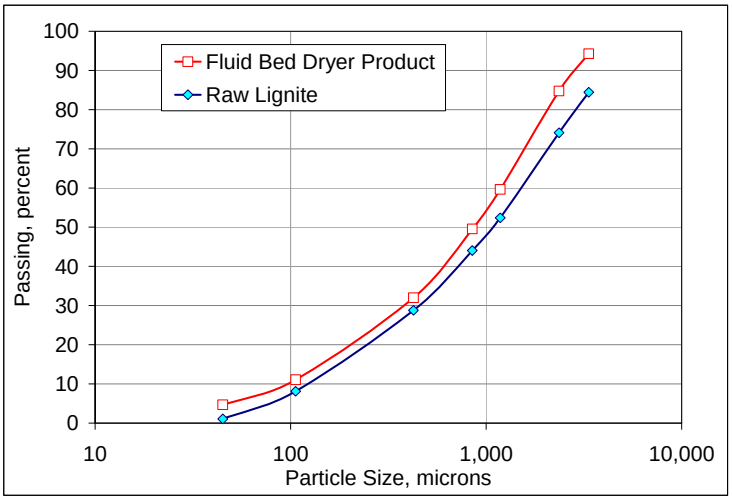

Figure 2-11. Particle Size Distributions of Lignite Processed in Fluid Bed Dryer and of Raw Lignite.

Parametric testing consistently demonstrated the positive relationship between bed temperature and coal moisture content, and the operating data established the minimum bed operating temperature. Figure 2-12 plots the moisture content of the fluid bed dryer product versus the bed temperature. As expected, testing also showed that lower hot water supply temperature resulted in a higher required mass flow rate of hot water but did not affect the coal moisture content.

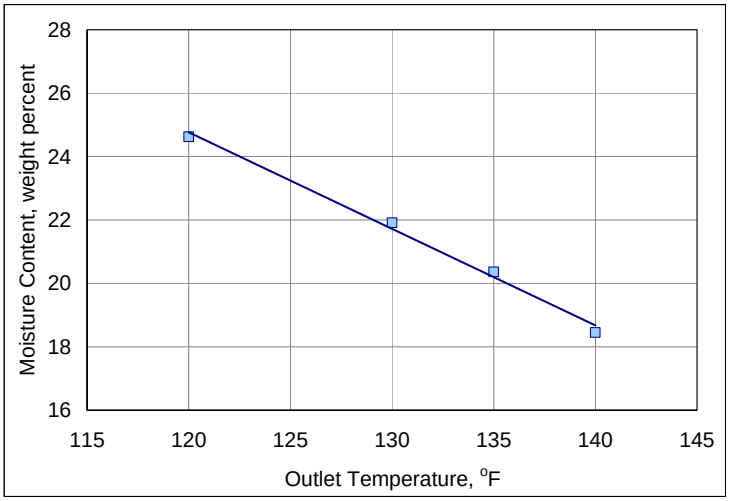

Figure 2-12. Product Moisture Content versus Fluid Bed Dryer Outlet Temperature.

The oversize (reject) removal rate was about 4 to 5 percent of the dryer feed rate. At this rate, dryer fluidization and bed differential pressure remained stable. Oxygen and CO analyzers were used to ensure safe operation of the process and provided accurate readings. Significant progress was made on control automation, with only three main control loops requiring additional tuning after completion of commissioning activities.

Operation of the Fluid Bed Coal Dryer System to Support the July 2008 Test Run. In preparation for TC25, the fluid bed dryer was started on June 23, 2008, and operated for about 100 hours, processing 365 tons of lignite. The system performed well with no operational problems. The dryer operating temperature was held constant at about 135°F while the lignite flow rate varied from about 4,500 to 13,000 lb/hr to evaluate how the system operated at different flow conditions. The fluid bed dryer reduced the moisture content of the lignite from about 41 weight percent as-received to about 19 weight percent. The particle size of the dryer produced material, at about 900 microns MMD, was consistent with previous testing. The dryer product had 42 weight percent oversize material (greater than 1,180 microns) and about 7 weight percent fines (material less than 45 microns).

The lignite processed in the fluid bed dryer was then pulverized in the coal mill pulverizers to reduce the amount of oversize material. The pulverizers reduced the MMD to about 475 microns and the weight percent of oversize particles to about 21 weight percent. Figure 2-13 compares the particle size distribution curves for the fluid bed dryer

product and the pulverized material. The additional pulverizing slightly increased the amount of fine material, which averaged about 18 weight percent. In addition, the pulverizers were operated without heat input from the electric heaters resulting in minimal added moisture reduction (lignite moisture content averaged 18 weight percent). The mill system was shut down after pulverizing about 195 tons of lignite.

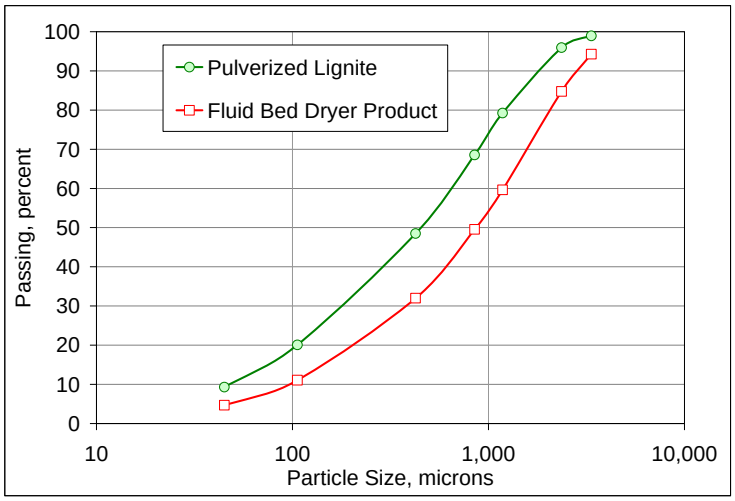

Figure 2-13. Particle Size Distributions of Pulverized Lignite and of Lignite Processed in Fluid Bed Dryer.

During on-line operation in TC25, the fluid bed dryer system operated without major operational issues for 469 hours, processing 2,800 tons of the high moisture lignite. The MMD particle sizes of the processed lignite as sampled from the coal feeders are shown in Figure 2-14. The lignite MMD particle size varied mostly from 300 to 500 microns for most of TC25 with some outliers ranging from 95 to 720 microns. The lower MMD around Hour 650 resulted from accumulated fines as the silo was emptied in preparation for a test with a slightly larger particle size.

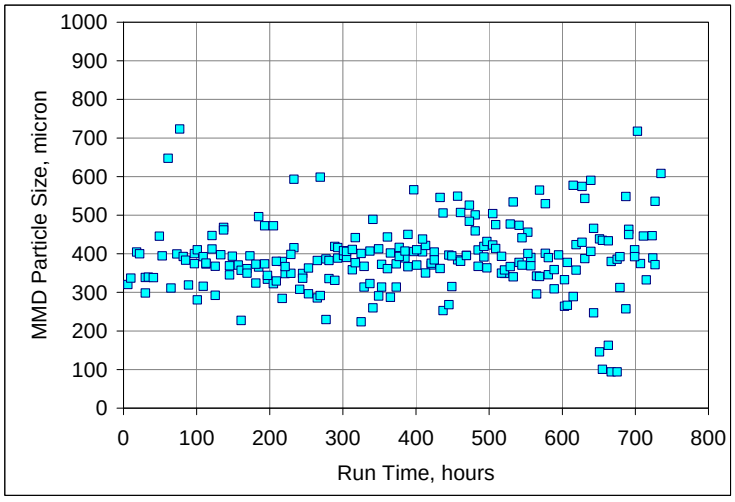

Figure 2-14. Particle Sizes of As-Fed Lignite.

Figure 2-15 shows the percentage of oversize coal (above 1,180 microns), and Figure 2-16 gives the percentage of fine coal (below 45 microns). The oversize particles varied mostly from 15 to 25 percent with outliers ranging between 5 and 33 weight percent of the coal. Fines concentrations varied mostly from 12 to 20 percent with outliers ranging from 9 to 32 percent.

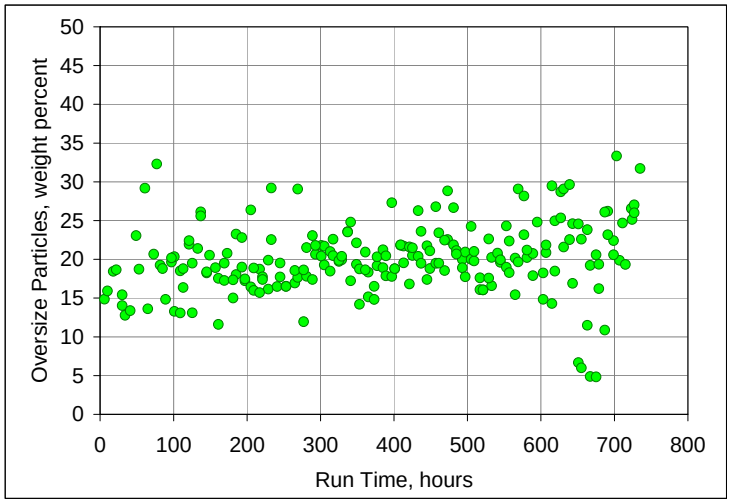

Figure 2-15. Percentage of Oversize Particles in As-Fed Lignite.

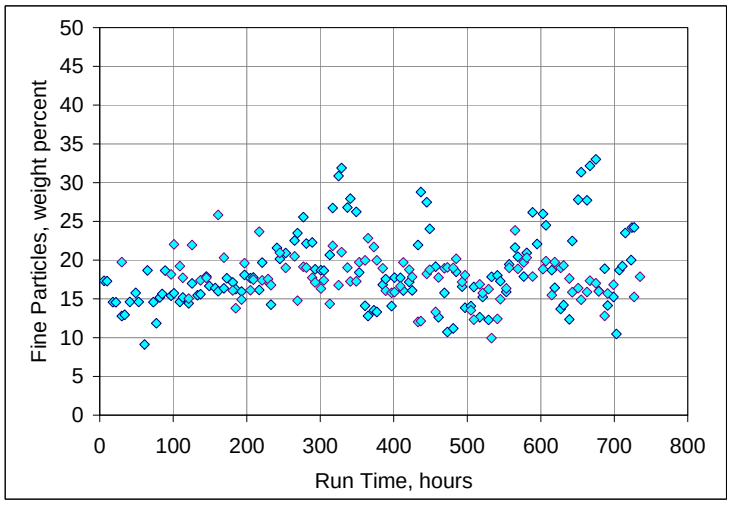

Figure 2-16. Percentage of Fine Particles in As-Fed Lignite.

Figure 2-17 plots compares the processed as-fed moisture content of the Mississippi high moisture lignite during TC22 (before the fluid bed dryer was installed) and during TC25, when the dryer was operating.

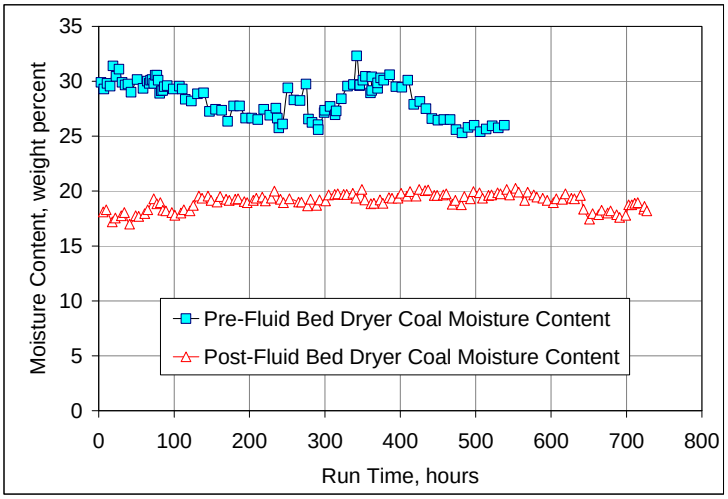

Figure 2-17. Moisture Content of As-Fed Lignite before and after Fluid Bed Dryer Installation.

2.2 Coal Feeders

Two feed systems, the original and the developmental systems, provided coal feed to the Transport Gasifier. Both feeder systems utilize lock hopper designs to pressurize the coal to gasifier operating pressure, but differ in the feed delivery systems. Numerous hardware and control logic modifications have been made to improve the reliability and operability of both systems over a wide range of coal particle sizes and moisture contents.

2.2.1 Original Coal Feeder

Equipment Description. The original coal feed system supplied by Clyde Materials Handling is a lock hopper, horizontal pocket feeder design with a "rotofeed" dispenser. The coal feed system receives coal from the pulverized silo into the surge bin, which always operates at atmospheric pressure. The system also has two pressure vessels, with the coal pressurized in the upper lock vessel and then gravity fed into a dispense vessel, which is always pressurized. The material is fed out of the dispense vessel by the rotofeed dispenser, which is driven by a variable speed electric motor and delivers the material into the discharge line where it is conveyed by air or nitrogen into the gasifier. A schematic of the system is shown in Figure 2-18.

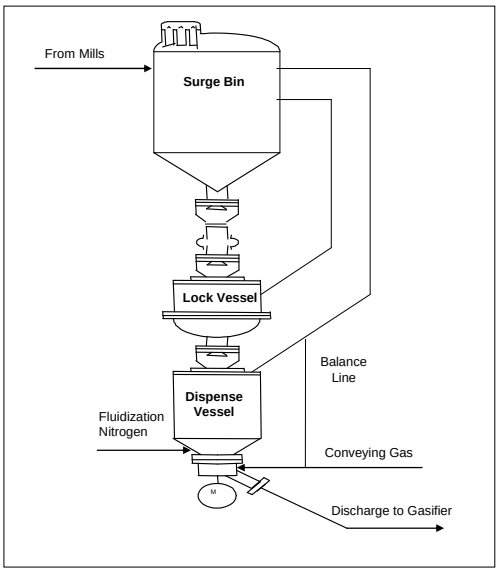

Figure 2-18. Original Coal Feed System.

Operational Challenges. Numerous operational issues have been encountered during testing, most related to the particle size and moisture content of the material, such as material plugging the vent lines, lock vessel, and discharge line. Operating parameters such as the transport gas velocity and dispense vessel fluidization were varied to improve operations and hardware, and control modifications were made to improve operations.

Vent Valve Modifications. Relocation of the vent valves on the lock vessel prior to TC19 resulted in fewer operating problems as compared to previous test campaigns. The particle size distribution occasionally varied outside of the developed operating envelope, and at these times the coal feeder experienced problems with the dispense vessel vent lines plugging. For example, coal feed was interrupted for 20 hours in TC19 to unplug the vent lines. To reduce downtime, the two-inch vent valve and associated 7/64-inch flow orifice were removed and replaced with a one-inch ceramic V-ball control valve, which is shown in Figure 2-19.

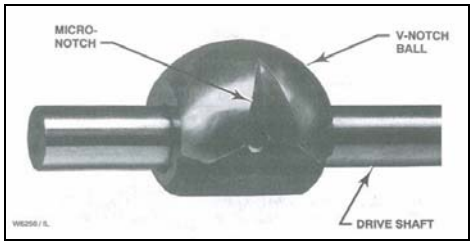

Figure 2-19. Vent Valve Replacement on Original Coal Feeder.

Figure 2-20 shows a schematic of the coal feeder with the location of the new vent valve circled in the figure. Operation of the new dispense vessel vent valve on the original coal feeder resulted in decreased frequency of vent line plugging compared to previous test

campaigns. The vent lines plugged occasionally during periods of variability in coal particle sizes, although downtime was limited to less than nine hours in TC20.

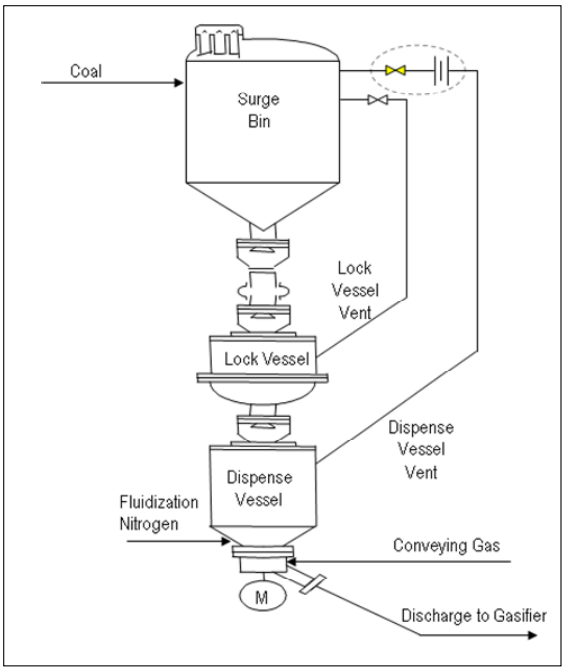

Figure 2-20. Original Coal Feeder Vent Valve Location.

Balance Line. A balance line was installed from the dispense vessel to the transport gas supply line and tested during operations in November 2006 operations. Figure 2-21 shows the location of the balance line. The balance line successfully minimized the occurrence of vent line plugging in this coal feeder.

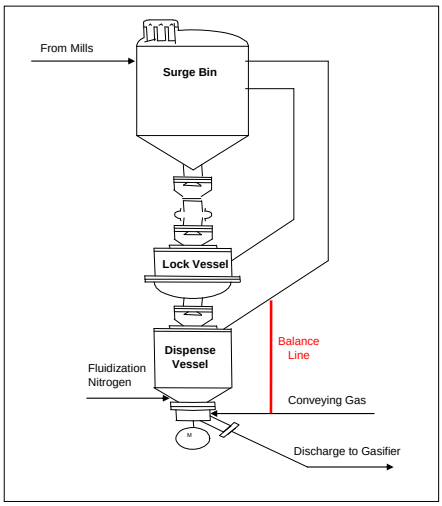

Figure 2-21. Original Coal Feeder Balance Line Location.

Operations. The original coal feed system has been tested for more than 16,000 hours with many different fuels over a wide range of operating conditions, including:

- Feed size from 100 to 800 microns MMD
- Pressures ranging from 110 to 290 psig
- Feed rates between 500 and 5,500 lb/hr
- Feed moisture contents from 3 to 30 percent
- Both air and nitrogen used as the conveying medium

Limiting the percentage of particles greater than 1,180 microns and the moisture content below 25 percent and modifications to eliminate low velocity regimes in the feed line have provided more stable operations, essentially eliminating occurrences of pluggages in the discharge line. Limiting the percentage of particles less than 45 microns and controlling the moisture content as well as modifying the lock vessel vent valve arrangement have minimized vent line pluggages.

Coal Feeder Operating Envelope. Based on the last five years of operations, the original coal feed system operating range for the coal moisture content and particle size was evaluated. Figure 2-22 illustrates the original coal feeder operating envelope for coal particle size versus coal moisture content. The operating envelope (shown in blue) represents reliable coal feeder operation during recent test campaigns (TC20 through TC25).

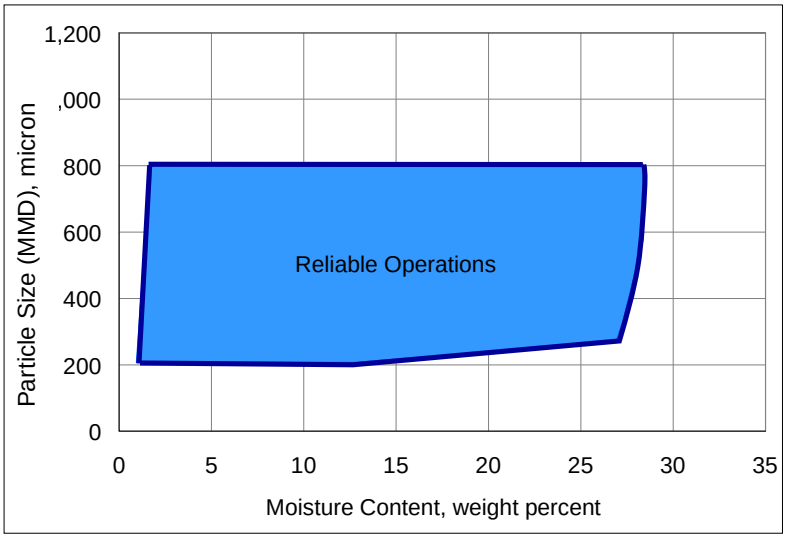

Figure 2-22. Original Coal Feeder Operating Envelope.

2.2.2 Pressure Decoupled Advanced Coal Feeder

The Pressure Decoupled Advanced Coal (PDAC) feeder concept was first tested in the PSDF cold flow unit, and following this initial concept validation, the system was scaled up to a size meaningful for testing in the PSDF gasification process.

Equipment Description. Installed to support high-pressure coal feeder development, the PDAC feeder is a non-mechanical feed control device with no moving parts. The design of PDAC combines some of the successful concepts developed at the PSDF (such as continuous ash depressurization) with traditional designs for flow rate control. Details of the design and its operating principles are proprietary. Like the original feeder, the PDAC system is a lock hopper-based feeder. PDAC differs in that it uses conveying gas flow to control the solids feed rate.

Off-Line Testing. The PDAC feeder was installed on the secondary coal feeder and was first commissioned in an off-line test system in December 2007. The off-line system allows testing at conditions similar to gasification operation, with pressures up to 250 psig and coal feed rates up to 6,000 lb/hr.

The PDAC feed system was tested off-line again in May and June 2008 with high moisture lignite. Three main operating challenges were encountered:

- Repeated plugging of the lock vessel
- Conveying line differential pressure increase without a corresponding increase in density
- Frequent plugging of one of the off-line feeder vessel discharge lines

To identify needed improvements in the lock vessel operation, the pulverized lignite was tested in the laboratory and the cold flow unit. The testing revealed that compared to subbituminous coal, the lignite had a higher angle of repose and more easily packed together when pressurized. Testing also showed the need for pressurization logic modifications to allow a slower pressurization ramp rate to the desired lock vessel pressure setpoint and to permit more frequent fluidization of the vessel during the fill cycle. In addition, the lock vessel pressure setpoint was lowered relative to the pressure of the dispense vessel. By operating the lock vessel in this under-pressurization state, additional fluidization of the lock vessel was achieved upon attempting to transfer material to the dispense vessel.

Additional data analysis showed that the conveying line pressure differential variations were due to the piping configuration of the off-line testing system. Booster nitrogen was added to address the off-line feeder plugging issue. Additional off-line operations occurred in June 2008 to test the modifications. After working through some initial issues and modifying the pressurization logic, the PDAC feed system operated well over a range of feed rates.

On-Line Commissioning with Coke Breeze. During February 2008 (TC24), the PDAC feed system was successfully operated for 36 hours, feeding coke breeze to the gasifier during start-up and hot re-starts. Coke breeze was fed to heat the gasifier from the maximum start-up burner temperature of 1,200^{o}F to a temperature high enough for coal feed (about 1,700^{o}F for the bituminous coal).

The PDAC system operated well, feeding about 20 tons of coke breeze to the gasifier at relatively low feed rates of about 1,100 lb/hr. The controls system operated well, with the feed rate responding as desired to changes in the conveying nitrogen flow rate. During initial operation, several trips occurred due to a problem with the interlock logic. Logic modifications prevented further trips, and thereafter, the feed system had 100 percent availability.

Coal Feed to the Gasifier. The PDAC feed system was successfully operated for 441 hours in July and August 2008 (TC25), feeding 885 tons of high moisture lignite to the gasifier. Feed rate controllability was an issue at certain conditions, so additional modifications were planned to improve the feed rate control.

3.0 TRANSPORT GASIFIER

At the conclusion of the reporting period (through January 2009), the Transport Gasifier had operated for 11,581 on-coal hours, including 1,757 hours in oxygen-blown mode. Optimization of operating parameters and design enhancements have allowed efficient gasification of a variety of fuels. The fuels tested include low-rank fuels such as lignite and subbituminous coals and as well as several bituminous coals.

3.1 Gasifier Description

The Transport Gasifier is a pressurized, advanced circulating fluidized bed reactor consisting of a mixing zone, riser, solids separation unit, seal leg, standpipe, and J-leg. Figure 3-1 provides the location of the Transport Gasifier components as well as the gas and solids flow path.

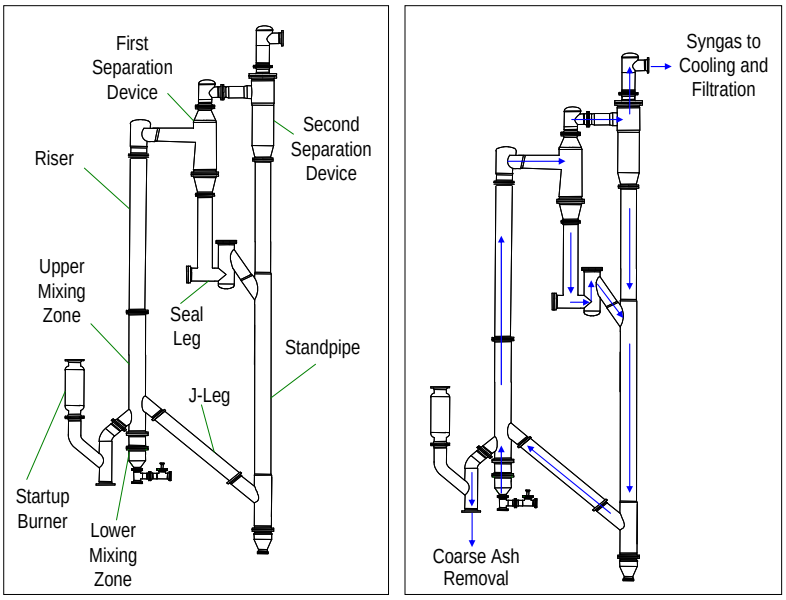

Figure 3-1. Schematic of Transport Gasifier.

The gasifier is equally capable of using air or oxygen as the gasification oxidant. A mixture of air or oxygen with steam is fed into the mixing zone at different elevations and orientations to evenly distribute heat generated from the partial combustion of the circulating solids. The oxygen from the air or pure oxygen feed is completely consumed in this section of the gasifier. Coal is fed at a higher elevation in the mixing zone where the atmosphere is reducing, or oxygen-free.

As the coal devolatilizes and chemical reactions occur to generate syngas, the gas and solids move up the riser and enter the solids separation unit. This unit contains two solids separation devices, which use cyclonic action to remove particles. Between the first and second solids separation devices is the seal leg, which prevents backflow of gas. The solids collected by the solids separation unit are recycled back to the mixing zone through

the standpipe and J-leg. The gasifier solids inventory is controlled by removing gasification ash through the continuous coarse ash depressurization (CCAD) system, which cools and depressurizes the solids. The nominal gasifier operating temperature is 1,800°F, and the gasifier system is designed to have a maximum operating pressure of 294 psig with a thermal capacity of about 41 MMBtu/hr.

Key features of the Transport Gasifier include:

- Simple, well established design based on technology in use for 70 years which does not require expansion joints
- Equally effective gasification in either air- or oxygen-blown modes of operation, making it suitable for power generation or production of liquid fuels and chemicals
- High reliability non-slagging design, which allows a 10- to 20-year refractory life
- Operation without burners enhances reliability and minimizes maintenance requirements
- Use of coarse, dry coal feed, which requires fewer, lower power pulverizers, and less drying than other dry-feed gasifiers
- Cost-effective operation and high carbon conversion with high moisture, high ash, and low rank fuels, including subbituminous and lignite coals
- Excellent heat and mass transfer due to a high solids mass flux, with a solids circulation rate 80 to 100 times greater than the coal feed rate

3.2 Gasifier Modifications

The original design of the Transport Gasifier was based on a combined combustor/gasifier operation, so modifications were needed to optimize gasifier operation and improve operational stability and performance. These modifications include changes to the gas feed distribution systems and the gasifier configuration.

3.2.1 Gas Flow Distribution Modifications

Upper Mixing Zone Modifications. Separate steam, oxygen, and air/nitrogen flow control valves and measurement devices were installed on the oxygen and steam supplies to the upper mixing zone (UMZ). The air and steam flow control valves and measurement devices were fully commissioned and operated as expected. Testing confirmed uniform distribution of the oxygen flow to the UMZ and verified the oxygen flow measurement accuracy. Adding oxygen into the UMZ resulted in a lower temperature differential between the UMZ and the gasifier outlet.

Lower Mixing Zone Modifications. Modifications to the lower mixing zone (LMZ) were made to increase the air flow rate to the LMZ to evaluate the hydrodynamics of the circulating bed, the amount of carbon being recycled into the LMZ, and the effect on the gasifier temperature profile. The supply valve was resized, and the piping configuration was re-designed to minimize the pressure drop in the supply line.

About 200 hours of testing was completed with air flow rates ranging from about 3,000 to just over 7,000 lb/hr. As expected, the density in the LMZ decreased about 10 to 15 percent, while the density in the UMZ and riser increased 30 percent on average. The solids circulation rate was higher at the higher flows due to less resistance to solids flow from the J-Leg into the mixing zone.

As the air flow rate to the LMZ was increased, the LMZ temperatures increased until the air flow rate was greater than that required stoichiometrically for complete combustion of the carbon re-circulated into the LMZ. At that point the temperatures decreased. As a result, the high temperature zone shifted to the upper mixing zone. The gasifier operated steadily during the test, and there was no negative impact on operations.

3.2.2 Gasifier Configuration Modifications

Modifications to the original Transport Gasifier configuration were initiated to overcome the limits based on its combined combustor/gasifier design, as well as to improve solids collection efficiency that had degraded over time. Testing in February 2004 showed a significant decline in the primary cyclone performance. The resulting high solids carryover rate to the PCD caused low gasifier solids inventory and necessitated continuous sand feed to the gasifier to maintain the solids inventory. Post-run inspections revealed that a notch had formed in the inlet flow path and that there was some damage to the cyclone roof causing the loss of collection efficiency. The gasifier cyclone notch was removed and the damaged roof was repaired in the outage following these tests. However, the notch at the cyclone inlet eventually re-formed, significantly limiting performance in 2005.

3.2.2.1 Description of Gasifier Configuration Modifications

In 2006, changes to the gasifier provided new, more robust solids separation and recycle systems as well as a larger diameter riser. These changes consisted of replacing approximately 85 percent of the existing refractory-lined gasifier. Different types of refractory were installed for evaluation of these materials.

While not precluding future testing in combustion mode, the modifications were designed specifically to enhance performance during gasification operation. The primary goals were to improve the solids collection efficiency and to increase the residence time in the gasifier as well as to demonstrate a solids collection system better suited for commercial scale-up. Increasing the solids collection efficiency improves the carbon conversion by retaining and recycling more of the carbon solids in the gasifier. Increasing the residence time also improves the carbon conversion to combustible syngas components.

With the original design, the particulate laden syngas from the riser passed through a disengager and then into a cyclone before exiting the gasifier. The disengager separated the gas and solids mixture by utilizing gravity settlement and operated with about 70 percent collection efficiency. The new design incorporated a two-stage solids separation unit utilizing cyclonic action for both stages of separation. In addition, the

solids flow path exiting the second device was improved to eliminate fine gasification ash from packing in the line before flowing back into the standpipe.

The modifications to the solids separation unit were designed to result in higher overall solids capture efficiency. By retaining more carbon containing gasification ash in the gasifier, more solid-phase carbon is converted into syngas. Higher carbon conversion results in a higher syngas heating value and thus a higher gasification efficiency. This positively affects the overall process economics. In addition, the higher capture efficiency alleviates the need to add gasifier circulating solids make-up material during normal operation.

Related to scale-up of the disengager, the complex flow field inside the disengager made it difficult to develop a set of design equations that could confidently be used for significant scale-up. If a simple scale-up model which uses the linear velocity in the vessel is utilized, the size of the disengager needed for the commercial process is too large to be economically feasible. Thus, the first stage solids separation device was designed to use cyclonic action.

Erosion was the main concern when using cyclonic action for the first stage separation due to the abrasiveness of the gasification ash and the high solids loading. The design of the first stage device focused on addressing the erosion issues with a design that was scalable to commercial size. Cold flow modeling was performed to develop the design equations based on first principles.

The riser diameter was increased to have the same diameter as the mixing zone. This modification doubled the gas residence time and more than doubled the solids residence time. Increases in the gas and solids residence time resulted in a higher first pass carbon conversion. The increased carbon conversion resulted in a lower carbon content in the gasifier circulating solids, which then resulted in a higher solids capture efficiency since the solids separation devices have low collection efficiencies for carbon.

3.2.2.2 Performance Results of Gasifier Configuration Modifications

The gasifier modifications were commissioned and initially tested with PRB coal in August 2006. This test campaign demonstrated the most stable gasifier operations since gasification testing began, with significant improvements in solids collection efficiency, syngas heating value, and carbon conversion. Efficiency of the first stage of the gasifier solids separation unit improved significantly, increasing from less than 85 percent to greater than 99 percent. The higher carbon conversion to combustible syngas components increased the raw syngas lower heating value by about 20 percent compared to operation with the previous gasifier configuration.

Because the modifications were expected to affect the PCD particulate characteristics, these effects were evaluated as well. The cyclonic action of the improved gasifier solids collection had the potential to retain the largest particles while allowing smaller particles to pass through. Thus, the size distribution of the particulate was expected to be smaller,

which could cause a higher PCD pressure drop. In addition, better solids collection would reduce the total solids mass entering the PCD, which would result in a lower areal loading on the filter elements and potentially lower pressure drop. Testing demonstrated that the particle size distribution did indeed become significantly finer with MMDs in the range of about 6 to 12 microns compared to typical particle size MMD of 15 to 20 microns in previous test campaigns. The improved gasifier particulate collection efficiency resulted in an average PCD inlet mass rate that was about 30 percent less than seen in previous test campaigns. Overall, the gasifier modifications did not adversely affect PCD performance.

Table 3-1 shows the maximum and steady state particle sizes and minimum bulk density of the gasifier circulating solids and the average particle size and bulk density of PCD solids for the August 2006 operations (TC20) and all the previous PSDF gasification test campaigns which used PRB coal. As shown in the table, the solids particle sizes and densities decreased significantly following the gasifier configuration modifications. These changes in physical properties after the gasifier modification verified that the solids collection devices were more efficient in retaining smaller particles than in prior operation. The improved solids retention in the gasifier eliminated the need for occasional addition of relatively high density sand, and the solids density was therefore lower. Testing with high sodium lignite showed similar results.

Table 3-1. Gasification Ash Characteristics with PRB Operation before and after Gasifier Modifications.

		Gasifier Circulating Solids			PCD Solids	
		Maximum Particle Size (SMD), microns	Steady State Particle Size (SMD), microns	Minimum Bulk Density, lb/ft^3	Average Particle Size (SMD), microns	Average Bulk Density, lb/ft^3
Pre-TC20 PRB Test Campaigns	Average	213	175	79	11	21
	Minimum	156	140	75	8	15
	Maximum	300	230	84	19	28
TC20		140	98	55	6	15

Table 3-2 summarizes the performance comparison for high sodium lignite and PRB coals before and after the modifications. There was an improvement in all performance indices for both fuels.

Table 3-2. Gasifier Performance at Comparable Operating Conditions.

	High Sodium Lignite		PRB	
	Before Modifications	After Modifications	Before Modifications	After Modifications
Syngas Heating Value, Btu/scf	35-40	65-80	62-65	72-76
Carbon Conversion, %	83-87	96-98	94-96	97-99
Hot Gasification Efficiency, %	69-73	83-86	88-90	90-92
Cold Gasification Efficiency, %	50-54	54-56	52-60	60-64

3.2.2.3 Refractory Evaluation

When the gasifier configuration modifications were incorporated, several different types of refractory materials were installed for evaluation in the various sections of the gasifier based on operating conditions in these sections. Figure 3-2 is a simplified diagram of the gasifier (not an exact representation of the gasifier configuration) included to illustrate the locations of the different refractory types.

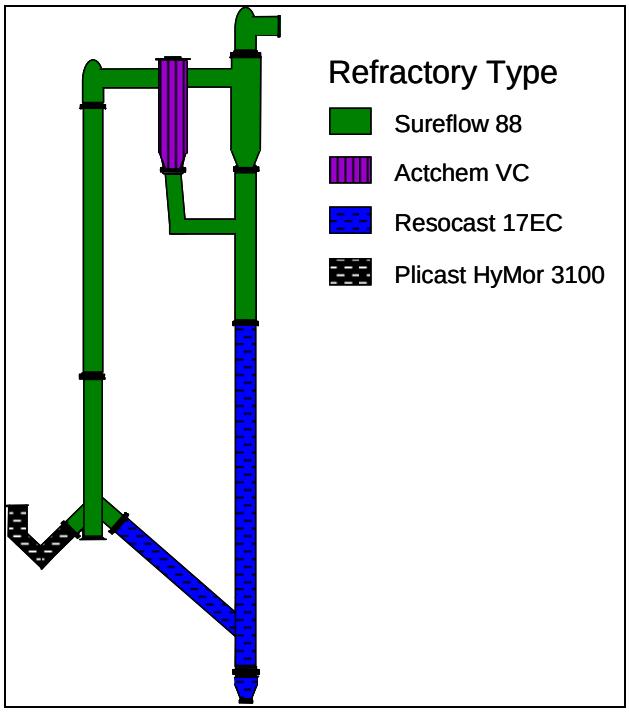

Figure 3-2. Gasifier Refractory Layout.

The modified gasifier refractory includes an insulating layer throughout using Resco RS-3A material, which was designed for reducing atmospheres. Prior to the modifications, the hot-face refractory used throughout the gasifier was Resco Resocast 17EC, which features an extended working life. The lower standpipe, which was not modified, contains the original Resocast 17EC material. The largest hot-face portion of the gasifier employs Resco Sureflow 88, an erosion resistant material designed for ease of mixing and replacement. Actchem VC from Vesuvius was utilized in the first solids separation device, and this material features a high corrosion resistance and high coefficient of thermal expansion, although it can be susceptible to cracking. The Plibrico Plicast Hymor 3100 material in the burner leg was selected for its low thermal expansion and thermal shock resistance.

Refractory Results. Detailed inspections were performed after test campaigns to evaluate the new and original refractory condition in the gasifier. The new refractory installed was in service for 2,500 hours and experienced 15 thermal cycles. (A full thermal cycle is a temperature increase from ambient temperature to 1,800°F combined with a decrease

in temperature below 200°F at a rate of 100°F/hr. A half thermal cycle designation is a temperature decrease below 1,000°F at a rate of 100°F/hr.) The original refractory in the lower standpipe that was not replaced during the gasifier configuration modifications was in service for 16,500 hours (including both combustion and gasification operation) and experienced over 80 thermal cycles.

In general, the new gasifier refractory was in excellent condition with two exceptions: the inlet of the first separation device and the seal leg. The original refractory was still in acceptable condition with only minor cracking observed. Figure 3-3 is a photograph taken of the lower standpipe refractory after 70 thermal cycles.

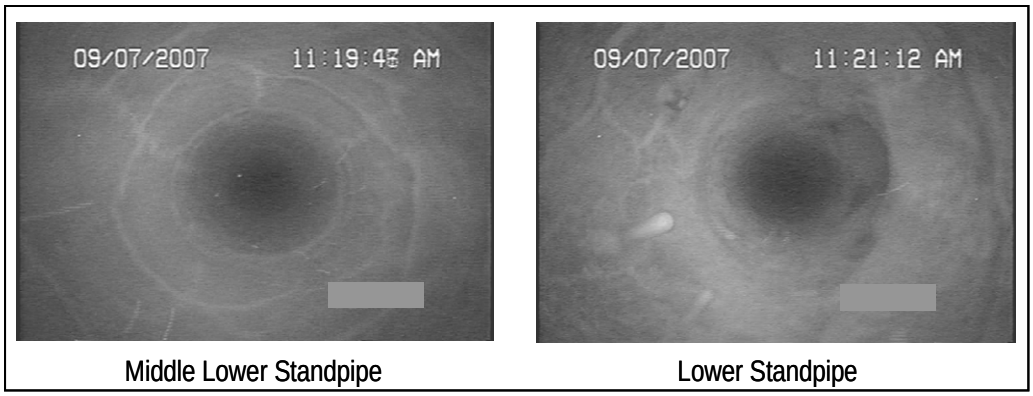

Figure 3-3. Lower Standpipe Refractory after 70 Thermal Cycles.

First Separation Device Inlet. Following the gasifier modifications, the first separation device contained Actchem 85 refractory. The Actchem 85 properties include a high erosion resistance and high coefficient of thermal expansion, which make it resistant to wear but susceptible to cracking. The Actchem 85 refractory life is heavily dependent on the number of thermal cycles and its rating is about 30 thermal cycles (a ten-year commercial life).

The first solids collection device appeared to be in good condition during visual inspections conducted following the first test run with the new refractory. However, there was some wear present. At the left of Figure 3-4 is a hairline crack seen from the entrance of the inspection nozzle that was approximately 1.5 inches deep. There was also a small area at the inlet with missing refractory, as shown on the right side of Figure 3-4.

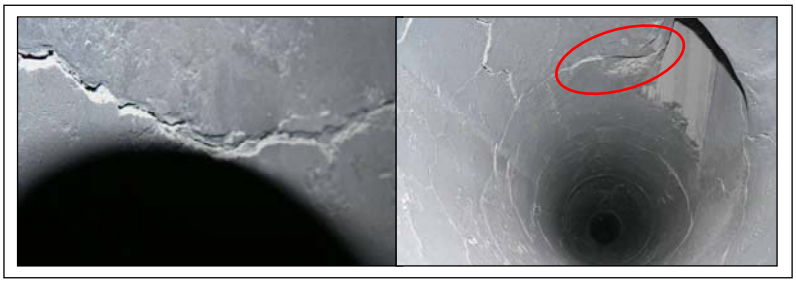

Figure 3-4. Inspection of Actchem 85VC Refractory following Initial Operation.

Degradation of the Actchem 85 refractory was noted during inspections after 11 thermal cycles, about half the thermal life (post-TC23). The refractory had been exposed to about 900 operating hours of solids circulation. Inspections showed that a portion of refractory was missing in the first stage solids separation inlet. Figure 3-5 shows examples of the cracking in this refractory.

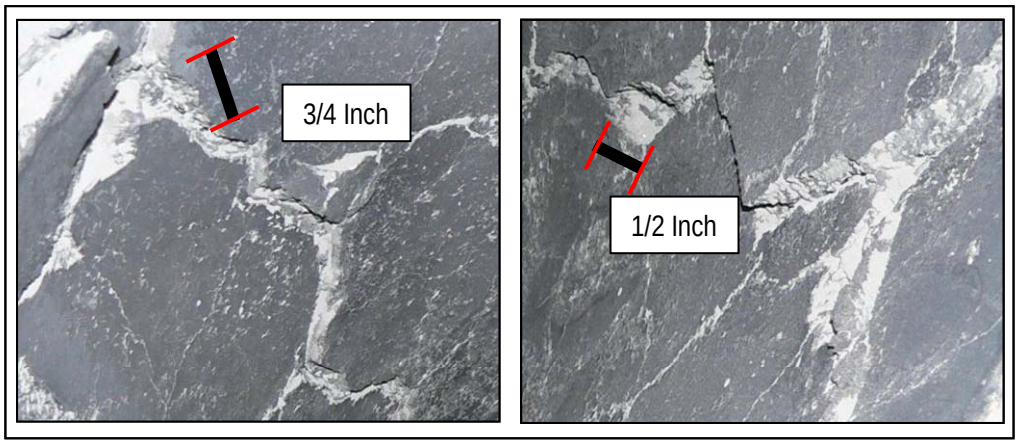

Figure 3-5. Cracking of Actchem 85VC Refractory after Eleven Thermal Cycles.

During the February 2008 test run, several pieces of separated refractory (the largest being about 12 inches long, 8 inches wide, and 2 inches thick) were found in the solids separation unit. The refractory condition at the inlet of the first solids separation device was of particular concern due to the large refractory pieces recovered and the previous loss of refractory in this area. At the conclusion of the February 2008 test run (TC24), the thermal cycles totaled 15. Inspection of the first stage solids collection revealed that the refractory loss at the inlet had progressed. Figure 3-6 shows the progression of refractory loss the inlet of the first solids separation device from post-TC23, post-TC24B, and post-TC24C inspections.

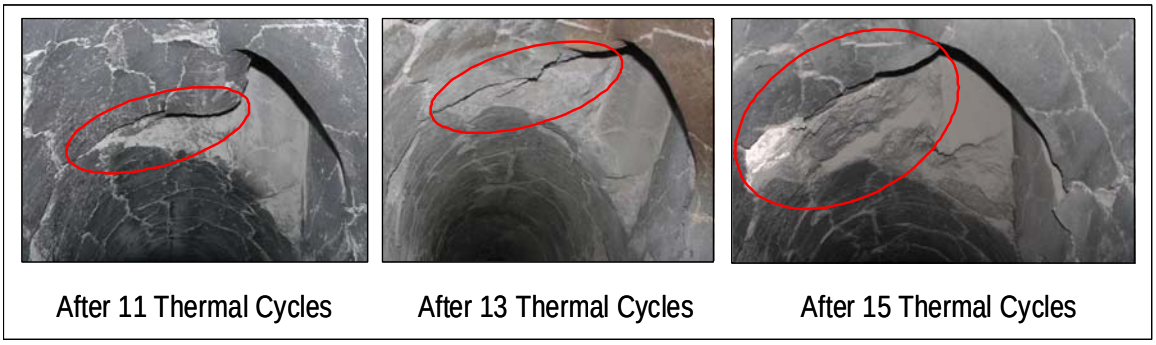

Figure 3-6. Refractory Loss at the Inlet of the First Solids Separation Device.

The extent of refractory damage made a complete replacement necessary. The Atchem 85VC was replaced with Resocast 88VC. Based on the operating experiencing at PSDF, the Atchem 85VC was not suitable in this application due to the high number of thermal cycles associated with multiple startups and shutdowns.

First Separation Device Inlet. Refractory obstructing the gasifier circulating flow path was found in the slant leg of the seal leg after the July 2008 run (TC25). Figure 3-7 is a photograph of the refractory and the location from which it was removed. The refractory piece shown in the figure was approximately 18 inches by 12 inches. Chemical analysis of a sample from the piece removed confirmed that it was Sureflow 88 refractory. The restricting refractory likely originated from the upper portion of the slant leg. Repairs were not necessary, and the obstructing refractory was removed.

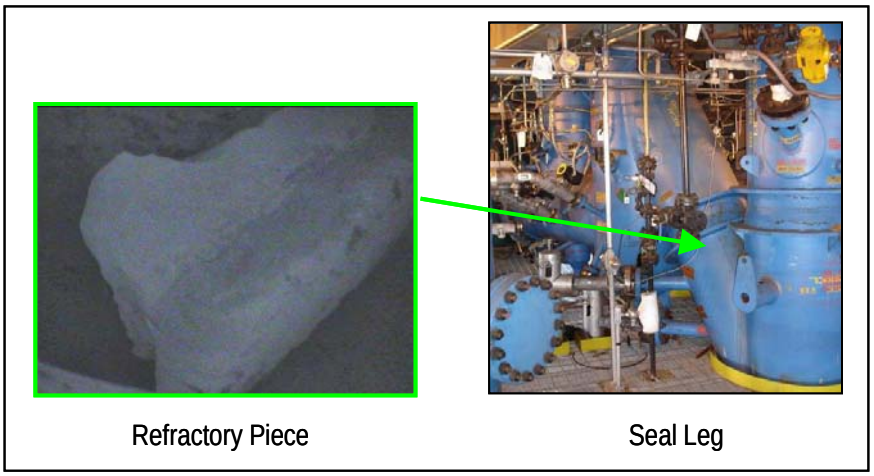

Figure 3-7. Gasifier Seal Leg Obstruction.

3.3 Gasifier Operations and Performance

The PSDF gasification process was operated with a variety of fuels. This section discusses operations and performance of the Transport Gasifier for each of the fuels

tested. Appendix A provides the properties of the coals tested at the PSDF in the last five years.

3.3.1 Lignite Operations

Lignite coals tested were from three mines: Freedom, Falkirk, and Red Hills. Lignite from the Freedom mine is also characterized by the differing sodium oxide content in the coal ash.

Falkirk. Lignite from the Falkirk mine in North Dakota was successfully operated in air-blown mode in April 2003 for 192 hours. The system was transitioned directly to lignite fire after heat up with the startup burner. Gasifier operations were stable despite coal feed issues related to insufficient drying of the coal mill system. The gasifier operated with high circulation rates and riser densities, resulting in high carbon conversions syngas heating values.

Freedom Low Sodium. Lignite from the Freedom mine in North Dakota with a relatively low sodium oxide content in the ash was successfully operated in air-blown and enriched air-blown mode in September 2003 and November 2006 for a total of 400 hours. The system was transitioned directly to lignite feed after heat up with startup burner. Gasifier operations were stable and the gasifier operated with high circulation rates and riser densities. The carbon conversions were high, and the syngas heating value was acceptable. There were no tars or oils in the syngas.

Freedom High Sodium. There has been significant testing over 790 hours with lignite from the Freedom mine in North Dakota that contains a high percentage of sodium oxide in the ash, as high as 10 percent. The high sodium lignite was first tested in September 2003 for 260 hours. The conditions were maintained from the previous operating period with low sodium lignite, which included oxygen-blown operation. During this operation at relatively higher temperatures, about 1700°F, agglomerations leading to deposits occurred within the first 15 hours of operation.

Testing later in air-blown mode at significantly lower temperatures, about 1,400°F prevented solids agglomeration and deposition. The reduced temperature did, however, negatively affect performance, causing a significant reduction in carbon conversion and syngas heating value. However, there were no tar or oils in the syngas while operating at the lower temperatures. The carbon conversion ranged from 80 to 85 percent.

Additional operations with high sodium lignite took place in August 2004 with a focus on evaluating ash chemistry at slightly higher operating temperatures with dolomite feed. The gasifier operated for 174 hours on PRB with dolomite before transitioning to lignite to eliminate a high concentration of silicon dioxide in the circulation solids, which is due to sand being used as the startup bed material. Recycled solids were added for startup bed material after a mid-run shutdown during PRB feed. Initial conditions were conservative and the gasifier temperature and coal feed rate were gradually increased. Muffle furnace tests conducted in the lab on loop seal samples early in the test campaign

showed no agglomerations, but agglomeration of samples taken during last the three days of operation did occur during muffle furnace testing. Carbon conversions remained lower than desired and it was determined that configuration changes to the gasifier would improve the gasifier performance when feeding high sodium lignite.

Tests Following Configuration Modifications. High sodium lignite testing resumed in November 2006 after the gasifier modifications were complete. One of the benefits of the gasifier modifications was improved gasifier performance using fuels with inherent ash chemistry issues such as high sodium lignite, which require lower gasifier operating temperatures. The increased residence time and improved gasifier solids collection efficiency offset the affect of lower operating temperatures on carbon conversions.

Initial tests were performed in air-blown mode with no sorbent addition. After the transition to high sodium lignite, agglomeration started in the lower mixing zone (LMZ) and progressed into the upper mixing zone (UMZ) which restricted solids circulation and necessitated a system shutdown after about 40 hours of operation. The agglomerated material was removed during the outage and the system was restarted. Several operating changes were made such as increasing the steam flow rate and adding dolomite to the gasifier. Unfortunately, agglomeration occurred again and the system was shut down after about 30 hours of high sodium lignite feed. Previous operation with the Freedom mine high sodium lignite in July 2004 (TC16) had shown that agglomerations could be prevented by operating with lower temperatures and by adding dolomite sorbent. However, the higher sodium content in the November 2006 (TC21) lignite proved to more readily form sodium silicates, leading to large agglomerations (TC21 averaged 8.2 weight percent Na_2O in the coal ash as compared to an average of 4.9 weight percent in TC16).

Additive Evaluation. Several sorbents including vermiculite, kaolin, kaolinite, dolomite, calcite, sand flour, and bauxite were evaluated in the laboratory as additives for testing with the high sodium lignite to address the agglomeration issues in the gasifier. Lab tests were performed using combinations of the sorbents with the lignite heated in a muffle furnace, and Energy Dispersive X-Ray analyses of the various reaction products were completed. The analyses showed that the sorbent effectiveness extent of sodium capture, based on, from greatest to least was: sand flour, kaolinite, kaolin, waste-derived kaolinite, Arkansas bauxite, vermiculite, and high-alumina bauxite. The finer kaolin and kaolinite showed a similar degree of consolidation as that with sand flour; however, the larger kaolin particles, of about 1,000 microns, did not show any signs of consolidation.

Initially, sand flour was selected as the additive for high sodium lignite testing since the amount of additive required is much lower than with kaolin or kaolinite due to the lower molecular weight. The existing sorbent feed system could not be used to feed the sand flour due to the small particle size. Thus, a slurry feed system was designed, procured, and installed to feed the sand flour.

In preparation for the August 2007 run (TC23), PSDF personnel consulted with researchers at the Energy and Environmental Research Center, a non-profit technology

branch of the University of North Dakota. Experiments at the University of North Dakota in a test unit at similar gasification conditions showed kaolin and kaolinite were successful in eliminating agglomeration in the gasifier. The suggested chemical process was the reaction of kaolin with sodium to form the sodium aluminum silicates with a higher melting point than the maximum gasifier operating temperature. However, due to the chemical properties of kaolin and kaolinite, a high kaolin- or kaolinite-to-sodium ratio is required. Since commissioning the slurry feed system was progressing slowly and feeding kaolin or kaolinite could be accomplished through existing systems, it was decided to first test kaolin since it was available locally. Kaolin is a mineral consisting mostly of equal amounts of silica and alumina.

The sorbent feed system, a lock hopper-based system with a volumetric feeder, was used to feed kaolin into the Transport Gasifier during high sodium lignite operation. The kaolin tested, shown in Figure 3-8, was a minus 14-mesh, CK-46 Meta-kaolin purchased from CE Minerals. Meta-kaolin is calcined kaoline clay with approximately 1.5 percent loss on ignition (LOI) and generally less than 1 percent quartz. The particle size distribution of the material is given in Figure 3-8. The kaolin feed rate varied from about 100 to 400 lb/hr.

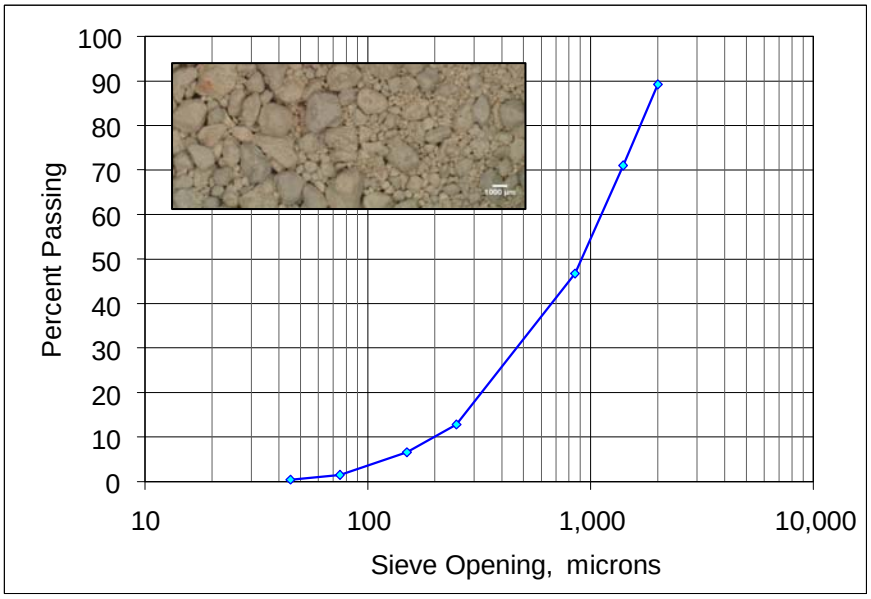

Figure 3-8. Kaolin Particle Size Distribution.

Testing in August 2007 confirmed that the kaolin was effective in preventing particle agglomeration and deposition in the gasifier. After start-up and initial operation with PRB coal, during which steady state operation was achieved and the start-up sand bed material was replaced with gasification ash, the gasifier feedstock was transitioned to high sodium lignite. Several parametric tests were performed during lignite operation to evaluate and optimize gasifier performance at various operating conditions. Gasifier operation was stable, achieving carbon conversions up to 97.6 percent and projected

syngas lower heating values from 125 to 140 Btu/SCF at the turbine inlet. However, fouling of the primary gas cooler caused a problematic reduction in heat transfer.

Red Hills High Moisture Lignite. High moisture lignite from the Red Hills Mine in Ackerman, Mississippi, was used as the fuel for two test campaigns, the first in March 2007 (TC22) and the second in July and August, 2008 (TC25). The system operated for about 1,285 hours in air-blown mode. Although gasification operation in March 2007 was successful, operation of the coal feed systems was problematic due to a high as-fed lignite moisture content. A fluid bed coal dryer was installed to reduce the moisture content of the Mississippi lignite to a sufficiently low content for reliable feeding to the gasifier.

The Transport Gasifier operated smoothly in the 2008 run over a range of conditions. The standpipe level was operated at the highest level to date and the aeration flows were reduced to the minimum levels operated to date. Recycle gas aeration requirements were minimal due to high flowability of the lignite ash. The gasifier carbon conversion was high, at over 97 percent for all conditions tested.

3.3.2 Subbituminous Coal Operations

The subbituminous coal extensively tested at the PSDF was a blend of coals from Southern PRB mines, including Jacobs Ranch, Black Thunder, North Antelope/Rochelle, and Antelope mines. The gasification process operated for 7,891 hours using PRB coal, with over 6,290 hours in air-blown and 1,600 hours in oxygen-blown mode. About 835 operating hours with PRB were achieved after the gasifier configuration modifications.

PRB was the coal used during most of the early gasification tests, and it was used to optimize gasifier parameters and hardware. Initial testing resulted in an uneven temperature profile due to lack of air distribution. Adding oxygen feed nozzles improved the temperature profile in later tests. Modifications made based on operating experience improved the operational stability, and the configuration modifications in 2006 significantly improved operations. During all testing of PRB, gasification yielded high carbon conversions and syngas heating values due to the high reactivity of this coal.

3.3.3 Bituminous Coal Operations

Early testing with bituminous coal from the Illinois Basin was conducted in October 2004 for 220 hours. This testing featured air for coal transport (instead of the typically used nitrogen) as well as feeding dolomite as a sorbent for sulfur capture. The steam flow was high (compared to operation with PRB coal) to control temperature in LMZ due to high carbon content in circulating solids. The gasifier temperatures were slightly higher (about 30 to 50°F) than PRB operations. Operations were stable, and the gasifier maintained good solids circulation rates and a stable temperature profile. However, the carbon conversion was low during bituminous coal testing (between 80.4 and

88.5 percent) due to the low coal reactivity and low solids collection efficiency before the gasifier configuration modifications.

Tests in February and March 2008 after the gasifier modifications with a more reactive bituminous coal from Utah was conducted for 237 hours in air-blown gasification mode. Gasifier operations were challenging due to a number of factors, such as particle agglomeration; a large percentage of oversize coal particles (greater than 1,180 microns); and lower overall gasifier solids collection efficiency due to degradation of refractory in the solids separation unit. The carbon conversion ranged from 75 to 95 percent, with the lower values attained during periods when the gasifier operating temperature was low due to limited solids circulation.

3.3.4 Operations Summary

Table 3-3 summarizes the operating parameters of the Transport Gasifier.

Table 3-3. Transport Gasifier Operations and Performance Summary after Configuration Modifications.

	Lignite			Subbituminous	Bituminous
	North Dakota	North Dakota	Mississippi	Wyoming	Utah
	Freedom Mine High Sodium	Freedom Mine Low Sodium	Red Hills Mine	Blend from Four PRB Mines	Sufco Mine
Operating Hours, Total	794	594	1,285	7,891	546
Oxygen-Blown Operating Hours	0	58	0	1,600	80
Maximum Gasifier Temperature, °F	1,510-1,690	1,710-1,800	1,620-1,820	1,700-1,820	1,840-1,920
Outlet Gasifier Temperature, °F	1,420-1,590	1,540-1,680	1,530-1,740	1,650-1,730	1,730-1,825
Gasifier Outlet Pressure, psig	130-220	170-210	120-260	160-240	170-205
Coal Feed Rate, lb/hr	2,080-4,640	3,300-5,400	2,640-4,880	3,500-5,340	1,140-3,770
Air Feed Rate, lb/hr	8,910-11,790	10,980-15,050	7,740-13,380	11,160-14,070	7,140-14,300
Steam Feed Rate, lb/hr	1,210-3,480	1,320-2,210	0-1,330	890-2,110	700-2,190
Recycle Gas Feed Rate, lb/hr	0-2,430	0-1,620	0-1,990	0	0-1,450
Maximum Carbon Conversion, percent	99	98	99	99	96

3.3.5 Parametric Test Results

A number of tests were performed to characterize operation and evaluate performance of the Transport Gasifier with different fuels after the configuration modifications. Parametric tests completed included variations in a number of operating parameters.

Table 3-4 summarizes the parametric tests performed and the main results. To obtain meaningful analyses, data were selected from steady state periods with other variables held nearly constant to focus on the variable of interest.

Table 3-4. Gasifier Parametric Tests.

Variable	Range	Results
Gasifier Outlet Temperature,	1,520–1,825°F	Carbon conversion increases as the temperature increases.
Standpipe Level	57– 302 inH_2O	Circulation rate increases as the standpipe level increases.
Coal Feed Rate	1,140–5,415 lb/hr	Syngas heating value increases with increasing coal feed rate.
Gasifier Outlet Pressure/ Riser Velocity	125–212 psig	Methane content increases with increasing pressure/reducing riser velocity.
Air Distribution	25–95 percent	The optimum percentage of air to the lower mixing zone is 35 percent. At this level, the temperature difference is about 100°F, which is optimum, and flow to the ash removal system is stable.
Transport Air	0-800 lb/hr	Syngas heating value increases when air is utilized for coal transport instead of nitrogen.
Recycle Gas Utilization	0-1,500 lb/hr	Syngas heating value increases when recycle gas is utilized.
Sorbent Addition	0–4.0 Ca/S molar ratio	Up to 35 percent removal achieved at Ca/S molar ratio of 4.0.
Steam-to-Coal Ratio	0.1–0.6 molar ratio	Increasing hydrogen-to-carbon monoxide ratio with increasing steam-to-coal ratio due to the water gas shift reaction. The lignite has higher hydrogen-to-carbon monoxide ratio at similar steam-to-coal ratios.
Fluidization Flow	Minimum to Maximum	Fluidization flow in seal leg and standpipe were minimized with no negative impact on the gasifier pressure differential profile or solids circulation rate.

Temperature Effect on Carbon Conversion. Figure 3-9 plots the carbon conversion as a function of temperature for the high and low sodium lignite, the high moisture lignite, the mix of PRB coals, and bituminous coal. At a given temperature, the carbon conversion was highest when using the high moisture lignite and lowest with the bituminous coal due to the relative reactivity of the fuels. Note that two data sets are shown for the high moisture lignite. Data collected from the TC22 test run show a lower carbon conversion and a greater dependency on temperature. The lower carbon conversion and greater temperature dependence (also seen with the bituminous coal) are related to lower solids collection efficiency that was caused by the loss of the refractory in the first solids separation device inlet.

The carbon conversion was excellent at over 97 percent for the low sodium lignite, PRB, and high moisture lignite over the range of temperatures tested. Additional testing is needed to improve the carbon conversion with bituminous coal. The operating

temperature was limited during bituminous coal operations due to material constraints with the second solids separation device.

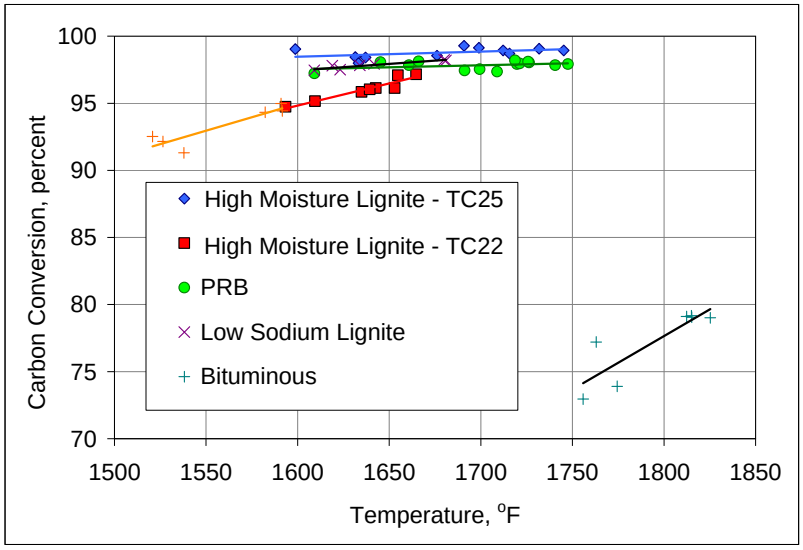

Figure 3-9. Carbon Conversion as a Function of Gasifier Outlet Temperature.

Standpipe Level Effect on Circulation Rate. Figure 3-10 shows the relative solids circulation rate as a function of standpipe level when using high sodium lignite, high moisture lignite, and PRB. The solids circulation rate had a positive linear correlation with standpipe level as expected for the fuels tested. The solids circulation rate was lowest at a given standpipe level for the high moisture lignite due to the low solids density of the high moisture lignite gasification ash.

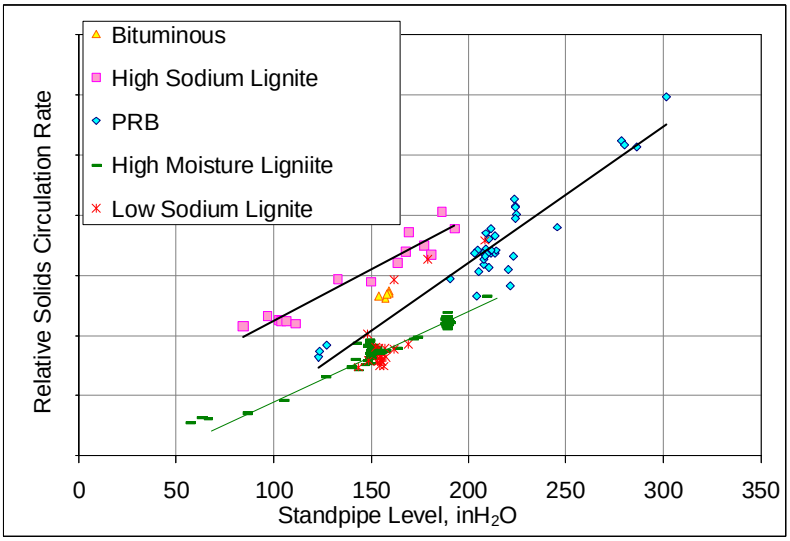

Figure 3-10. Solids Circulation Rate as a Function of Standpipe Level.

Coal Feed Rate Effect on Syngas Heating Value. Figure 3-11 is a plot of the raw wet syngas heating value versus the coal feed rate. There is a positive linear correlation for all fuels tested as seen in the figure. The higher coal feed rates produced higher syngas lower heating values (LHVs) because the testing is done at relatively constant nitrogen feed rates, so the syngas concentration of nitrogen is lower at higher coal feed rates.

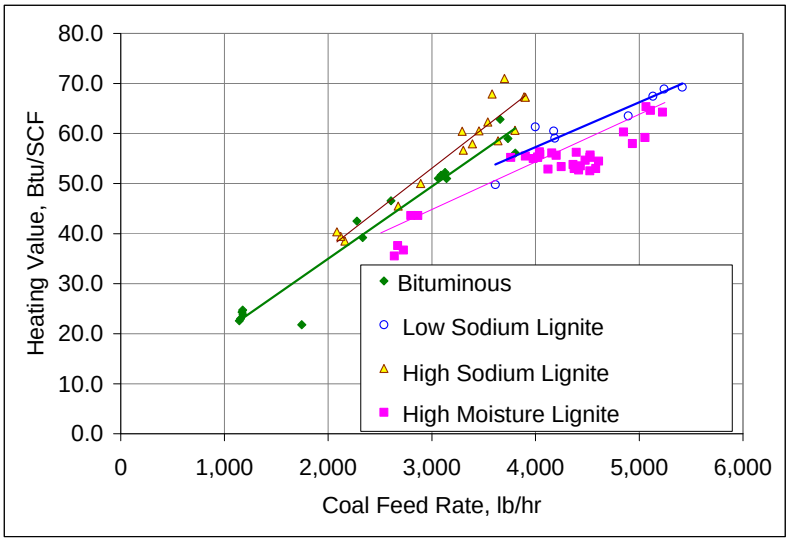

Figure 3-11. Syngas Heating Value as a Function of Coal Feed Rate.

Gasifier Pressure Effect on Methane Content. The gasifier pressure was varied to evaluate its effect on the methane content in the syngas. Figure 3-12 shows the effect of pressure on the syngas methane content, represented by a relative value, the methane factor. The methane content showed a positive correlation with gasifier pressure for all of the tests.

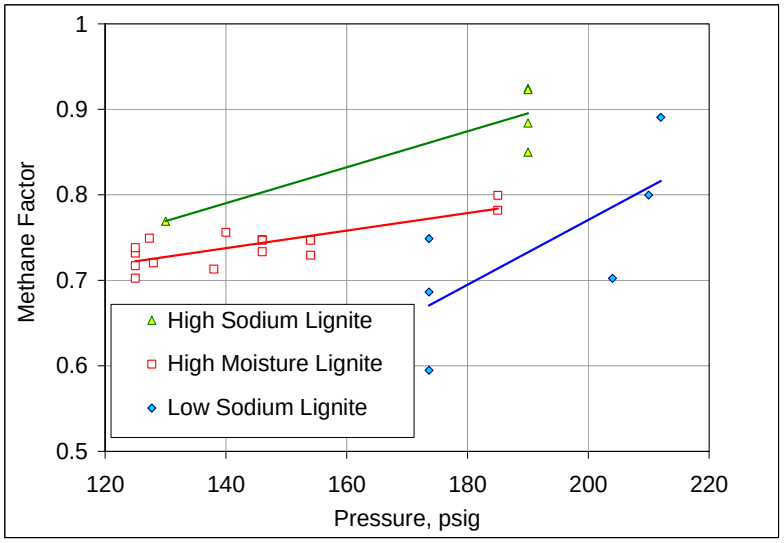

Figure 3-12. Syngas Methane Content as a Function of Pressure.

Air Distribution Effect on Temperature Profile. Another area of parametric testing assessed the effect of varying the air flow rate to the lower mixing zone (LMZ), specifically examining the effect of LMZ air flow rate on the gasifier temperature profile. Figure 3-13 shows the gasifier temperature differential between the maximum gasifier temperature and the LMZ temperature as a function of air flow rate to the LMZ (as a percentage of total air flow to the gasifier) for tests with PRB and high moisture lignite. For tests with PRB, as the air flow to the LMZ increased, less carbon was available for combustion in the LMZ. The temperature drop in the LMZ resulted in a larger temperature differential between the maximum gasifier temperature and the LMZ temperature. A similar phenomenon was observed in testing with high moisture lignite.

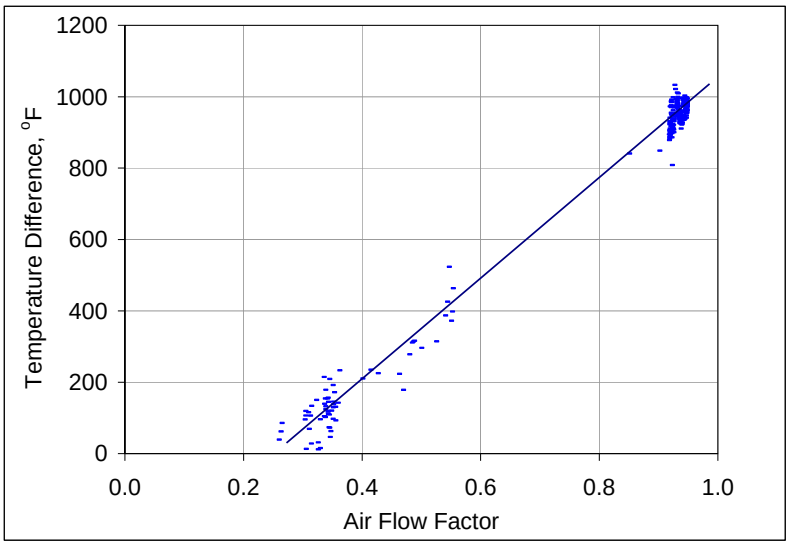

Figure 3-13. Temperature Difference as a Function of Air Flow to LMZ.

Effect of Using Transport Air on Syngas Heating Value. Figure 3-14 shows the instantaneous effect of using transport air to convey the low sodium lignite (instead of nitrogen) on the syngas heating value. After the transfer to transport air, the syngas heating value immediately increased and stabilized with an increase of 15 Btu/SCF, a 23 percent increase in the syngas heating value. The data shown below is for all low sodium lignite steady state periods and for coal feed rates ranging from 3,300 to 5,400 lb/hr.

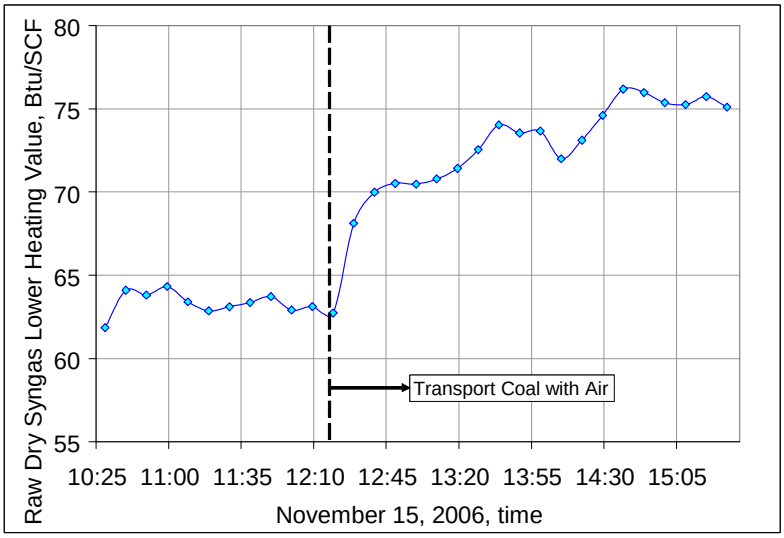

Figure 3-14. Effect of Transport Air on Syngas Lower Heating Value.

Effect of Using Recycled Syngas on Syngas Heating Value. Figure 3-15 shows the instantaneous effect on syngas heating value when utilizing recycle gas for aeration during testing of low sodium Freedom mine lignite. The plot shows the syngas heating value versus a relative time for two different time periods when the aeration gas was transitioned from nitrogen to recycle gas. The syngas heating value increased about 5 Btu/SCF, an 8 percent increase. Gasifier operation was stable, and the coal feed rate was constant during both time periods.

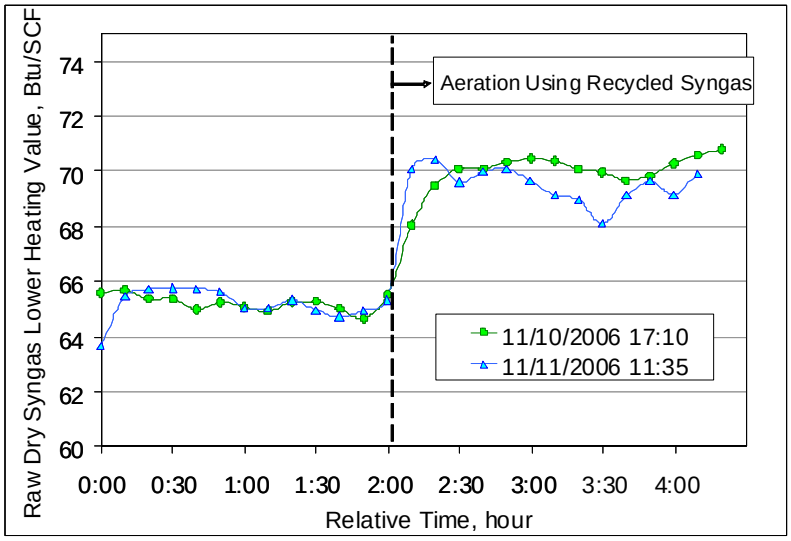

Figure 3-15. Effect of Recycle Gas Use for Gasifier Aeration on Syngas Heating Value.

Sulfur Removal as a Function of Ca/S Molar Ratio. Figure 3-16 shows the sulfur (in the form of H_2S and COS) removal as a function of calcium-to-sulfur molar ratio (Ca/S). Calcium

originated from the coal ash and from dolomite. The data used were from steady state periods with mixing zone temperatures between 1,620 and 1763°F, recycle gas in use for gasifier aeration, and the coal feed rate within a 250 lb/hr range. Without dolomite feed, at Ca/S values of about 1.5, sulfur removal averaged 13.2 percent, the result of sulfur reaction with the coal ash calcium. At higher Ca/S values reached with dolomite feed, the average sulfur removal was about 32 percent, with up to 35 percent removal achieved at the highest dolomite feed rate.

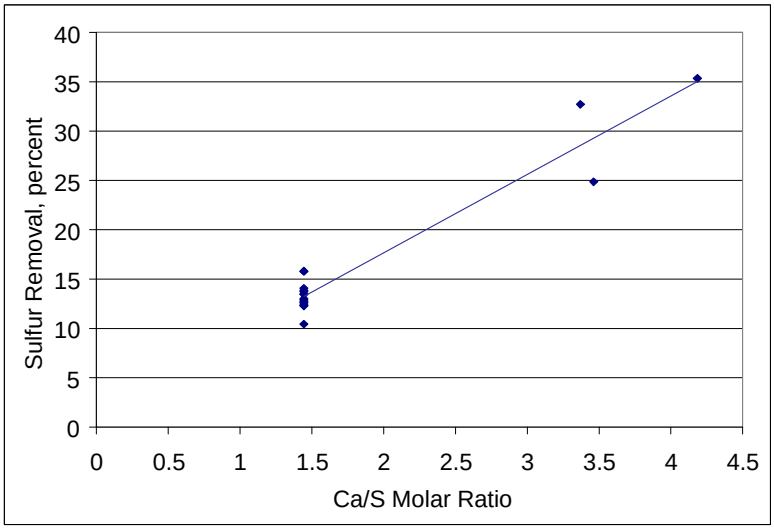

Figure 3-16. Sulfur Removal as a Function of Calcium-to-Sulfur Molar Ratio.

Effect of Steam-to-Coal Ratio on Syngas Hydrogen-to-Carbon Monoxide Ratio. Figure 3-17 plots the syngas hydrogen-to-carbon monoxide (H_2/CO) ratio and the steam-to-coal ratio. The positive correlation is due to the water gas shift reaction.

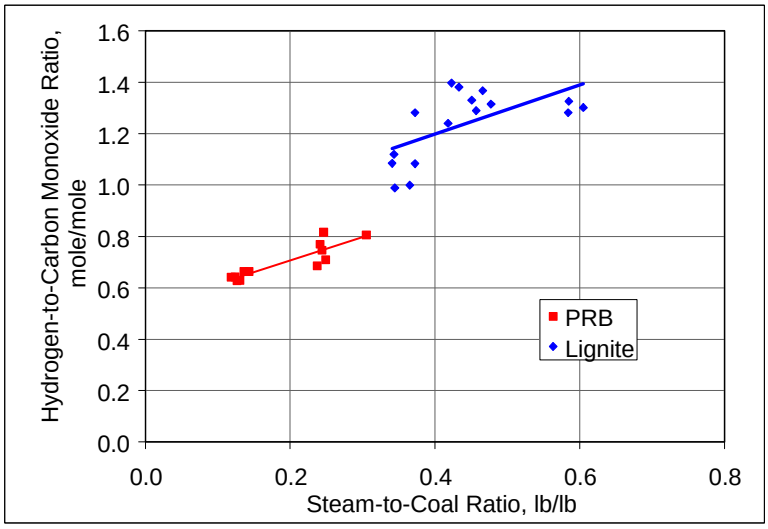

Figure 3-17. Syngas Hydrogen-to-Carbon Monoxide Ratio versus Steam-to-Coal Ratio.

4.0 PARTICULATE CONTROL DEVICE

During testing of the PSDF gasification process, all syngas filtration was performed with the Siemens Particulate Control Device (PCD). Although early operation of the PCD was problematic and characterized by low availability, system improvements over time enabled highly reliable operation of the filter vessel. Following these improvements, the PCD consistently demonstrated excellent collection efficiency during normal operation, reducing the gasification ash concentration from 10,000 to 30,000 ppmw at the PCD inlet to less than 0.1 ppmw at the outlet.

In the advancement of hot gas filtration technology, efforts focused primarily on:

- Testing filter element materials
- Identifying reliable failsafe designs
- Understanding and addressing ash bridging
- Enhancing instrumentation
- Defining the relationship between gasification ash characteristics and PCD design requirements

4.1 Equipment Description

PCD Filter Vessel. The PCD, located downstream of the primary gas cooler houses up to 91 candle-type filter elements. Figure 4-1 provides a photograph and a schematic drawing of the Siemens PCD.

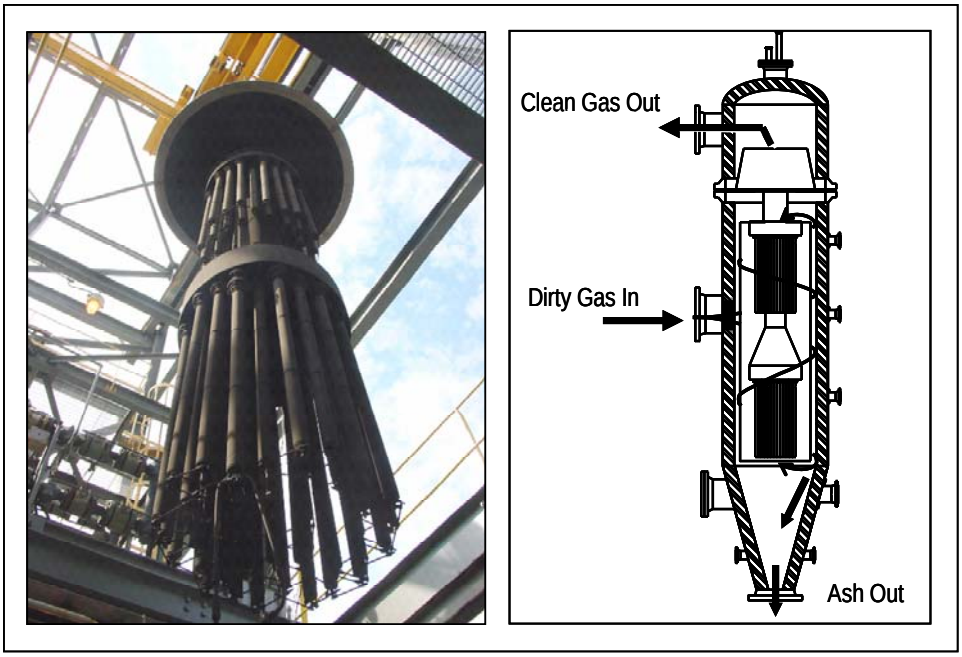

Figure 4-1. Siemens Particulate Control Device.

Syngas flows into the vessel through a tangential entrance, around a shroud, and through the filter elements into the plenums. High pressure gas is used to pulse clean the elements periodically to remove the accumulated gasification ash and control the pressure drop across the tube sheet. A failsafe device is located on the clean side of each element to prevent solids leakage in the event of filter element failure by acting as a back-up filter. Table 4-1 lists the nominal parameters for PCD operation during gasification testing.

Table 4-1. Nominal PCD Operating Parameters.

Dustcake Drag, inH_2O/(ft/min)/(lb/ft^2) (Normalized to Room Temperature)	100
Temperature, ^oF (^oC)	750 (400)
Pressure, psig (bar)	200 (14)
Face Velocity, ft/min (cm/s)	3.5 (1.8)
Baseline Pressure Drop, inH_2O (bar)	80 (0.2)
Pressure Drop Rise Rate, inH_2O/min (bar/min)	10 (0.025)
Pulse Cycle Time, min	5
Pulse Duration, sec	0.2
Pulse Pressure, psig (bar)	450 (31)
Inlet Loading, ppmw	10,000 to 30,000
Particle Mass Median Diameter, micron	10 to 15

Particulate Sampling and Monitoring. The PCD collection efficiency is quantified based on isokinetic sampling performed at the PCD inlet and outlet. The sampling systems, described in Section 7.6.1, are in-situ systems that give the most accurate possible solids concentrations. The outlet samples have generally indicated particulate concentrations below the sampling system lower limit of resolution (0.1 ppmw), equivalent to greater than 99.9999 percent collection efficiency. On-line particulate monitors (see Section 6.5) also indicate PCD collection performance.

Off-Line Filter Element and Failsafe Evaluation Facilities. On-site equipment for evaluating performance of filter elements and failsafes (at ambient conditions) before and after operating in the PCD includes:

- A flow test unit for measuring pressure drop using nitrogen
- A bubble tester for checking structural integrity using isopropyl alcohol
- A cold flow model of the PCD used for collection efficiency measurements. The cold flow model, shown in Figure 4-2, uses the same type of particulate sampling utilized for the PCD.

Figure 4-2. Cold Flow PCD Model.

4.2 Filter Element Testing

Element Types. During the early operation of the PSDF process in combustion mode, flue gas entered the filter vessel at around 1,400°F. The majority of the elements tested were made of ceramic materials because of their ability to withstand high temperatures. The ceramic elements include three categories: monolithic alumina, monolithic silicon carbide, and composite ceramic. Operation with ceramic elements was characterized by frequent element failure. During this early period of PSDF operation, the PCD failsafe devices used did not provide adequate protection from particulate leakage, and filter element breakage caused system shutdowns to replace the failed elements.

For gasification operation, economic and engineering studies determined that the commercially viable operating temperature for syngas filtration was about 750°F. This temperature is sufficiently low to allow the use of metal filter elements, which are less prone to brittle failure than ceramic ones. Several types of metal filter elements were tested in gasification mode. During the last five years of testing, elements installed in the PCD mainly consisted of Pall PSS sintered powder element made of iron aluminide (FEAL) material and Pall Dynalloy sintered fiber elements constructed of an HR-160 alloy. Several other metal elements and one type of ceramic element were tested to a lesser extent. With the metal elements, testing focused on evaluating collection efficiency and corrosion tendencies.

Filter Element Evaluation Procedures. Filter elements evaluated at the PSDF were subjected to a series of tests. Before a filter element was installed in the PCD, the element was tested by:

- Examining visually to detect manufacturing defects or damage and examining with a microscopic to quantify pore or fiber size
- Bubble testing in isopropyl alcohol to detect holes or cracks in the filter media or weld joints
- Flow testing to establish a clean baseline pressure drop for the element type
- Measuring particulate collection efficiency using a cold flow filter vessel

Following syngas exposure in the PCD, representative filter elements were removed for detailed inspection, which included:

- Optical microscope examinations
- Flow tests to check for changes in pressure drop characteristics
- Bubble tests to identify damage to the filter media or welds
- Examinations with a scanning electron microscope (SEM) coupled with energy dispersive X-ray (EDX) analysis for assessment of corrosion and ash plugging (in selected filter element sections)

4.2.1 Pall PSS Iron Aluminide Filter Elements

Because of their extremely high collection efficiency and expected corrosion resistance, the Pall PSS FEAL sintered powder elements were the most extensively tested of the element types. Several individual elements were tested repeatedly for accumulated exposures times up to 10,940 hours.

4.2.1.1 Pall PSS FEAL Corrosion Observations

The PSS elements continued to demonstrate very high collection efficiency, although corrosion of the elements became apparent after about 2,000 to 3,000 hours of syngas exposure. Figure 4-3 provides photomicrographs of the FEAL filter media for a range of accumulated syngas exposure time from 834 to 5,471 hours. The figure shows the merger of iron oxide spots into a continuous surface scale.

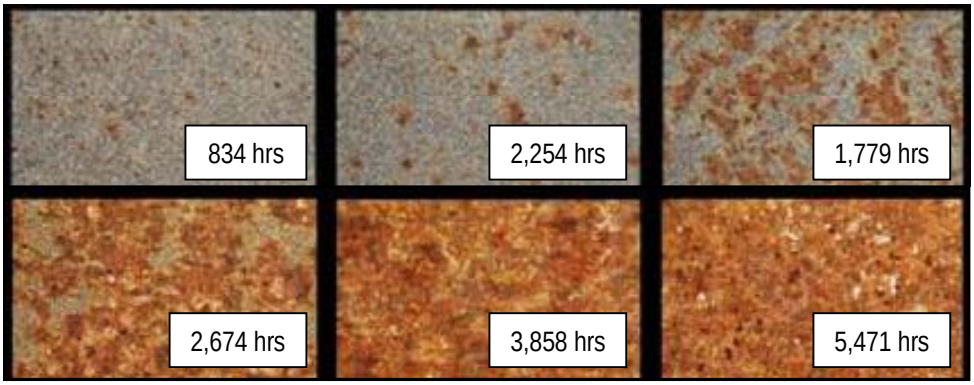

Figure 4-3. Micrographs of FEAL Filter Media Showing Progression of Iron Oxide Scale.

With accumulated syngas exposure in excess of about 6,000 hours, a black scale containing iron sulfide became visible. Figure 4-4, a photograph of PSS filter elements (which were pressure washed) arranged by syngas exposure time, shows the presence of the black scale progressing and dominating the filter media surface over time.

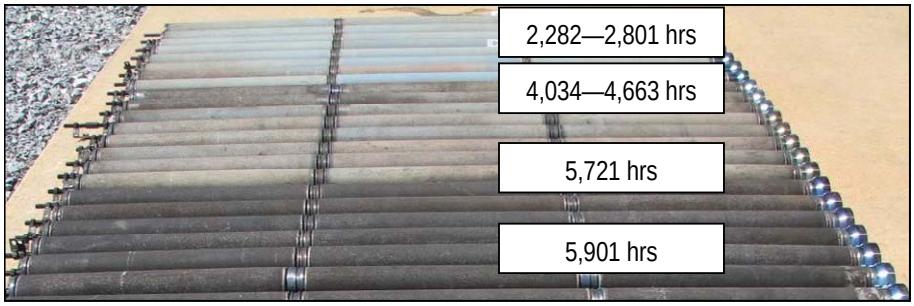

Figure 4-4. Cleaned FEAL Elements Arranged by Exposure Time.

Microscopic examination of the black colored elements revealed the presence of reddish-brown iron oxide in addition to the black scale. The iron oxide was generally present as borders around pitted areas, as shown in Figure 4-5. The filter media section shown in the figure was taken from an element which had accumulated 7,158 hours of syngas exposure.

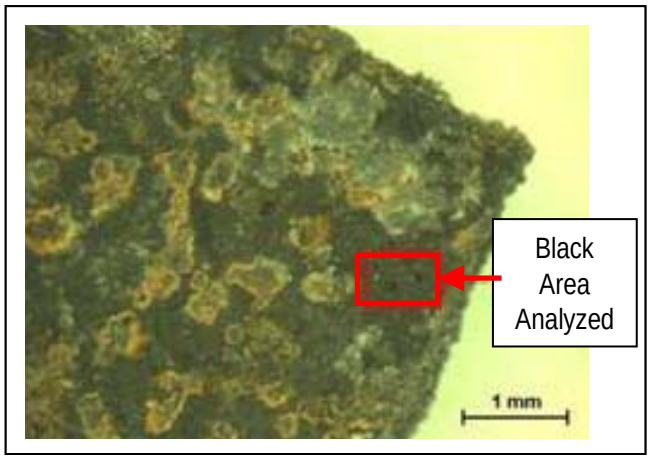

Figure 4-5. Photomicrograph of FEAL Filter Element Section Showing Pitted Areas with Iron Oxide Borders.

The EDX analysis of the region indicated in Figure 4-5 (provided in Figure 4-6) suggested the presence of iron sulfide along with bound ash components. The iron sulfide most likely formed through the reaction of the iron oxide scale with hydrogen sulfide in the syngas. Analysis of the reddish-brown borders confirmed that they were predominately iron oxide (Fe_2O_3). In the black areas, other iron oxides such as Fe_3O_4 and FeO, which are black in color, may have been present in addition to the iron sulfide (FeS).

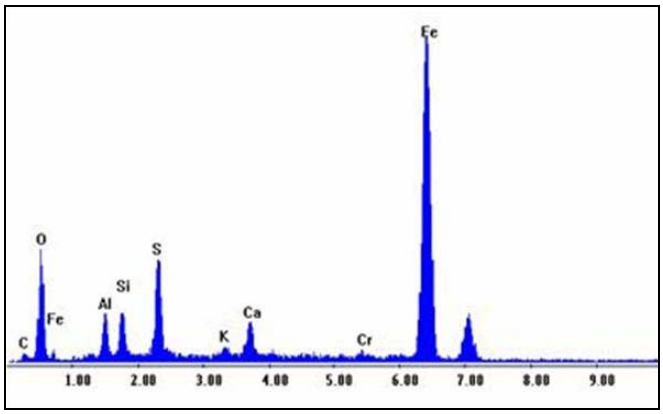

Figure 4-6. EDX Spectrum from Black Region Indicated in Figure 4-5.

Further examination of the PSS elements indicated a considerable degree of sulfidation and plugging in certain areas of filter element cross sections. Figure 4-7 shows an example of this where plugged areas near the outer diameter (OD) surface and open areas away from the OD surface can be seen in a filter cross section that was exposed for 7,158 hours to syngas.

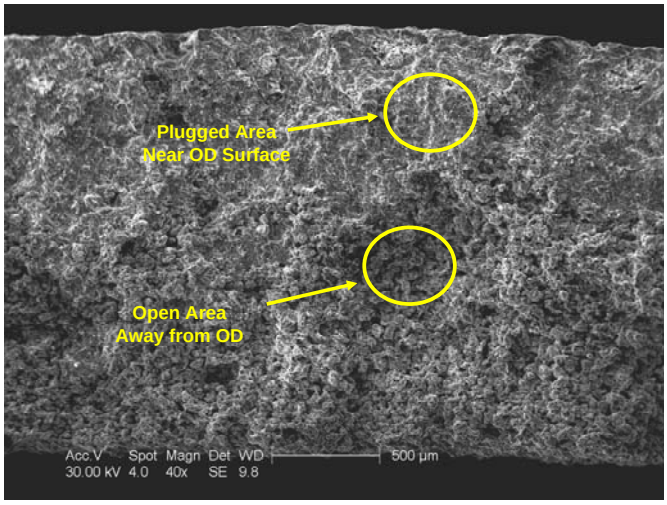

Figure 4-7. Photomicrograph of Plugged and Open Areas of FEAL Element.

Figure 4-8 provides EDX analyses of the plugged and open areas indicated in Figure 4-7. The significant presence of sulfur in the plugged area and the absence of sulfur in the open area suggest that sulfidation was responsible for the plugging. This same effect was observed in iron aluminide filter elements used at the Wabash River IGCC project (McKamey et al., 2002). However, it should be noted that the H_2S concentration in the syngas at the Wabash River facility was much higher than that at the PSDF because of higher sulfur feedstock. Both the PSDF and the Wabash River facility results confirm that sulfidation and plugging can occur in iron aluminide elements at temperatures of about 750 to 800°F.

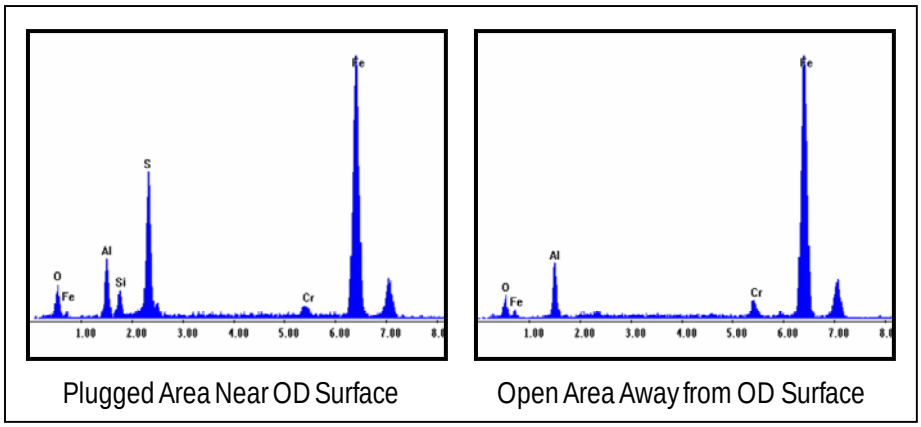

Figure 4-8. EDX Spectra from Plugged and Open Areas Indicated in Figure 4-7.

Corrosion Mechanism. During the manufacturing of Pall PSS FEAL filter elements, a pre-oxidation step forms a protective layer of alpha-alumina on the surface of the iron aluminide grains. If this layer is intact, it should prevent sulfidation and other forms of corrosion. However, compared to other alumina-forming alloys, the protective alumina layer on iron aluminide spalls more readily (Pint et al., 2001). Estimates of the expansion differential between the alumina and the underlying iron aluminide also show that cracking of the layer would be expected during startups when the filter element is heated from ambient temperature to 750°F. (More thermal cycling occurred at the PSDF due to the research nature of the project than would be expected at a commercial facility.)

Once the alumina layer is cracked, the iron in the underlying iron aluminide is susceptible to attack by H_2S, as well as other reactive gases such as steam. Steam attack should proceed more rapidly than attack by H_2S, since the partial pressure of steam in the PSDF syngas is two orders of magnitude higher than the partial pressure of H_2S. Moreover, steam is known to react very vigorously with finely divided iron. This may explain why the formation of iron oxide was observed on the PSDF filter elements as a precursor to the formation of iron sulfide.

Even though the steam attack is very rapid initially, it eventually forms an extensive layer of iron oxide that tends to be converted to iron sulfide because iron oxide reacts rapidly with H_2S at 750 to 800°F (Danielewski et al., 1982). The reaction rate increases with increasing temperature up to a point where the reaction product (FeS) becomes thermodynamically unstable. At a temperature of 750°F, both the thermodynamics and the kinetics are favorable for formation of FeS by the reaction of Fe_2O_3 with H_2S.

To summarize, a postulated mechanism of the iron aluminide corrosion is:

(1) The protective alumina layer is cracked by differential expansion during thermal cycles (startups, shutdowns, etc.)
(2) The underlying iron is attacked by steam to form iron oxide.
(3) Iron oxide is sulfidized to FeS by reaction with H_2S.

While the proposed mechanism has not been verified, each step of the mechanism is supported by observations at the PSDF and by published literature on iron aluminide behavior and sulfidation. The observed rate of corrosion with the PSS elements may be sufficiently low to allow a two-year life in commercial operation.

4.2.1.2 PSS Filter Element Performance

Collection Efficiency. Despite corrosion issues with the FEAL material, tensile strength and collection efficiency remained high for the PSS elements. Cold flow testing of a corroded, pitted PSS element with 7,700 syngas exposure hours showed that particulate penetration through the element was below the detection limit of 0.1 ppmw, which gave a collection efficiency greater than 99.9999 percent.

Element Breakage. The PSS elements were more prone to breakage than the fiber elements. During thermal upsets or build up of ash around the elements, breakage tended to occur in weld-affected areas due to the weakness of these areas and the difference in thermal expansion rates of the filter media and weld material. Some infrequent breakage occurred for unknown reasons. Overall, the failure rate was acceptably low.

Pressure Drop. The PSS elements showed an increase in pressure drop over time of syngas exposure. The pressure drop at fixed face velocity (3 ft/min) was measured on each of the filter elements both with the light residual dustcake and after pressure washing to remove all particulate. Figure 4-9 presents the data plotted as a function of gasification exposure hours for the PSS FEAL filter elements. Because all these elements were installed in the same test campaign, the data were not influenced by differences in dustcake drag or porosity that could bias the age comparison.

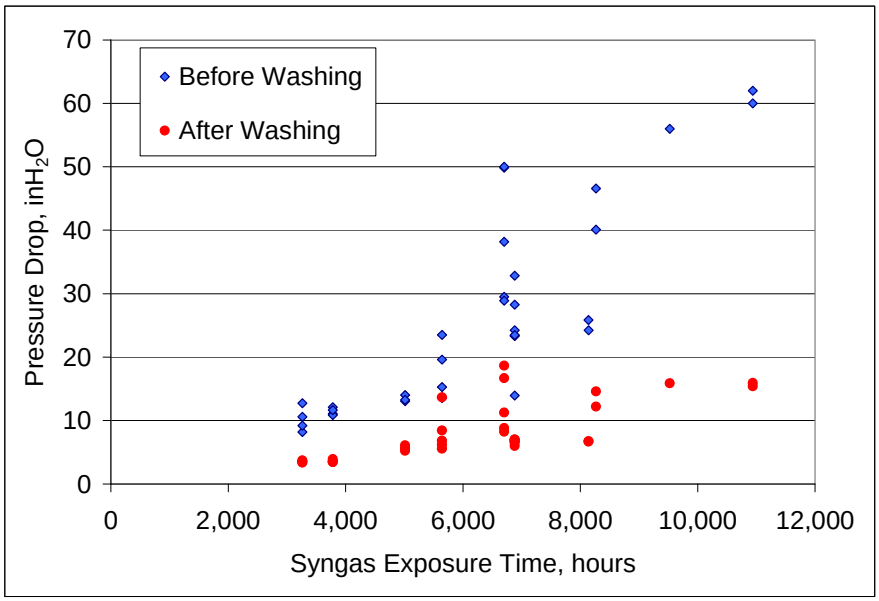

Figure 4-9. Pressure Drop versus Syngas Exposure Time for Pall PSS FEAL Elements.

Based on microscopic examination of the element surfaces and cross sections, the pressure washing effectively removed all of the gasification ash, and the ash had not penetrated into the elements. Therefore, the data for the washed elements in Figure 4-9 represents the effects of corrosion and sulfidation. As indicated in the figure, the rate of increase in pressure drop became distinctly more rapid at longer exposure times. Therefore, an interaction between the corrosion products and adherent dustcake appeared to accelerate the increase in pressure drop. Even at the higher baseline filter element pressure drops, the filter element pressure drops represent a small portion of the overall pressure drop with the gasification ash dustcake.

Overall Performance. Corrosion of the PSS elements caused an increase in pressure drop over syngas exposure time, with sharp increases noted after about 6,000 hours of exposure. However, the elements continued to demonstrate high collection efficiency and adequate strength, and the useful life of the elements could be reasonably considered to be greater than one year. The observed rate of element corrosion may be sufficiently low to allow a two-year life in commercial operation.

4.2.2 Dynalloy Filter Elements

Two types of Pall Dynalloy fiber filter elements were evaluated: coarse and fine fiber HR-160 alloys. Compared to sintered powder elements, the coarse fiber elements allow more particulate penetration (particularly when new or cleaned) although the collection efficiency is sufficient to meet turbine specifications. The fine fiber elements showed significantly higher collection efficiency, although corrosion was more of a concern with finer fibers.

4.2.2.1 Dynalloy HR-160 Corrosion Observations

Corrosion of the coarse fiber Dynalloy HR-160 was first observed in elements with over 2,500 syngas exposure hours. Figure 4-10 is a photomicrograph of a portion of a coarse fiber filter element showing corrosion with pits about 50 microns in size that appeared to be merging.

Figure 4-10. Coarse Fiber Dynalloy HR-160 Filter Media with 2,698 Syngas Exposure Hours.

Although the fine fiber Dynalloy elements were tested for less than 1,000 hours of operation, corrosion was also observed on these elements. Figure 4-11 shows discolored areas that indicate corrosion with small pits forming at the center of some areas.

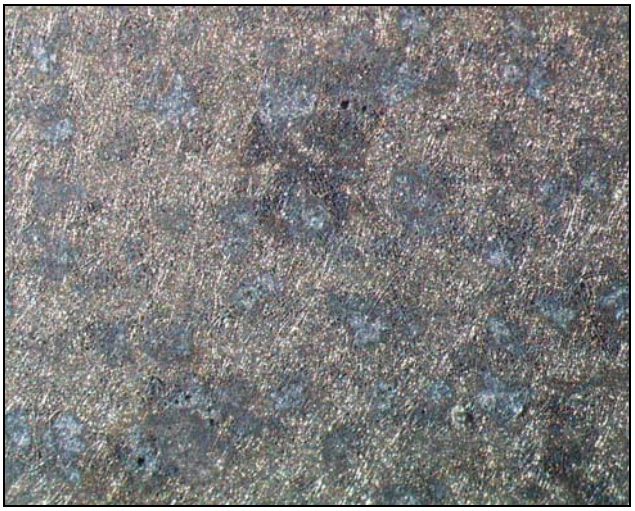

Figure 4-11. Fine Fiber HR-160 Filter Media with 979 Syngas Exposure Hours.

4.2.2.2 Dynalloy Filter Element Performance

Collection Efficiency. Table 4-2 provides cold flow model measurements of collection efficiency for the coarse and fine fiber Dynalloy HR-160 elements. While the collection efficiency of the Dynalloy elements was not as high as the Pall PSS elements, testing showed that seasoning of the Dynalloy elements through syngas exposure with gasification ash improved their performance.

Table 4-2. Collection Efficiency Measurements for Dynalloy Elements.

Element Type and Condition	Collection Efficiency, %	Particulate Penetration, %
Coarse Fiber Dynalloy New	99.9951	0.0049
Coarse Fiber Dynalloy Exposed 416 Hours	99.9998	0.0002
Coarse Fiber Dynalloy Exposed 725 Hours	>99.9999	<0.0001
Fine Fiber Dynalloy New	99.9997	0.0003

Pressure Drop. Figure 4-12 and Figure 4-13, respectively, show the pressure drop measured at a fixed face velocity (3 ft/min) versus exposure time for coarse fiber and for fine fiber Dynalloy elements. The plots indicated that the pressure drop before washing of the elements increased with time. However, since the dustcakes present on the elements prior to washing were collected from different test campaigns (using different coal types and operating conditions), the data could be biased by differences in dustcake flow resistance.

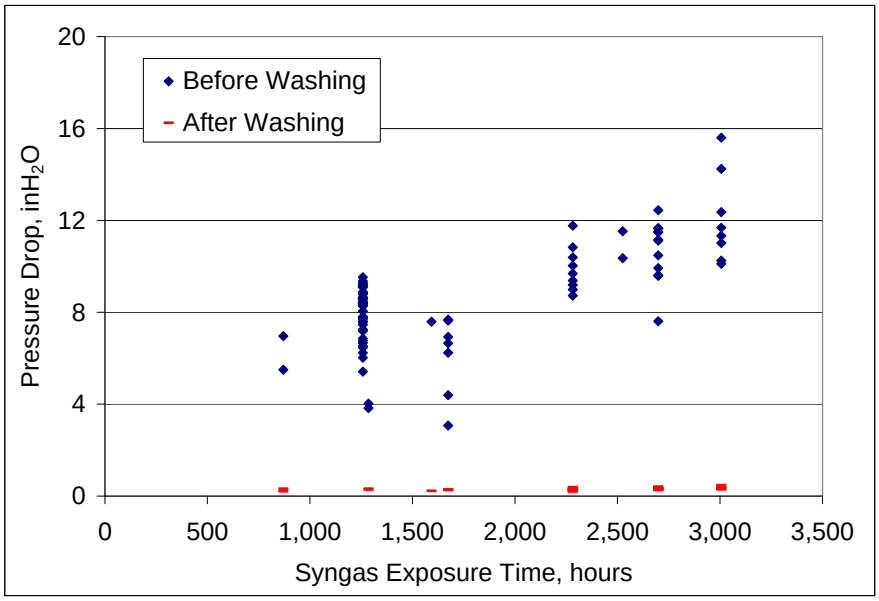

Figure 4-12. Pressure Drop versus Syngas Exposure Time for Coarse Fiber Dynalloy Elements.

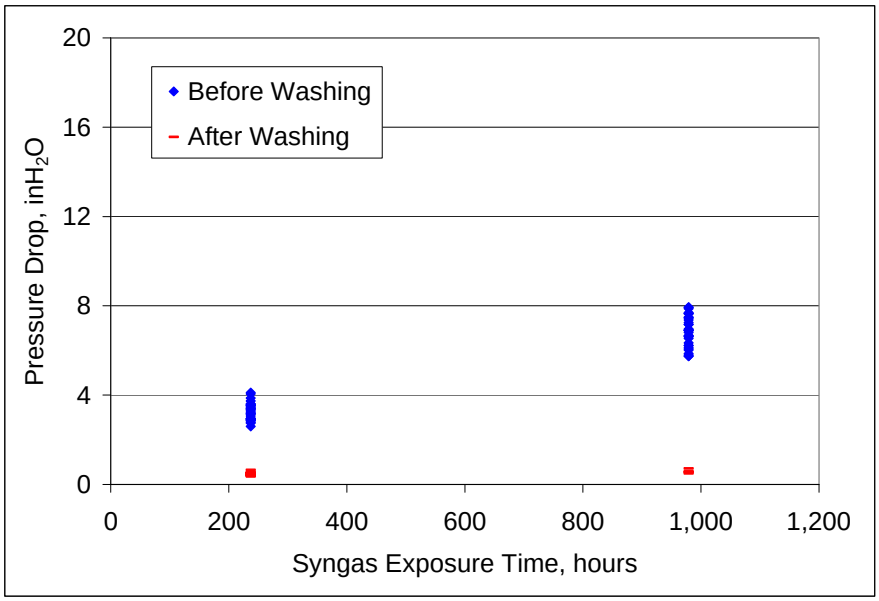

Figure 4-13. Pressure Drop versus Syngas Exposure Time for Fine Fiber Dynalloy Elements.

Overall Performance. Throughout testing, all Dynalloy HR-160 elements remained intact. While the collection efficiency of the Dynalloy elements was not as high as the Pall PSS elements, it is high enough to meet turbine specifications. Testing showed that seasoning of the Dynalloy elements through syngas exposure with gasification ash improved their performance. Corrosion of the coarse fiber elements began after about 2,500 hours of syngas exposure, and corrosion of the fine fiber elements was observed after about 1,000 hours of exposure. Further testing is needed to determine the useful lifetime of the Dynalloy HR-160 elements.

4.2.3 Fecralloy Filter Elements

Fecralloy fiber elements manufactured by Porvair were tested and exposed to syngas for 481 hours. No positive signs of corrosion were found on the elements. However, coupons made of the Fecralloy media that were exposed for 2,281 hours showed significant corrosion. Inspection of the coupons after cleaning showed that corrosion had completely penetrated through the fibers. EDX analysis confirmed that the primary corrosion product formed on the coupons was iron oxide, but further research is needed to determine the corrosion mechanism.

4.2.4 Titanium Filter Elements

Titanium sintered powder filter elements from Graver Technologies were tested for 1,342 hours of syngas exposure. These elements were constructed of a low-grade 99 percent purity material. During the test campaign, a coal feeder stoppage resulted in oxygen entering the PCD. At that time, a PCD pressure indicator showed a pressure swing of almost 9 psi in 3 seconds, and filter element thermocouples reached over 1,200°F momentarily, which tripped all air flow to the gasifier due to safety interlocks.

Inspection of the elements showed that the titanium elements were severely damaged, and a failsafe downstream of one of the titanium elements was destroyed and its media was expanded. Because the other elements installed (all Pall PSS FEAL) were undamaged, the reaction of the titanium elements with oxygen had apparently caused the pressure fluctuation.

Further inspection of the titanium filter elements after cleaning showed a white inner layer fused to the surface of the filter element which could not be removed. The bonded white inner layer was covered with a very thin layer of black ash. There was also an extremely thin black layer under the bonded white layer. The underlying black layer appeared to be some reaction product formed from the titanium. These observations suggested that some sort of bonding and/or reaction took place at the surface of the titanium elements, rendering them impermeable. A section of one of these elements is shown in Figure 4-14.

Figure 4-14. Section of Damaged Titanium Filter Element.

In light of the reactivity of the titanium elements indicated by this operating experience, further testing of this element type was not pursued.

4.2.5 Silicon Carbide Filter Elements

Three 2-meter silicon carbide 10-20 elements supplied by Schumacher/Pall were tested for 342 hours of syngas exposure. This type of element was the best performer of the ceramics used in combustion operation at the PSDF. Performance of the elements during this test campaign was unremarkable, although one element broke, apparently during removal following the testing. The crack was located at the element neck between the mounting flange and the main body of the element. Use of a filter neck gasket would likely have prevented the crack. While the ceramic elements could be a viable option due to their corrosion resistance, further testing was not considered beneficial.

4.3 Failsafe Testing

Since failsafes are necessary for reliable PCD operation, testing and development of failsafes became a major focus of research.

Failsafe Development Program. Improvements in failsafe operation were critical for the advancement of PCD technology, since the failsafes originally supplied with the PCD vessel did not function adequately to prevent significant particulate penetration following filter element failure. The failsafe test program included failsafe design as well as evaluation of various failsafes in the cold flow model and in simulated element failure modes under actual PCD operating conditions.

Failsafe Evaluation Procedures. The steps for failsafe evaluation include:

- Flow testing of the failsafe using nitrogen at ambient conditions to determine the pressure drop across the failsafe
- Measuring collection efficiency in the cold flow model
- Installing in the PCD for exposure to syngas at operating conditions to evaluate material compatibility with syngas and structural durability under backpulsing
- On-line testing in the PCD in simulated filter element failure conditions

4.3.1 On-line Failsafe Testing Methods

Three different types of filter element failures that produce small, moderate, or large particulate leaks have been simulated at the PSDF. Particulate sampling at the PCD outlet indicated how well the failsafe performed.

Simulation of Small Particulate Leak. To simulate a small particulate leak (e.g., a pinhole in a filter element), a low ash concentration of approximately 300 ppmw (in nitrogen gas) was injected into the clean side of a filter element to the failsafe. The gasification ash was injected from a fluid bed feeder into the clean side of the filter element through a solids injection line. The pressure drop across the filter and failsafe device was monitored to determine how the failsafe responded to the solids injection.

Simulation of Moderate Particulate Leak. For the moderate particulate leak simulation, unfiltered syngas with an ash concentration of approximately 5,000 ppmw was injected into the filter element. This setup used a bypass line to route the unfiltered syngas out of the PCD and into the clean side of the filter element. The dirty syngas flow rate was determined by a Venturi measurement, and pressure drop was monitored by the same technique used with the simulation of the small particulate leak.

Simulation of Large Particulate Leak. Two separate procedures for simulating a large particulate leak were used. The first procedure used a double-burst disk arrangement to introduce particulate flow to the failsafe. The burst disk device was installed below the failsafe onto the tubesheet of the PCD. The failsafe was exposed to particulate laden syngas by bursting the disks with high pressure nitrogen. The solids concentration for this test was equivalent to the inlet loading of the PCD. Although results were achieved with this system, it was difficult to prevent unplanned opening of the burst disks.

Because the burst disk method was unreliable, a different design that was simpler and easier to control was implemented. The new design was a direct injection system that

consisted of a metal pipe, flexible metal hose, and a specially designed ball valve installed inside the filter vessel through a nozzle. The valve actuator was located on the outside of the PCD vessel, and when opened allowed unfiltered syngas to flow through the flexible hose and into the metal pipe that contained the failsafe device.

4.3.2 Failsafes Tested

Several different types of failsafes have been used and tested at the PSDF, including:

- PSDF-designed metal fiber failsafe
- Pall FEAL sintered powder fuse
- Pall Dynalloy HR-160 metal fiber fuse
- CeraMem ceramic honeycomb failsafe
- Specific Surface ceramic honeycomb failsafe

4.3.2.1 PSDF-Designed Failsafe

The PSDF-designed failsafes were constructed of different types of metal fiber media supplied by Pall Corporation. The design incorporated a metal platform for collection of particulate to aid in preventing cleaning of the failsafe during backpulsing, and the failsafes were installed above the filter elements.

PSDF-designed failsafes with Haynes 188 and Haynes 230 media have accumulated over 8,120 hours and 9,435 hours respectively and have shown no signs of degradation. The HR-160 media has retained its integrity but has shown corrosion. Other media materials used with the PSDF-design were retired due to filter media flaws and cracking near welds.

4.3.2.2 Pall FEAL Fuse

The FEAL fuse is a commercially available product from Pall Corporation that fits inside the filter elements. Because this failsafe is welded in, it eliminates the need of failsafe gaskets and extra space above the filter elements.

Although the fuse design is commercially desirable, the FEAL material showed some problems. As with the FEAL filter elements, corrosion of the FEAL fuses was apparent. Additionally, separation of the fuses (by weld failure) from the elements was a significant concern. On several occasions, fuses were discovered following test campaigns completely separated from the filter elements. Fuses also tended to break off during filter element removal, despite the significant care taken by inspection personnel. The problem was apparently related to the difficulty of welding the FEAL material (the FEAL media makes up the entire structure of the fuses and of the filter elements) to the element flange.

4.3.2.3 Pall Dynalloy HR-160 Fuse

Since the fuse design is superior to externally mounted failsafes, testing of the fuse design was continued with a sturdier material: Pall Dynalloy HR-160 material. For

PSDF testing, the filter media was inverted (in relation to the HR-160 filter element media) to promote media plugging. The coarse mesh support media is on the outer failsafe surface, and the fine filter media is on the inner surface. This material has been tested for about 2,000 hours and has shown no signs of corrosion.

4.3.2.4 CeraMem Ceramic Failsafe

The CeraMem ceramic failsafes were constructed of re-crystallized silicon carbide in a honeycomb configuration for high surface area and low flow resistance. Compared to the metal failsafes, the ceramic failsafes can handle higher temperatures, are less susceptible to corrosion, and contain a larger filtration area. They are, however, more susceptible to damage from thermal shock and mechanical loads.

Following the first on-line testing of the CeraMem failsafe, the packing design was improved, which improved the failsafe performance. The failsafe then demonstrated very high collection efficiency and showed no signs of degradation.

4.3.2.5 Specific Surface Ceramic Failsafe

Like the CeraMem failsafe, the Specific Surface failsafe was made of a re-crystallized silicon carbide material in a honeycomb configuration. During normal failsafe operation of syngas exposure for 360 hours, the Specific Surface failsafe cracked, probably due to thermal and mechanical stresses during backpulse operation. A Specific Surface failsafe was also found broken following an on-line failsafe test. Design improvements are needed for acceptable operation of this failsafe.

4.3.3 Failsafe Test Results

Table 4-3 provides results of failsafe collection efficiency tests using the cold flow model, and Table 4-4 lists the results of the various on-line failsafe tests. Because of the effect of temperature and syngas constituents on particulate properties, the collection efficiencies measured in the PCD cold flow model may not match those in the actual PCD. Nevertheless, the magnitude of the differences measured in the cold flow unit are large enough to conclude that the Pall iron aluminide sintered powder fuse and the CeraMem ceramic honeycomb failsafe have better particulate collection efficiencies than do the Pall Dynalloy metal fiber failsafes during the initial plugging period.

Table 4-3. Cold Flow Model Failsafe Test Results.

Failsafe Type	Collection Efficiency, %	Particulate Penetration, %
PSDF-Design	99.9680	0.0320
Pall FEAL Fuse	99.9998	0.0002
Pall HR-160 Fuse	99.9980	0.0020
CeraMem	99.9992	0.0008

Table 4-4. On-Line Failsafe Test Results.

Failsafe Type	Leak Simulation Size	PCD Outlet Concentration, ppmw	Ash Injection Duration, hours
PSDF-Design	Low	< 0.1	2
	Moderate	0.16	2
	Moderate	0.18	27
	Moderate	< 0.1	48
Pall FEAL Fuse	Low	0.33	2
	Moderate	0.15	2
	Moderate	< 0.1	25
	Moderate	< 0.1	49
	Moderate	< 0.1	1
Pall HR-160 Fuse	High	0.45	1
	High	0.30	1
	High	< 0.1	26
Specific Surface	Low	0.45	2
CeraMem	Low	0.46	2
	Moderate	3.34	1
	Moderate	< 0.1	4
	Moderate	0.17	4
	High	< 0.1	7

All of the failsafes (with the exception of the Specific Surface failsafe) performed satisfactorily. The elevated particle penetration only occurred during the initial plugging process for a short time period. The plugging time depends on the type of failsafe design, its porous media structure, and particulate concentration. After the failsafe plugged, the overall particulate concentration in the PCD outlet stream usually remained below the sampling system lower detection limit. Even in the initial plugging period, the particulate collection efficiencies were high enough to meet particulate concentration limits specified by gas turbine manufacturers.

4.4 Gasification Ash Bridging

Ash bridging between the filter elements of the bottom plenum was a frequent problem during early gasification operation. The bridging caused high PCD pressure drop and excess strain on the filter elements. After gasifier operation was improved by equipment modifications and operating procedures, bridging became much less common. However, some instances of bridging occurred over the last few years of gasification test campaigns. The most likely causes of bridging were identified, and on-line removal of bridging by combustion was successfully completed. Filter element instrumentation enhancements, described in Section 4.4.2, were implemented for prevention and detection of bridging.

4.4.1 Causes of Bridging

The main causes of bridging identified were:

- Inter-plenum ash re-entrainment resulting from the tiered design of the Siemens PCD
- Insufficient backpulse intensity
- Overfilling the PCD hopper

Gasification Ash Re-Entrainment. The tiered Siemens PCD design apparently promotes re-entrainment of ash following backpulsing, particularly re-entrainment of ash onto the bottom plenum filters following the top plenum backpulse cleaning. The effect of re-entrainment of ash on the bottom plenum elements was apparent by the accelerated pressure drop increase across the PCD tube sheet immediately following a backpulse cycle. This effect does not normally interfere with operation, but may make the bottom plenum more prone to bridging following upset conditions.

Insufficient Backpulse Intensity. While optimizing backpulse parameters, one goal was to reduce backpulse pressure and frequency to the lowest levels needed for reliable cleaning. To that end, the backpulse pressure was lowered from the normal pressure of about two times the gasification system pressure (about 250 psi above system pressure, or 250 psid) down to 150 psid. The frequency was changed for the normal 5 minutes to 10 and then to 20 minutes. After two days of operation at these settings, bridging began to occur.

Overfilling PCD Hopper. Although careful attention was given to the PCD ash level, overfilling could occasionally occur undetected and lead to bridging. Additional thermocouples added to the PCD hopper (refer to Section 4.4.2.3) proved useful in early detection of ash overfilling.

4.4.2 Instrumentation Added to Address Bridging

4.4.2.1 Filter Element Thermocouples

Operational experience showed that bridging on the filter elements caused a noticeable change in temperature indications from filter element thermocouples. The number of filter element thermocouples (Type K bare-wire thermocouples) used was increased, and they were staged at different levels on the elements to give information about bridging growth. Figure 4-15 shows an installed filter element thermocouple.

Figure 4-15. Filter Element Thermocouple.

When covered by gasification bridging, filter element thermocouples tended to become unresponsive to backpulsing, and, relative to uncovered thermocouples, indicated a slight time lag and higher temperatures. Figure 4-16 shows a plot of responses from thermocouples, both covered and uncovered by bridged ash, during a test campaign when bridging occurred.

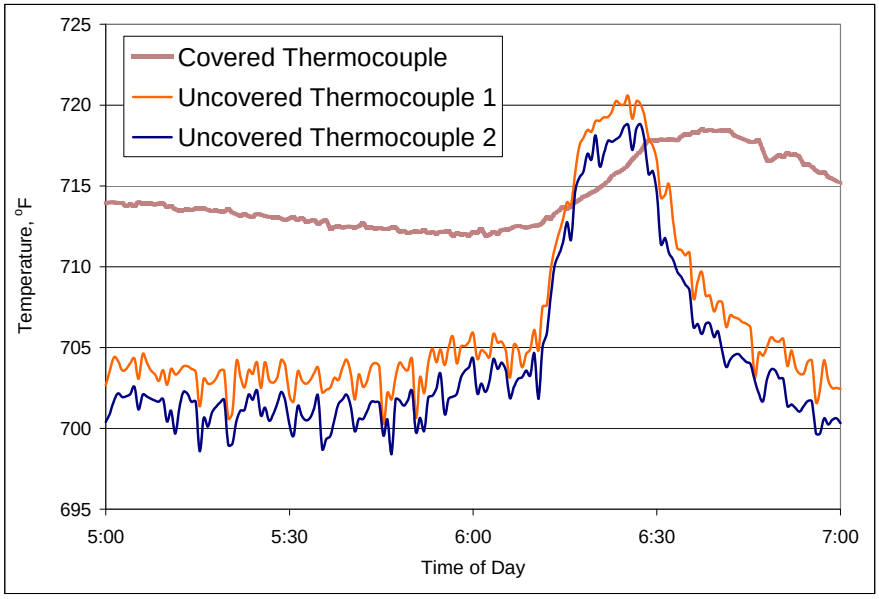

Figure 4-16. Filter Element Thermocouple Response during Bridging.

4.4.2.2 Resistance Probes

In addition to the filter element thermocouples, resistance probes were developed on site and installed on filter elements. These instruments, which register a change in electrical resistance caused by the presence of gasification ash, had the advantage of giving a discrete alarm, as opposed to the thermocouples, which require trend observation. Figure 4-17 shows a resistance probe installed on a filter element.

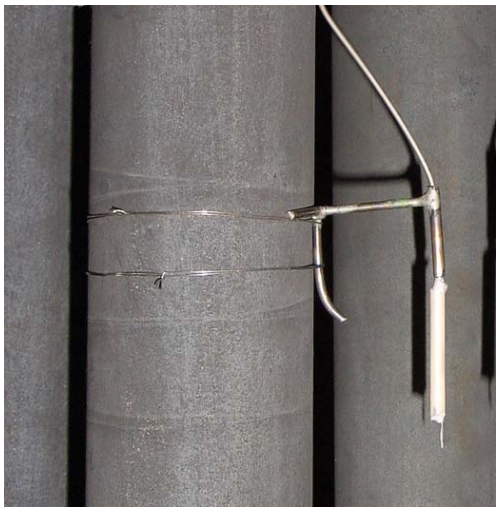

Figure 4-17. Filter Element Resistance Probe.

Figure 4-18 shows the response of the filter element resistance probes to bridging.

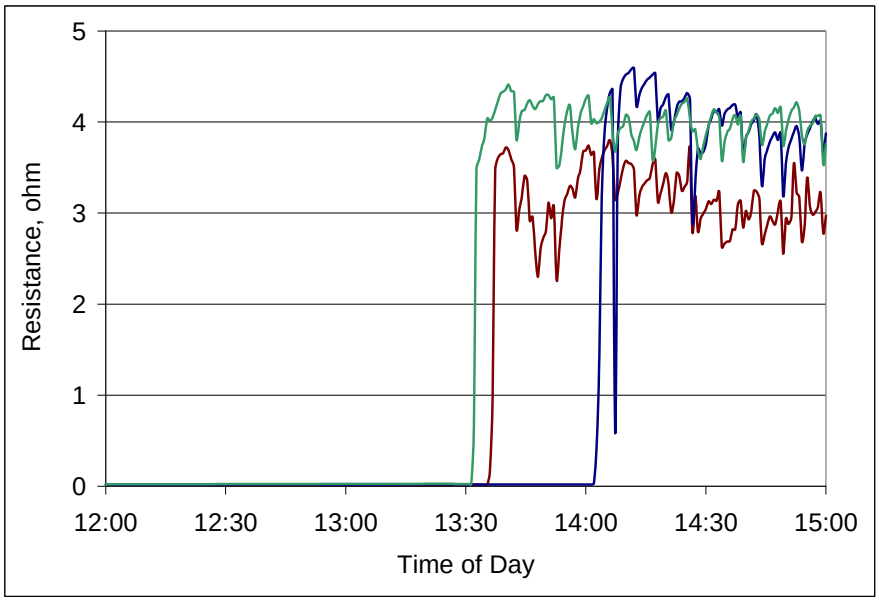

Figure 4-18. Filter Element Resistance Probe Response during Bridging.

4.4.2.3 Additional Hopper Thermocouples

The originally installed thermowell thermocouples located in the hopper of the PCD were slow responding and, since they were located on the hopper walls, did not necessarily indicate ash levels in the center of the PCD. For improved monitoring of ash levels in the PCD hopper, a structure was added to support centered thermocouples. This addition proved useful in providing much faster and more accurate temperature data than the original thermocouples. Figure 4-19 shows the structure and its location in the PCD hopper.

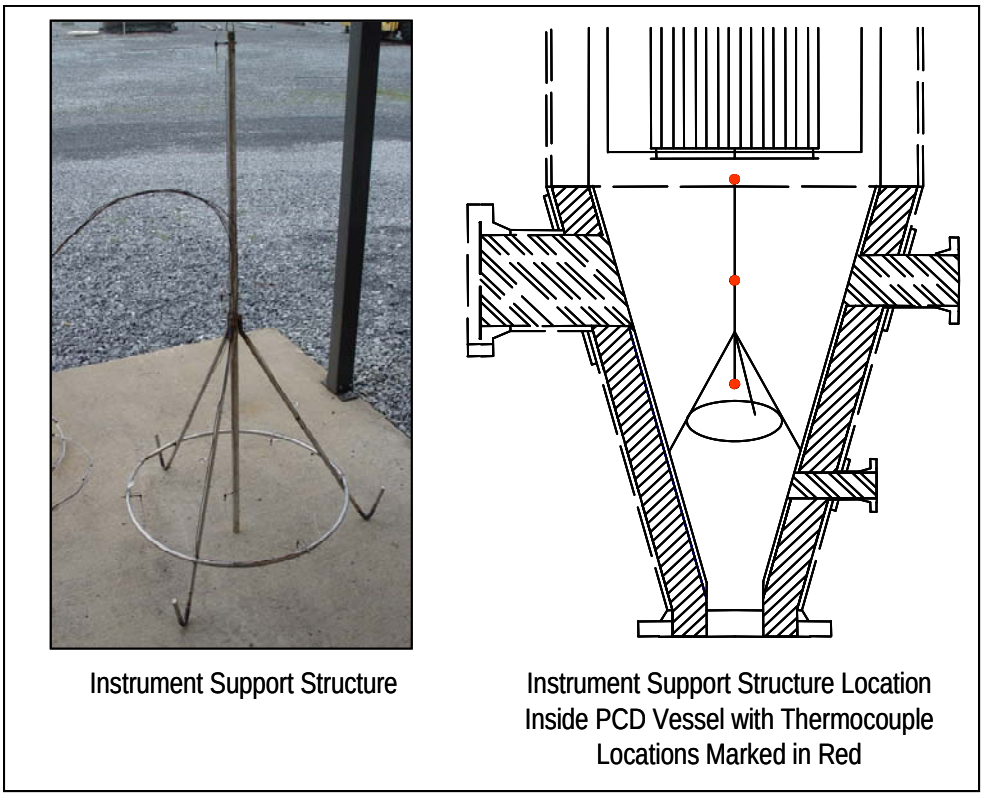

Instrument Support Structure

Instrument Support Structure Location Inside PCD Vessel with Thermocouple Locations Marked in Red

Figure 4-19. PCD Hopper Thermocouple Support Structure.

4.4.3 On-line Removal of Ash Bridging

Several attempts were made to remove bridging on-line by adjusting backpulse parameters (increasing backpulse valve open time, pulse pressure, etc.), but these methods did not affect the bridging. During an instance of bridging (test campaign TC17), rather than shut down the system due to the increasing pressure drop across the PCD, the bridging was removed on-line.

To accomplish the bridging removal, the gasifier was transitioned from gasification mode to combustion mode by increasing air flow to the gasifier and allowing a low level of oxygen to enter the PCD. After over 12 hours of combustion, the gasification ash was

removed, as indicated by the resistance probe responses (Figure 4-20) and the lower PCD pressure drop level was restored.

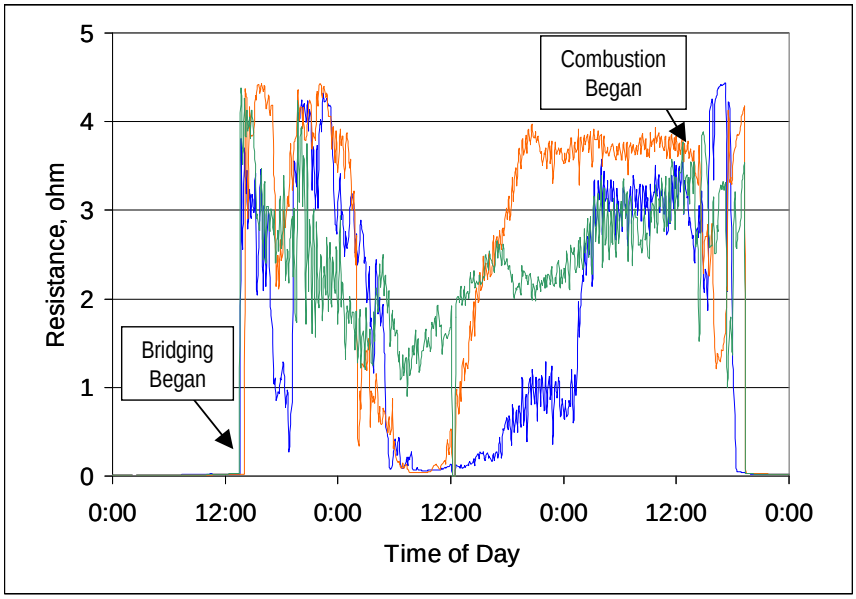

Figure 4-20. Resistance Probe Response during On-Line Bridging Removal.

4.5 Relating Particulate Characteristics to PCD Design Requirements

The PCD size required to maintain a given allowable pressure drop is a strong function of the dustcake drag, since most of the PCD pressure drop occurs across the dustcake. Given the significant relationship between dustcake drag and PCD size requirement, the design of the PCD system must take into account the particulate characteristics that affect drag. The following sections address some of the key particulate characteristics that govern dustcake drag, in particular the non-carbonate carbon content, particle size distribution, and morphology.

4.5.1 Non-Carbonate Carbon versus Particulate Drag

The pressure rise within a cleaning cycle of the PCD is a direct measure of the characteristics of the particulate being collected at that time. Under stable operation, the vast majority of this particulate is removed from the filter elements during cleaning, so this is referred to as the transient pressure drop. Since pressure drop is a function of the gas velocity, temperature (gas viscosity), particulate loading, and the flow resistance of the particulate, describing PCD operation in terms of pressure drop makes comparison of different conditions difficult. Instead, a value of normalized drag is calculated, which is pressure drop that is normalized to 1 ft/min face velocity, 1 lb/ft^2 areal particulate loading, and gas viscosity of air at 70°F. The result is a fundamental parameter that describes the flow resistance of the collected dustcake.

For each in-situ sample at the PCD inlet, the PCD transient drag was calculated using the measured particulate concentration along with the pressure drop increase and face velocity during the period of the in-situ test. All of the particulate measured at the PCD inlet is assumed to be collected on the filter elements and to contribute to pressure drop.

The results of the transient drag calculations are plotted as a function of the non-carbonate carbon content of the ash in Figure 4-21. The values plotted are the transient drag values normalized to the viscosity of air at room temperature (70°F). These values are directly comparable to the laboratory drag measurements, and, because they are normalized, can be compared across a wide range of test campaigns with different process operating conditions and different fuels. As seen in all previous test campaigns, Figure 4-21 clearly shows that transient drag increases with increasing carbon content in the gasification ash. The reasons for this effect will be discussed in more detail in Section 4.5.2 in conjunction with laboratory studies of the effects of particle size and carbon content on drag.

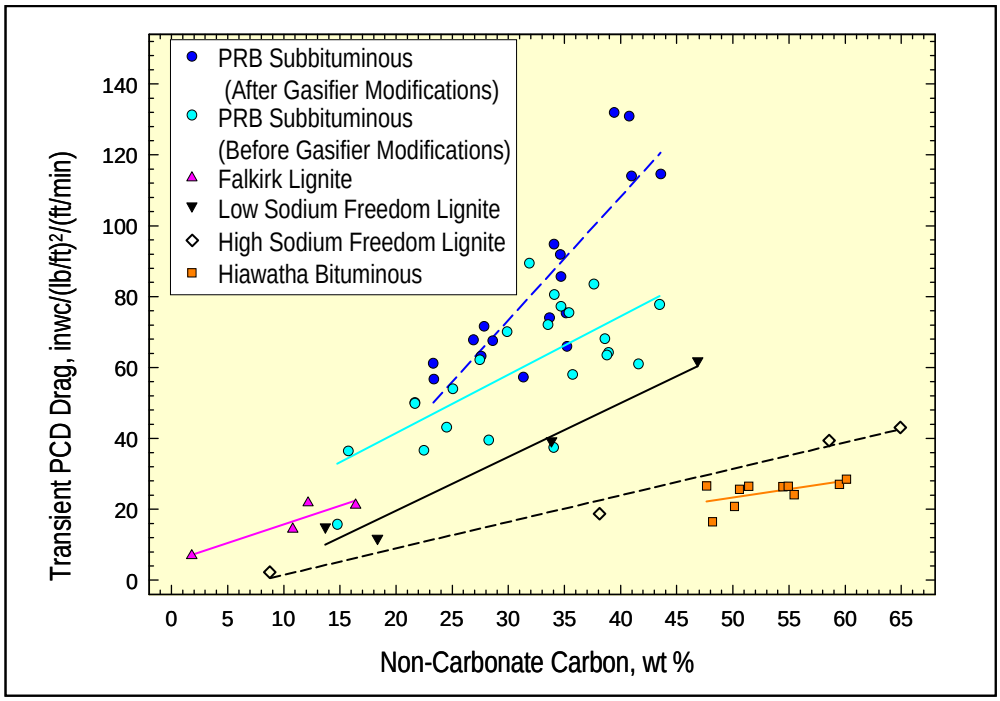

Figure 4-21. PCD Transient Drag versus Carbon Content of In-Situ Samples.

4.5.2 Particle Size versus Particulate Drag

To determine the effect of particle size on drag, the laboratory apparatus shown in Figure 4-22 is used. This apparatus uses a fluidized bed to entrain the gasification ash and blow it over to a collection chamber where it is collected on a sintered-metal filter. Various combinations of small cyclones are incorporated to remove larger particles, allowing the production of dustcakes having median particles sizes in the range of approximately 2 to 15 microns. The flow through the dustcake and the pressure drop across the dustcake are

monitored as the dustcake builds up on the sintered-metal filter. Since the viscosity of the room-temperature air used in the lab system is much lower than the viscosity of the hot syngas, the compressive force of the gas on the dustcake is less than it is in the actual hot-gas filter. To compensate for this effect, the laboratory drag measurement system is operated at a face velocity that is higher than that of the actual hot-gas. Experience with the laboratory system has shown that a face velocity of about 12 ft/min (6 cm/sec) is required to simulate the dustcake compaction that occurs in the actual hot-gas filter (Dahlin, 2002).

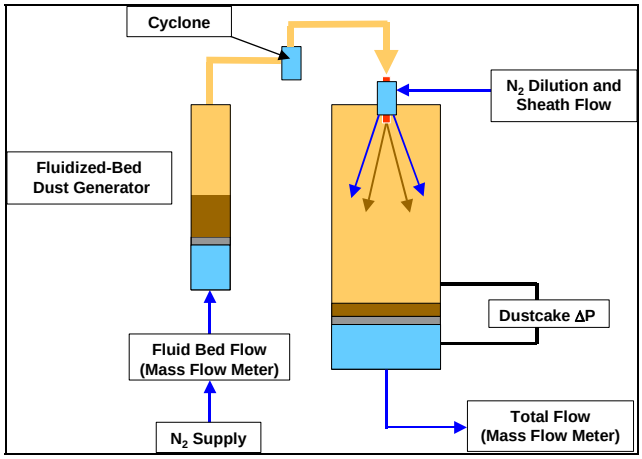

Figure 4-22. Laboratory Apparatus for Measuring Drag of Re-suspended Gasification Ash.

After the buildup of the dustcake is complete, the system is disassembled to measure the dustcake thickness and to weigh the dustcake. Based on this information, the normalized drag of the dustcake (R) is determined from the pressure drop across the dustcake (ΔP_d), the areal loading of the dustcake (L_a), and the filter face velocity (V_f):

$$R = \frac{\Delta P_d}{(L_a * V_f)} \qquad (1)$$

By using the system with various combinations of small cyclones, it is possible to determine dustcake drag as a function of mean particle size. Such measurements can be described by a linear regression in logarithmic coordinates:

$$\log(R) = m * \log(D) + b \qquad (2)$$

in which D is the mass-median particle size. The best-fit values of slope m varied from -0.9 to -1.1, suggesting that the drag was very nearly proportional to the inverse of the mean particle size.

Results obtained with the lab drag measurement apparatus are illustrated in Figures 4-23, 4-24, and 4-25, which show the normalized drag plotted against the MMD of the collected dustcake. The sets of drag data are arrayed with drag increasing with increasing

carbon content. As expected, all of the samples also show increasing drag with decreasing particle size. The relationship between drag, particle size, and carbon content (non-carbonate carbon, or NCC) can be evaluated by calculating a multiple regression. The resulting equation relating these values is given by:

$$\text{Drag} = 10\text{^}(A - (B * \text{Log}(\text{MMD})) + C * \text{NCC}) \qquad (3)$$

where A, B, and C are constants.

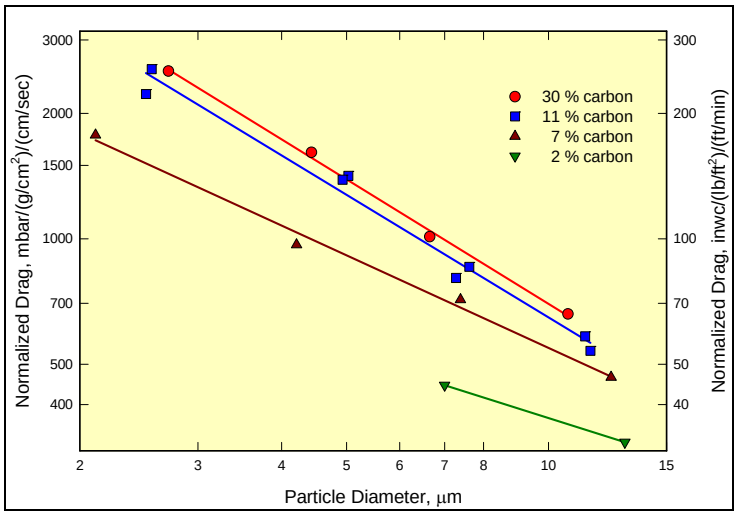

Figure 4-23. Lab-Measured Drag as a Function of Particle Size with Falkirk Lignite Ash.

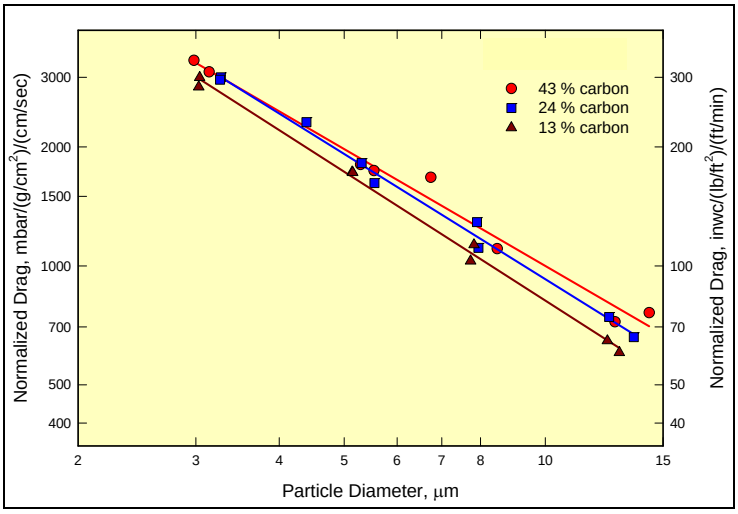

Figure 4-24. Lab-Measured Drag as a Function of Particle Size with PRB Subbituminous Coal Ash.

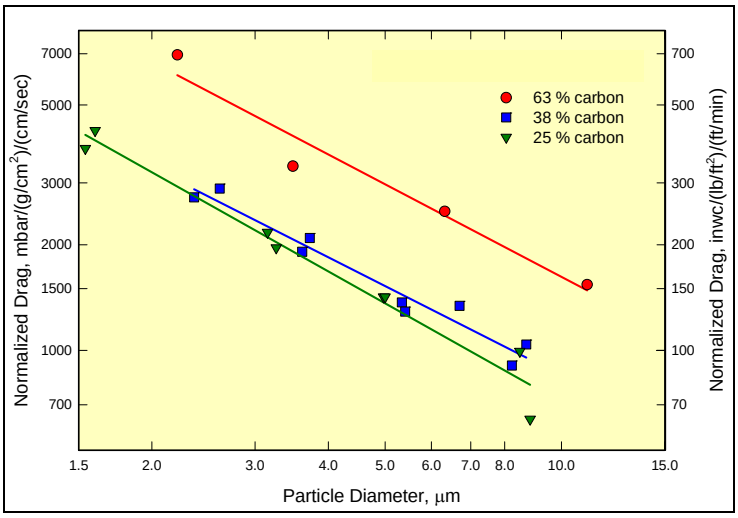

Figure 4-25. Lab-Measured Drag as a Function of Particle Size with High-Sodium Freedom Lignite Ash.

With all three coal types, the laboratory drag measurements show that drag increases with increasing carbon content, although the differences in the three PRB ash samples (Figure 4-26) may not be statistically significant. For the Falkirk lignite ash, a change in carbon content from 30 to 11 percent does not have a major impact on drag, but the effect of carbon on drag becomes much more dramatic as the carbon content drops to values approaching zero. The Falkirk gasification ash sample that contains only 2 weight percent carbon exhibits drag that approaches the drag of combustion ash. This result is not surprising since complete conversion of the carbon would produce a material similar to combustion ash, which generally has drag below 10 inwc/(lb/ft^2)/(ft/min).

Analysis of various particle size fractions showed that carbon content varies with particle size. However, over the particle size range of the laboratory drag measurements (2 to 15 microns) the carbon content of the gasification ash from the PSDF gasifier has been shown to be essentially constant. Therefore, the effect of carbon on drag shown in Figures 4-24 through 4-26 cannot be attributed to a variation of carbon with particle size.

To better understand the mechanism by which carbon content affects drag, selected samples from the drag studies were examined by SEM and EDX analyses. The SEM/EDX analyses were completed on three sets of samples. Each set of samples consisted of a low drag and a high drag sample from one of the three different coal types.

SEM photos of the low and high drag samples produced from each coal type are shown in Figures 4-26 to 4-28. The SEM photos show that the high drag samples contain more particles that are angular, while most of the particles in the low drag samples seem to have relatively smooth surfaces. The more angular, shard-like particles would be expected to produce more flow resistance than the smoother particles (Bush, et al., 1989). The high drag samples also have higher surface areas than do the low drag samples, and surface area is another factor that contributes to flow resistance.

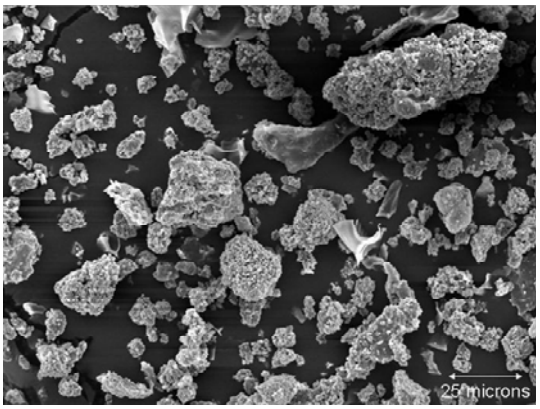

Low drag sample -- 3 wt percent carbon and 19 m^2/g surface area

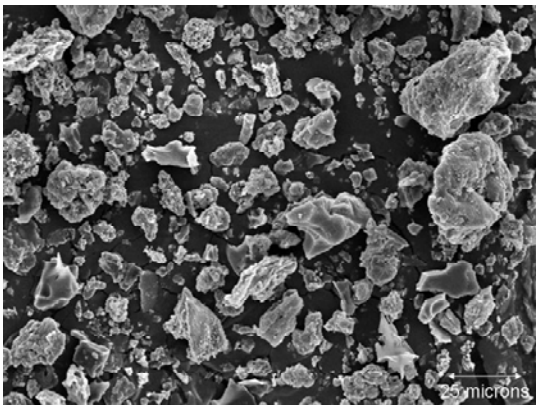

High drag sample -- 34 wt percent carbon and 99 m^2/g surface area

Figure 4-26. SEM Photographs of Low and High Drag Samples from Falkirk Lignite.

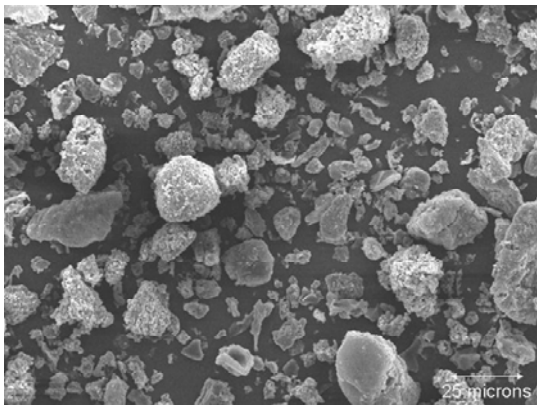

Low drag sample -- 13 wt percent carbon and 74 m^2/g surface area

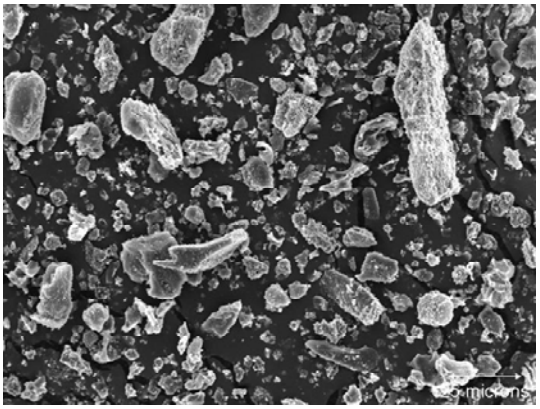

High drag sample -- 43 wt percent carbon and 185 m^2/g surface area

Figure 4-27. SEM Photographs of Low and High Drag Samples from PRB Coal.

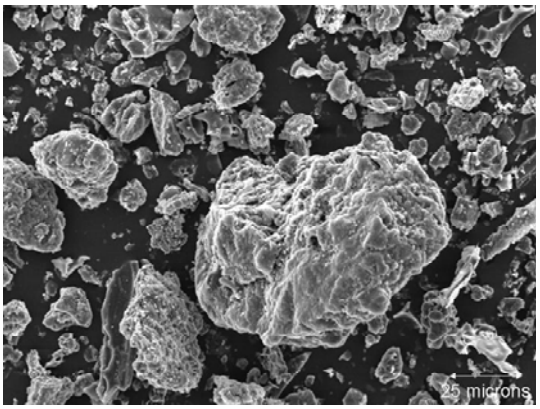

Low drag sample -- 18 wt percent carbon and 12 m^2/g surface area

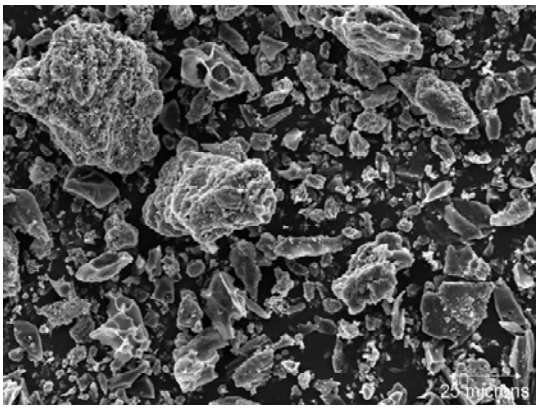

High drag sample -- 57 wt percent carbon and 75 m^2/g surface area

Figure 4-28. SEM Photographs of Low and High Drag Samples from Freedom Lignite.

EDX analysis revealed that the angular, shard-like particles contain much more carbon than do the lumpy, smoother particles. Based on optical microscopy, the angular, shard-like particles appear to be chunks of unconverted or partially converted coal. Most of the carbon is contained in these poorly converted coal particles, which have more internal porosity and more surface area than the fully converted particles of gasification ash. Since the partially converted coal particles also have irregular shapes that offer more flow resistance, it is not surprising that drag and surface area increase with increasing carbon content.

In the Transport Gasifier, carbon conversion is strongly influenced by the collection efficiency of the solids separation unit. With high gasifier collection efficiency, more carbon is retained in the gasifier loop, resulting in higher carbon conversion and lower drag. These factors must be considered when the gasifier and hot-gas filter systems are scaled up for commercial application.

4.5.3 Relative PCD Sizing Requirements for Different Fuel Stocks

For a commercial IGCC application, the PCD system must be designed to allow the plant to operate at full-load conditions with the entire range of fuels that will be used in the plant. The PCD must be sized to operate within acceptable limits of baseline pressure drop and peak pressure drop, even for the "worst-case" fuel. In this context, the worst-case fuel is the one that produces the dustcake with the highest drag under the planned filter operating conditions. In other words, the sizing of the filter must be based on the highest anticipated value of dustcake drag. Thus, a reliable determination of the dustcake drag is essential to ensure that the filter system is properly sized for a given application.

In determining the value of dustcake drag to be used for sizing the filter system, it is important to consider the drag characteristics of both the residual dustcake and the

transient dustcake. The residual dustcake, which is sometimes referred to as the "permanent" dustcake, remains on the filter elements for time periods that are very long compared to the filtration cycle, while the transient dustcake is removed with each cleaning cycle. Measurements made at the PSDF have shown that there can be significant differences between the residual and transient dustcakes. Some of these differences have been attributed to the enrichment in fine-particle content that occurs in the residual dustcake over repeated cycles of backpulsing and fine-particle re-entrainment and recollection. The prolonged exposure of the residual dustcake to hot syngas may also result in additional sulfidation in the residual dustcake. Since the molar volume of calcium sulfide is larger than the molar volume of the calcium oxide that it is replacing, the additional sulfidation produces a change in the dustcake porosity, which results in a change in dustcake drag. Consolidation reactions within the residual dustcake may also contribute to the observed differences in drag characteristics between the residual and transient dustcakes.

From these results, it is clear that residual and transient dustcakes can be characterized by substantial differences in their resistance to gas flow. These differences must be taken into account when sizing the PCD system. The baseline pressure drop across the filter just after cleaning will be governed by the properties of the residual dustcake, while the properties of the transient dustcake will govern the additional pressure drop that is accumulated during the filtration cycle and hence the peak pressure drop. The baseline pressure drop (ΔP) across the PCD just after cleaning may be separated into three components: (1) the ΔP across the residual dustcake, (2) the ΔP across the filter elements themselves, and (3) other pressure losses associated with flow in other vessel internals.

The ΔP attributable to the filter elements and vessel internals may be inferred from flow ΔP measurements made on a clean filter system if available. If these measurements are not available, the ΔP across the filter elements can be estimated from flow ΔP measurements made on individual filter elements, and the vessel losses can be calculated using various computational fluid dynamics models. In either case, it is important to make sure that the values of ΔP are adjusted to the same face velocity and gas viscosity that will be experienced during stable filter operation at full load conditions. The estimated values of ΔP due to the vessel losses and the filter elements themselves can then be subtracted from the allowable baseline ΔP to obtain the maximum allowable ΔP across the residual dustcake. (Graphical illustrations of these pressure drop terms and the other terms used in the filter sizing calculations are given in Figures 4-29 and 4-30.)

$$\Delta P_{residual} = \Delta P_{baseline} - \Delta P_{vessel} - \Delta P_{elements} \qquad (4)$$

This value of residual dustcake pressure drop ($\Delta P_{residual}$) can then be used along with the measured drag of the residual dustcake ($R_{residual}$) and the areal loading of the residual dustcake ($L_{residual}$) to calculate the required filter face velocity (V_{face}).

$$V_{face} = \Delta P_{residual} / R_{residual} / L_{residual} \quad (5)$$

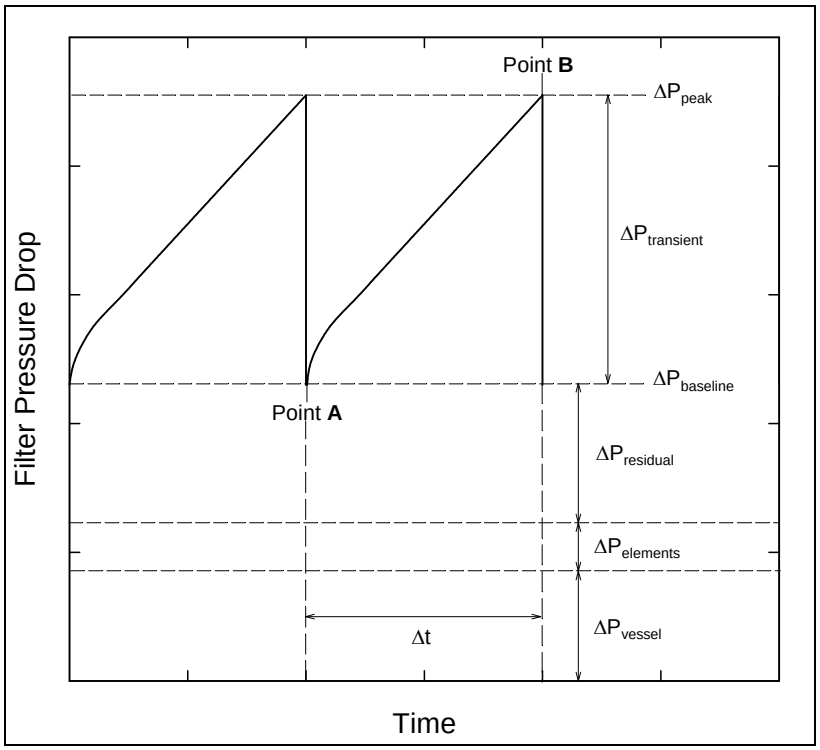

Figure 4-29. Graphical Illustration of Terms Used in PCD Sizing.

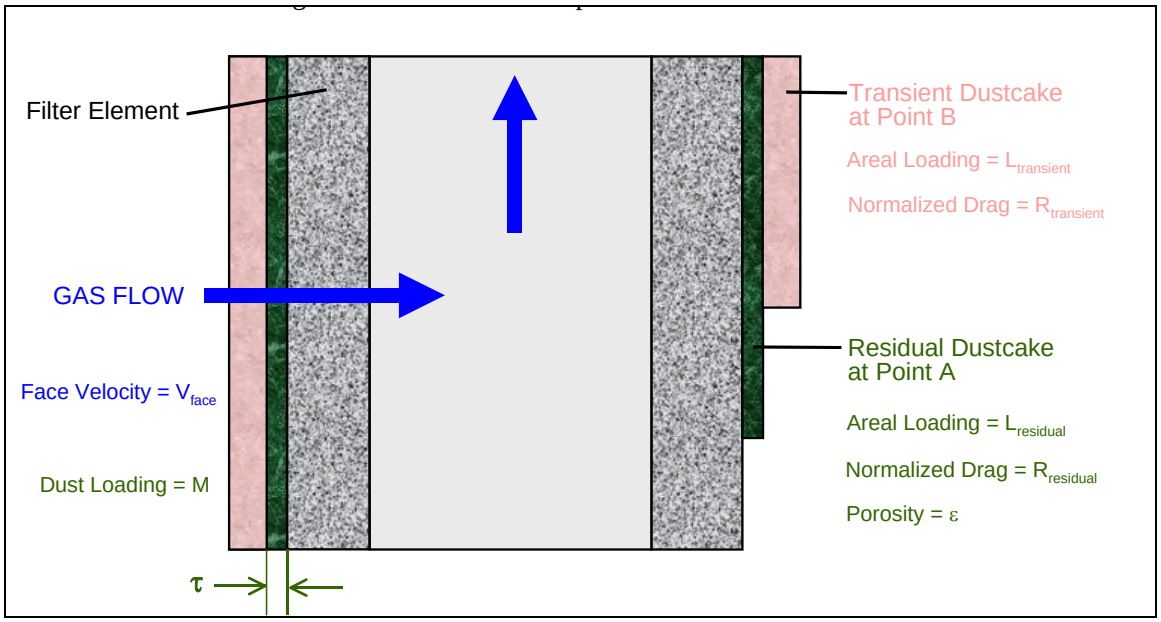

Figure 4-30. Dustcake Development at Points A and B in Figure 4-29.

In this relationship, both the residual dustcake drag ($R_{residual}$) and the areal loading ($L_{residual}$) are functions of the dustcake porosity, which is the key unknown parameter. Estimates of the dustcake porosity and drag may be obtained using the laboratory drag measurement apparatus described earlier. The dustcake porosity (ε) determined from these measurements may be used along with the measured true particle density (ρ_{true}) and an assumed value of dustcake thickness (τ) to calculate the areal loading ($L_{residual}$).

$$L_{residual} = \tau * \rho_{true} * (1- \varepsilon) \qquad (6)$$

This value of areal loading may then be used in the previous relationship to determine the required face velocity, which in turn establishes the total required filtration area, or total number of required filter elements. Of course, there are many other factors that must be considered in the design of the hot-gas filter system, but the relationships given above provide a relatively simple method of determining the total required filter surface or the number of filter elements required to maintain an acceptable baseline ΔP.

A procedure similar to the one discussed above can be used to insure that the maximum allowable peak pressure drop (ΔP_{peak}) is not exceeded based on the estimated transient dustcake drag ($R_{transient}$). In this procedure, drag measurements are made on an ash sample that simulates the ash arriving at the filter elements. The measured value of transient dustcake drag ($R_{transient}$) is then used along with the face velocity (V_{face}) determined previously and the areal loading of the transient dustcake ($L_{transient}$) to calculate a transient dustcake pressure drop ($\Delta P_{transient}$).

$$\Delta P_{transient} = R_{transient} * V_{face} * L_{transient} \qquad (7)$$

Transient drag values to be used in this relationship may be obtained from laboratory drag measurements made with the laboratory drag measurement apparatus. The effect of the transient dustcake drag on PCD size is illustrated qualitatively in Figure 4-31. The areal loading of the transient dustcake ($L_{transient}$) may be calculated directly from the inlet particulate loading (M), the total gas flow (Q), the fraction of particulate mass that drops out in the filter vessel before reaching the filter elements (f), and the total filtration area (A) determined previously, and the time interval between cleaning cycles, Δt:

$$L_{transient} = M\ (ppmw) / 1{,}000{,}000 * Q\ (lb/hr) * (1 - f) * \Delta t\ (min) / 60\ min/hr / A \qquad (8)$$

Using the above relationship for the areal loading, the transient dustcake ΔP may then be calculated from the previous expression, and the peak ΔP may be determined by adding in the estimated baseline ΔP determined previously. If the peak ΔP exceeds the maximum allowable value even with very frequent cleaning (short Δt), it may be necessary to increase the filtration area beyond what was previously estimated based on residual dustcake properties alone.

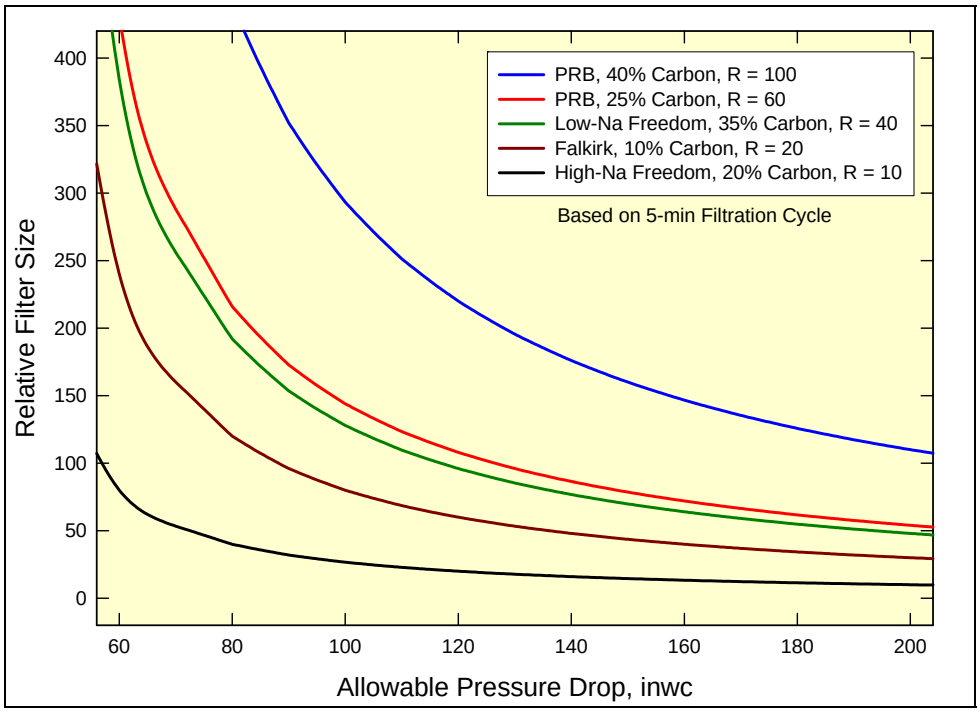

Figure 4-31. Effect of Transient Drag on Required PCD Size at a Given Allowable Pressure Drop.

The reliability of the foregoing relationships for the sizing of PCD systems has been assessed using in-plant measurements of peak and baseline ΔP, inlet particulate loading, residual dustcake areal loading, and laboratory measurements of dustcake porosity and drag. Results obtained to date suggest that the relationships provide a reasonably accurate means of sizing a filter system for IGCC applications.

5.0 ADVANCED SYNGAS CLEANUP

Work in advanced syngas cleanup began in 2004. To provide flexible test conditions, the syngas cleanup slipstream unit was designed to allow for off-line operations with bottled gases as well as on-line operations with a slipstream of syngas generated in the Transport Gasifier. Early tests focused on sulfur and nitrogen species removal as well as reformation of hydrocarbons. Syngas cleanup for fuel cell testing was also performed in these early tests.

Later studies included testing of water-gas shift reactions with a catalytic filter element and a fixed bed reactor, direct oxidation of hydrogen sulfide (H_2S) in a fixed bed reactor, and CO_2 capture in a batch reactor. Additional tests were also performed with a hydrocarbon cracking catalysts, trace metals sorbents, and sulfur sorbents. The syngas cleanup unit was also used to support researchers from the Department of Energy (DOE) National Energy Technology Laboratory, Media Process Technology, TDA Research, and Johnson Matthey.

5.1 Desulfurization

Sud-Chemie Sulfur Sorbent. In 2005, syngas desulfurization tests were conducted with the Sud-Chemie sulfur sorbents RVS-1 and RVSLT-1. The nominal properties of these two sorbents are listed in Table 5-1.

Table 5-1. Sud-Chemie Sulfur Sorbent Properties and Nominal Operating Parameters.

Sorbent/Catalyst	RVS-1	RVSLT-1
Chemical Composition, weight percent		
Zinc Oxide	40 – 60	50 – 70
Calcium Sulfate	15 – 25	15 – 30
Calcium Oxide	5 – 10	5 –15
Nickel Oxide	5 –15	
Bentonite	5 –15	5 – 15
Silica, Quartz	< 5	< 5
Physical Properties		
Shape	Spheres	Spheres
Size, mm	3 – 4	3 – 4
Density, lb/ft^3	60 – 85	60 – 85
Bed Mass, lb	16	16
Bed Height, in	28	28
Syngas Flow Rate	30	30
Pressure, psig	200	180
Temperature, ^oF	635	570
Space Velocity, hr^{-1}	1,950	1,950
Inlet H_2S and COS, ppm	215	215

During the first 76 hours of testing the RVS-1 sorbent, the H_2S content was reduced to below the detectable limit. There was no sulfur breakthrough experienced during this

test; however; in the subsequent test conducted in November 2005, sulfur breakthrough was observed after 145 hours of operations. Desulfurization tests with the RVSLT-1 sorbent were also performed in November 2005 achieving over 98 percent removal.

Synetix Sulfur Sorbent. In November 2006 and March 2007, the syngas from the carbonyl sulfide (COS) hydrolysis unit was sent through a two-step desulfurization process to supply syngas with ultra low concentrations of sulfur for trace metals removal testing by TDA Research. Two sulfur sorbents from Synetix, Puraspec 2010 and Puraspec 2020, were used to reduce sulfur in the syngas. Desulfurization of the syngas was accomplished in fixed bed reactors arranged in series, with the first reactor filled with Puraspec 2010 for bulk sulfur removal and the second reactor filled with Puraspec 2020 for sulfur polishing. The sorbents are composed mainly of zinc oxide with a proprietary active ingredient. The sorbent properties and desulfurization operating parameters are given in Table 5-2. The sulfur concentration at the outlet of the second reactor was below the detection limit, which is typically 1.5 ppmv.

Table 5-2. Synetix Sulfur Sorbent Properties and Nominal Operating Parameters.

Sorbent Type	Puraspec 2010	Puraspec 2020
Physical Properties		
Zinc Oxide Content, wt %	84—91	84—91
Shape	Spheres	Spheres
Size, mm	2.8—4.75	2.8—4.75
Density, lb/ft^3	62—84	47—62
Catalyst Bed Mass, lb	45	35
Catalyst Bed Height, in	51	44
Operating Parameters		
Pressure, psig	200	200
Temperature, ^{o}F	620	385

The Puraspec 2010 was used in the July 2008 run to reduce the syngas sulfur levels below the detection limit, typically 1.5 ppmv, to condition the syngas prior to use in the fuel cell and mercury sorbent test skids.

5.2 Direct Oxidation of H_2S

Off-Line Tests. Direct oxidation of H_2S was performed off-line with bottled gases (nitrogen, hydrogen sulfide, and sulfur dioxide) in preparation for on-line testing with syngas. The primary objective of this test was to investigate bulk sulfur removal efficiency by converting H_2S at low concentrations to elemental sulfur using sulfur dioxide (SO_2).

The oxidation catalyst used was BASF DD-431 activated alumina in 6 mm diameter spherical form. Off-line testing was conducted at 200 psig pressure and gas flow rates of 11.5 to 12 lb/hr. The first test was performed at a reactor bed temperature of about 475^{o}F and achieved conversions up to about 88 percent. During the second test, the reactor bed

temperature was maintained at 417ºF, and the H_2S conversion was slightly higher, at about 93 percent.

On-Line Tests. In August 2007 the H_2S oxidation test using the DD-431 catalyst was conducted using syngas generated from high sodium lignite. One objective of the test was to ensure that high H_2S conversions achieved during off-line testing could be achieved with actual syngas containing low H_2S concentrations. Another test objective was to observe how a stoichiometric amount of SO_2 selectively reacts with H_2S in the presence of CO and H_2. Levels of COS were monitored to ensure that additional amounts of COS were not formed.

The on-line testing took place for about 40 hours. Operating conditions included pressures from 110 to 200 psig, temperatures of 260 to 550°F, and a syngas flow rate of 30 lb/hr. Bottle gas containing 1 percent SO_2 and 99 percent N_2 was fed at rates from 0 to 3 lb/hr. During the testing, the reactor inlet concentration of H_2S generally ranged from 0.07 to 0.10 percent on a dry basis.

The first part of the direct oxidation on-line test was performed at temperatures up to 550ºF. It was observed during this test that H_2S concentration at the outlet of the reactor increased with the increase of SO_2 flow, indicating that SO_2 was reacting with H_2 present in the syngas, forming additional H_2S. No oxidation reaction of H_2S with SO_2 to form elemental sulfur was observed.

The second part of the direct oxidation on-line test was at a lower temperature of about 280ºF. During this test, the H_2S concentration at the outlet of the reactor was unchanged, and ammonia present in the syngas was significantly reduced from the reactor inlet to the outlet. Direct oxidation of H_2S was observed only when excess SO_2 was used.

Post-Test Evaluation. The BASF DD431 catalyst was removed from the direct H_2S oxidation fixed bed reactor after the 40 hour test. The catalyst shape, 6 mm diameter spheres, was unchanged, although the color had changed from white to grayish black. The used catalyst was sent to BASF for analysis. According to BASF, the sulfur content had increased to about 12 percent, higher than the 3 to 4 percent increase typically seen with oxidation catalysts.

5.3 COS Hydrolysis

The first COS hydrolysis test was conducted in November 2005 with a Sud-Chemie COS hydrolysis catalyst, C53-2-01. Testing was conducted at temperatures between 400 and 500ºF and pressures ranging from 170 to 200 psig. The tests lasted for 250 hours, and the COS concentrations at the reactor outlet were near equilibrium.

In August 2006, the tests were expanded to include COS hydrolysis catalysts supplied by Engelhard, Johnson Matthey, and Alcoa. Aluminum oxide was the basic material of the catalysts, with proprietary amounts of additional materials. The testing was performed in 310 stainless steel reactors with 5.2 inch inner diameters and heights of 5 feet. Space velocity was maintained at 2000/hr. Nominal catalyst properties and operating

parameters for the COS hydrolysis tests are shown in Table 5-3. The COS conversions ranged from 80 to 93 percent.

Table 5-3. COS Hydrolysis Catalyst Properties and Nominal Operating Parameters.

Catalyst Supplier	Sud-Chemie	Engelhard	Johnson Matthey	Alcoa	Alcoa
Catalyst Type	C53-2-01	Selexcat	Puraspec 2312	Selexsorb	F200
Physical Properties					
Aluminum Oxide Content, wt %	--	84-96	100	84-96	94-100
Shape	Extrusion	Spheres	Spheres	Spheres	Spheres
Size, mm	3.2	2	3	3.7	3.2
Density, lb/ft^3	30	45.6	43.7	46.8	43.1
Catalyst Bed Mass, lb	6.5	9.8	9.4	10.1	9.3-10.8
Catalyst Bed Height, in	17.7	17.6	17.6	17.6	17.6-19
Operating Parameters					
Pressure, psig	190	225	180	165	100-200
Temperature, ^{o}F	420	390	390	400	375-430
Inlet COS Concentration, ppm	22.5	26.5	27.0	23.5	16.5-57.2
Outlet COS Concentration, ppm	4.5	1.7	2.3	4.3	2.4-4.8
COS Conversion	80	93	92	82	90
Operating Time, hr	342	120	101	58	527

5.4 Ammonia Cracking and Hydrocarbon Reforming

Three Sud-Chemie nickel-based catalysts (G 117RR, G-31, FCR-4) were tested to crack ammonia and reform hydrocarbons. The nominal properties of the nickel-based catalysts are shown in Table 5-4.

Table 5-4. Ammonia Cracking and Hydrocarbon Reforming Catalyst Properties.

Catalyst Type	G-117RR	G-31	FCR-4
Physical Properties			
Shape	Rings	Spheres	Spheres
Size, mm	3 - 4	1	3
Density, lb/ft^3	55 - 75	65 -100	72
Chemical Composition			
Magnesium Oxide, weight percent	75 – 90	---	---
Nickel Oxide, weight percent	5 – 15	1 – 25	10 - 14
Calcium Oxide, weight percent	1 - 5	---	---
Aluminum Oxide, weight percent	1 - 5	75 - 99	86 - 90

G-117RR Catalyst. A Sud-Chemie nickel-based catalyst, G-117RR, was tested in a slipstream reactor to assess the catalyst reactivity and sulfur poisoning effect using ammonia, benzene, and sulfur dioxide. A bottled ammonia gas simulation test was conducted at 1,650^{o}F and 2 to 10 psig pressure for 4 hours. The inlet ammonia concentration was maintained at 3,000 ppm, while the outlet ammonia level measured

below 20 ppm. A benzene bottle gas simulation test was conducted at 800 to 1,600ºF and at pressures from 2 to 10 psig for 3 hours. The inlet benzene concentration was maintained at 1,000 ppm. The outlet benzene level was obtained below 50 ppm at 1,600°F. A hydrogen sulfide bottle gas was used to study contaminant effects at temperatures from 1,000 to 1,600ºF and at pressures of 2 to 10 psig for 8 hours. The inlet concentration of ammonia and benzene were maintained at 3,000 and 550 ppm respectively. The outlet concentrations of both ammonia and benzene measured below 50 ppm. At these high temperatures, the catalyst performance was not affected by contaminants such as hydrogen sulfide.

In June 2005, during tests on syngas with the G-117RR catalyst (which was tested for 290 hours) the ammonia concentration was reduced by about 96 percent on average; benzene was reduced by about 75 percent; ethylene was reduced by 97 percent; acenaphthene was reduced by 97 percent; phenanthrene was reduced by 88 percent; and naphthalene was reduced by 81 percent.

G 31 Catalyst. In June 2005, ammonia cracking and hydrocarbon reforming testing was conducted for 13 hours using the G 31 catalyst. About 99 percent reduction in ammonia, benzene, ethylene, acenaphthene, and phenanthrene was achieved. Naphthalene was reduced by about 98 percent.

Testing with the G 31 catalyst continued in November 2005 at temperatures of 1,700°F and low pressures. The reactor used for this testing was a two-inch inner diameter, four foot tall vessel. The tests lasted for over 300 hours, and the ammonia concentration was reduced from about 2,250 ppm to less than 10 ppm. Benzene concentrations were reduced from about 800 ppm to about 20 ppm. Other hydrocarbon concentrations measured included ethylene, phenanthrene, and naphthalene, which were typically reduced by 99 percent or more, and acenaphthene, which was reduced by about 89 percent.

FCR-4 Catalyst. The Sud-Chemie hydrocarbon cracking catalyst FCR-4 was tested and reduced concentrations of organics such as benzene and naphthalene by 90 to 99 percent.

5.5 Syngas Cooler Fouling Testing

Syngas cooler fouling tests were conducted from June 2005 to March 2007 using a slipstream of syngas. The syngas temperature was lowered below the dew point of the syngas stream to evaluate potential deposition during condensation. The syngas flow was varied from 18 to 40 lb/hr. The syngas temperature at the cooler inlet was 430 to 500ºF, and that at the outlet was 120 to 130ºF. The gas velocity in the cooler tube was varied from 49 to 65 ft/s. Testing showed that the exchanger tube was not plugged with organics in over 621 hours of operation at these conditions; however, exchanger tube fouling with organics was observed when the chiller water inlet temperature was lowered to 50ºF. The condensate removed was clear and free of any heavy organic compounds.

5.6 TDA Research Trace Metals Removal

As part of development of a DOE sponsored project for sorbent-based high temperature removal of trace metals from coal-derived syngas, TDA Research performed testing at the PSDF in November 2006 using the syngas cleanup slipstream. The sorbent-based high temperature trace metal removal process was designed to remove trace metals, including mercury, arsenic, selenium, and cadmium, from coal-derived syngas in a single step. Single step high temperature removal is potentially beneficial for future gasification power systems because of improved overall efficiency compared to cold gas cleanup systems and lower capital and operating cost due to the reduced amounts of sorbent required as compared to currently available trace metals removal technologies.

Initial testing by TDA Research was performed with syngas generated from low sodium lignite that had sulfur concentrations reduced below the limit of measurement (about 1.5 ppmv). Testing continued in March 2007 with syngas generated from Mississippi lignite. During this test, over 200,000 SCF of syngas was treated. Post testing analysis indicated that the sorbent would achieve high mercury removal efficiency.

5.7 Water-Gas Shift Reaction Testing

Water-gas shift reaction testing using the Sud-Chemie T-2822 shift catalyst was started in August 2007. The approximate composition of the Sud-Chemie T-2822 shift catalyst used for the water-gas shift testing is shown in Table 5-5.

Table 5-5. Water-Gas Shift Catalyst Properties.

Catalyst Supplier	Sud-Chemie	Johnson Matthey
Catalyst Trade Name	T-2822	Katalco K8-11
Chemical Composition		
Aluminum Oxide Content, wt %	50-70	
Magnesium Oxide Content, wt %	15-35	
Molybdenum Oxide Content, wt %	5-15	10
Cobalt Oxide Content, wt %	1-10	4
Calcium Oxide Content, wt %	3-7	

5.7.1 Catalytic Filter Elements

Tests in the Syngas Cleanup Slipstream Unit. For water-gas shift (WGS) testing using catalytic filter elements, the T-2822 WGS catalyst was pulverized and sieved into a particle size range of 180 to 500 microns for packaging in an iron aluminide filter element. This testing was conducted during the initial portion of TC23 when the gasifier was operating on PRB coal. Testing with the catalytic filter element showed a need for increased catalyst material due to difficulties controlling the low gas flow rate. Pressure typically ranged from 150 to 200 psig, and temperatures varied from 500 to 600ºF, with a short period of testing done at temperatures up to 800ºF. The syngas flow rate ranged from 6 to 30 lb/hr, and the steam flow was varied from 0 to 6 lb/hr. Post run inspections revealed that the pulverized catalyst had changed color from pale green to black due to in-situ sulfidation.

In February 2008, testing of the catalytic filter elements for the WGS reaction was continued and 40 hours of operation on syngas was achieved. Two catalytic filter elements were installed in parallel to test the Sud-Chemie T-2822 shift catalyst and the Johnson Matthey Katalco K8-11 shift catalyst. Table 5-5 lists the catalyst properties. During the outage preceding TC24, the catalysts were pre-sulfided using a gas mixture of 5 percent H_2S and 95 percent H_2 to convert the cobalt and molybdenum, the active ingredients of the catalyst, to the sulfided form. The pre-sulfidation was performed at 200 psig and 660°F. After the pre-sulfidation was completed, the catalysts were pulverized and sieved to a particle size of 106 to 212 microns and then packed in iron aluminide filter elements.

While operating on syngas, the operating conditions were varied to evaluate the performance of the catalytic filter elements. The inlet temperature was varied from 450 to 850°F, and the pressure ranged from 150 to 160 psig. The face velocity was varied between 1 and 3.6 ft/min, and the H_2O-to-CO molar ratio was varied from 0.8 to 6.2 mole/mole.

The CO conversions ranged from 5.3 to 94.4 percent for the T-2822 catalyst during 30 hours of testing, while the CO conversion for the Katalco K8-11 catalyst ranged from 10.5 to 75.4 percent during 10 hours of testing. The CO conversion was dependent upon operating temperature, face velocity, and catalyst type. Figure 5-1 presents the data collected during the T-2822 catalyst testing, which shows a positive linear relationship for two different face velocities with a H_2O/CO ratio of 4.5 to 6.0 mole/mole. The data demonstrated the expected trends of increasing conversion with increasing temperature and increasing conversion with decreasing face velocity. Figure 5-2 shows the positive linear relationship for the K8-11 catalyst at a face velocity of 1.3 to 1.9 ft/s and a H_2O/CO ratio of 4.5 to 6.0 mole/mole.

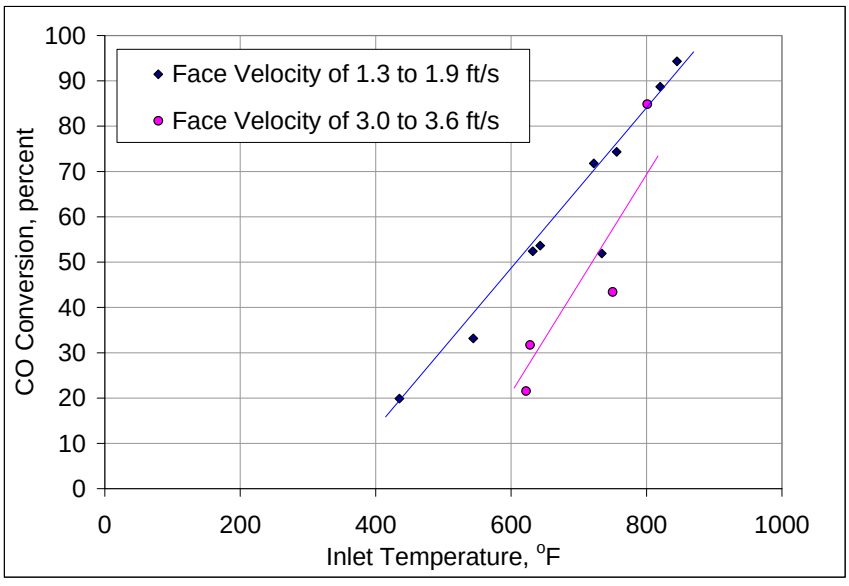

Figure 5-1. Sud-Chemie T-2822 Shift Catalyst Performance.

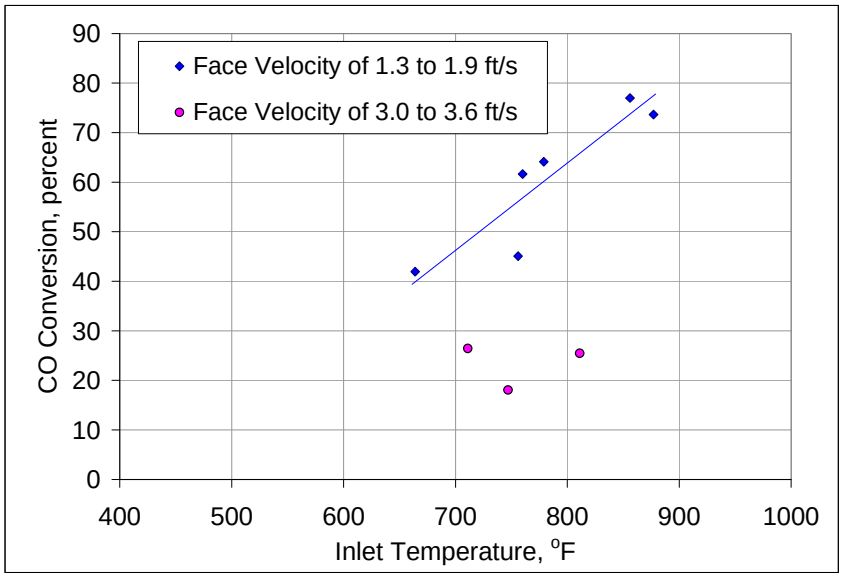

Figure 5-2. Johnson Matthey Katalco K8-11 Shift Catalyst Performance.

Figure 5-3 compares the performance of the two catalysts over a range of temperatures at face velocities from 1.3 to 1.9 ft/s and H_2O/CO molar ratios ranging from 4.5 to 6.0. Based on this data, the T-2822 catalyst performed slightly better than the K8-11.

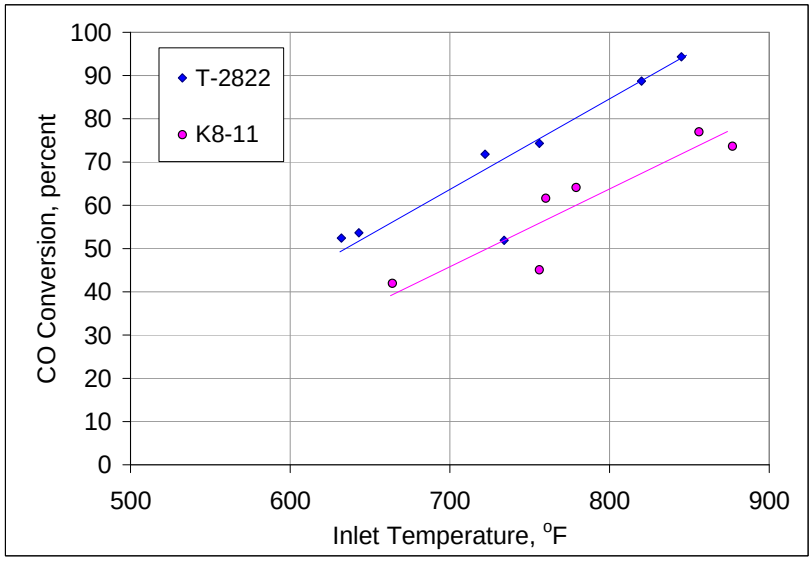

Figure 5-3. T-2822 and Katalco K8-11 Shift Catalyst Performance Comparison.

The catalytic elements were tested again during the July 2008 test run (TC25) for about 538 hours in the syngas cleanup unit. Two filter elements, one with an inner tube filled with the Sud-Chemie shift catalyst and one with an inner tube of the Johnson Matthey shift catalyst, were installed in a pressure vessel. During the outage preceding TC25, the catalysts were pre-sulfided as described previously. After the pre-sulfidation was

completed, the catalysts were pulverized and sieved to a particle size of nominally 100 to 200 microns and then packed in iron aluminide filter elements, with an annular surface layer approximately 1 cm thick. While operating on syngas, the operating conditions were varied to evaluate the performance of the catalytic filter elements. Table 5-6 gives the operating conditions during the catalyst testing.

Table 5-6. Water-Gas Shift Catalyst Test Conditions.

Shift Catalyst	Sud-Chemie T-2822	Johnson Matthey K8-11
Syngas Exposure Time	162	372
Operating Pressure, psig	150 to 200	150 to 200
Operating Temperature, ^{o}F	600 to 800	650 to 780
Syngas Flow Rate, lb/hr	50	25 to 50
Steam Flow Rate, lb/hr	5	0
Filter Element Face Velocity, ft/min	2.4 to 3	0.8 to 2.5
H_2O-to-CO molar ratio	2.4 to 3.4	0.8 to 1.2
Shift Conversion, percent	22 to 94	20 to 50

Figure 5-4 and Figure 5-5 show the Sud-Chemie and Johnson Matthey Katalco catalysts, respectively, before and after testing in TC25B. Sintering seen in Figure 5-5 (after testing) was due to a thermal excursion (as described below) that occurred prior to syngas testing. After the thermal excursion, the Sud-Chemie catalyst in the filter element was replaced, and the Johnson Matthey catalyst in another filter element in the same pressure vessel was not replaced.

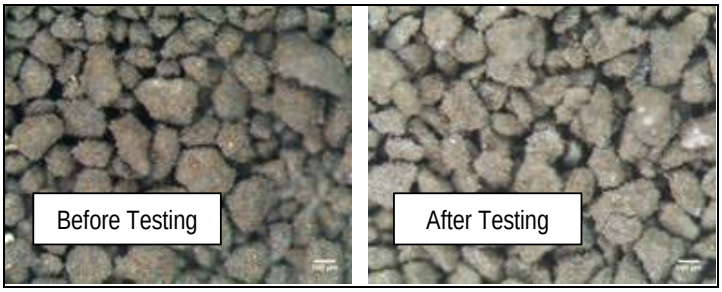

Figure 5-4. Photomicrographs of Sud-Chemie T-2822 Shift Catalyst before and after Testing.

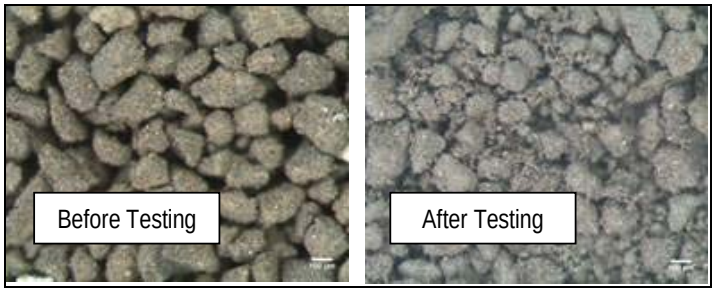

Figure 5-5. Photomicrographs of Johnson Matthey Katalco K8-11 Shift Catalyst before and after Testing.

Catalytic Filter Elements in the PCD. Three catalytic filter elements were installed in the process PCD for operation during the July 2008 run. The elements inner tubes were filled with the Sud-Chemie catalyst. During the first portion of the test campaign, thermocouples on these elements indicated a thermal upset, as shown in Figure 5-6. High temperatures were not measured on other PCD filter elements. The upset occurred during the time of combustion mode operation for removal of syngas cooler fouling when the maximum oxygen concentration in the PCD inlet gas was 1.8 mole percent.

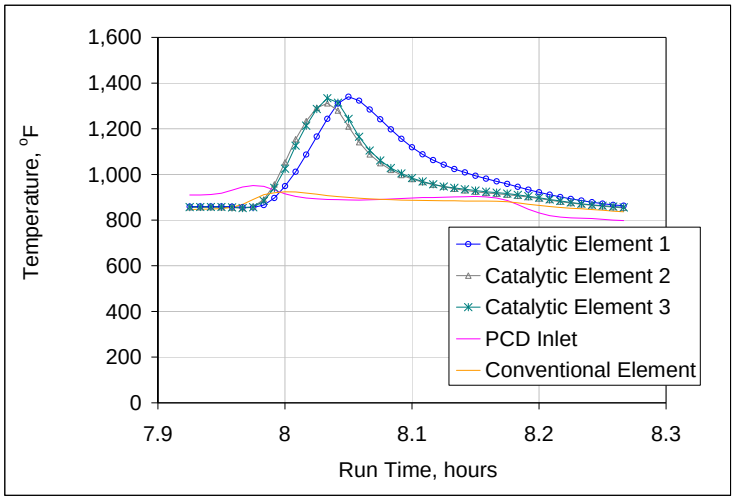

Figure 5-6. Catalytic Filter Element Temperatures during Thermal Upset at Hour 8.

During the subsequent system restart, the same PCD catalytic filter element thermocouples indicated a dramatic temperature increase, which is shown in Figure 5-7. As before, the thermocouples on these filter elements read higher than any other PCD thermocouples and exceeded the high end of their scale of 2,000°F. This temperature upset occurred when the measured oxygen level was below three percent.

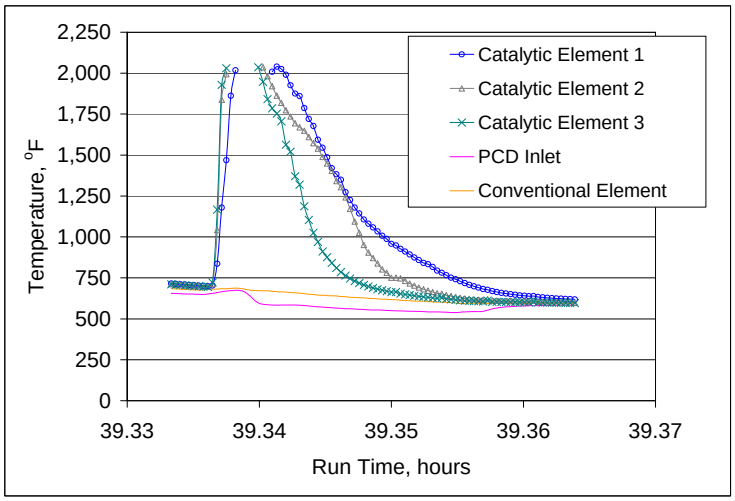

Figure 5-7. Catalytic Filter Element Temperatures during Thermal Upset at Hour 39.

The thermal transients were apparently caused by a highly exothermic reaction of sulfide oxidation. After the catalyst material (which had been pre-sulfided prior to installation) was exposed to a reducing atmosphere, it became highly reactive with oxygen. The catalytic elements were removed from the PCD during an 8-day outage. The catalytic elements remained in the syngas cleanup unit for further testing, since in the cleanup unit, the elements could be isolated from process gas flow during re-starts when oxygen is present at low concentrations.

5.7.2 Fixed Bed Reactor

Fixed bed reactor testing of water-gas shift was also conducted during gasifier operation with PRB coal and employed the T-2822 catalyst in pellet form. Operating pressures ranged from 110 to 190 psig with temperatures of 550 to 800°F. Syngas flow through the fixed bed reactor ranged from 15 to 30 lb/hr while steam flow rates varied between 0 and 18 lb/hr. Approximately 22 hours of testing with the fixed bed water-gas shift reactor was completed, and this preliminary testing gave results of 40 to 88 percent shift conversion, with higher rates achieved at higher temperatures. Inspections showed that the pelleted catalyst had also changed color from pale green to black, as the active material in the catalyst changed to a sulfided form.

5.8 NETL Fuel Cell Module

In February 2008 the NETL Fuel Cell Module utilizing solid oxide fuel cell (SOFC) technology was installed at the PSDF, and shakedown tests were successfully completed. Figure 5-8 is a photograph of the Fuel Cell Module during the completion of installation.

Figure 5-8. NETL Fuel Cell Module.

The Fuel Cell Module is a multi-cell array (MCA) mobile platform developed to test different solid oxide fuel cells in parallel on coal-derived syngas. The unit was designed to enable testing for up to 12 individual fuel cells simultaneously over a range of electric load conditions for extended periods of time to provide data on the influence of trace coal

contaminants such as arsenic, phosphorous, selenium, and mercury on fuel cell performance. This information is critical for development of fuel cells for coal-based power generation.

The shakedown tests were performed on bottled hydrogen gas and lasted for over 100 hours. The test cells were operated at an average temperature of 1,400°F with 68 mole percent H_2 and 32 mole percent H_2O. At initial hydrogen feed, eight cells produced output indicative of proper operation; however, only five cells were functioning properly by the end of the 100-hour test. Cell 7, which was typical of the five operating cells, had a current density of about 150 mA/cm^2 and steadily maintained a voltage of about 0.73V.

After the initial shakedown tests were completed, new button cells were loaded. The module was then re-started. The two subsequent re-starts initially demonstrated good cell response, but through the first 24 hours, cell failure reduced the number of operable cells. Diminishing cell operation was attributed to seal failure and thermal degradation of the current collecting wires. Needed improvements to the seal method were identified.

Testing of the NETL fuel cell module continued in July 2008. NETL researchers continued field modifications to resolve previously identified issues related to gas seals and current leads. Following the repair, a brief 30 hour test run was successfully conducted on hydrogen and syngas on 3 of the 12 cells in the MCA. With this success, the MCA was shut down in order to rebuild all 12 cells. The test was successfully restarted with hydrogen as the fuel with 11 of 12 cells in good condition. Unfortunately, an attempt to load the current failed due to an unexpected high resistance possibly due to corrosion on the cathode nickel current leads. Replacement of the nickel leads with sliver leads resolved this issue, and testing was restarted with hydrogen fuel. After the cells stabilized, the testing transitioned to syngas fuel for the remaining duration.

Analyses for low-level sulfur compounds, hydrocarbon content, and feed gas composition were supplied during this testing effort. The chiller unit allowed for continuous sulfur and composition analyses during fuel cell operation. FTIR samples taken once a day to verify the operation of a hydrocarbon cracking catalyst. Other services included provision of compressed gas supplies (hydrogen and liquid argon) and the construction of gas manifolds for the uninterrupted delivery of hydrogen.

After NETL researchers resolved issues previously identified, the solid oxide fuel cell (SOFC) MCA was restarted successfully with hydrogen fuel and switched to conditioned syngas in August. Fuel cell operation on syngas lasted for a total of 200 hours and shut down eight days later as planned. The experience gained and data collected through the combination of the exposure and electrochemical tests under real syngas conditions should yield valuable information to assist in future SOFC technology development fueled on coal derived gas. During this period, a NETL modified gas chromatograph with inductively coupled plasma/mass spectrometer was also successfully commissioned for accurately measuring syngas trace metals at the sub-ppm level.

The fuel cell module was dismantled and shipped back to NETL. This marked the conclusion of the SOFC test project. During this test period (January 31 through August 13, 2008), PSDF provided support to the project on many fronts including project coordination, equipment installation and dismantling, gas supply and analysis, test stand repair, and necessary test monitoring.

5.9 Media Process and Technology Carbon Molecular Sieve Membrane

An advanced carbon molecular sieve (CMS) membrane was installed and commissioned in February 2008. Working in cooperation with NETL, researchers at Media Process and Technology (MPT) developed the membrane, which is highly selective for hydrogen and particularly well suited for coal-derived syngas. The membrane separates hydrogen from syngas with membrane materials that were extensively lab-tested. The objective of the testing at PSDF was to evaluate material stability of the membrane under gasification conditions with particulate-free coal-derived syngas containing both major and minor contaminants including hydrocarbons at the parts per million level. Figure 5-9 is a photograph of the CMS membrane installed at the PSDF.

Figure 5-9. MPT Carbon Molecular Sieve Membrane Installed at PSDF.

After installation, the membrane unit was connected to a slip stream of syngas from the process that utilized bottled H_2 to increase the hydrogen content of the syngas. Upon review of the system, modifications to the control system were made. Two low flow switches were installed and interlocked with the existing trip-monitoring device to stop syngas flow to the unit if purge nitrogen flow was lost to the main process cabinet or to the H_2 bubbler flow meter box. In addition, the emergency shutdown logic was reprogrammed to ensure a proper shutdown in the case of loss of power. Due to delays associated with modifying the system and with gasifier operation, testing with syngas was postponed to the test run in July 2008.

The advanced CMS membrane was re-installed and tested in July 2008. MPT successfully tested a single tube of the CMS on syngas with and without hydrogen augmentation. For the raw syngas without enrichment, the hydrogen concentration was 8 to 10 percent in the feed and 40 to 50 percent in the permeate. For enriched syngas, the

hydrogen concentration was 18 to 20 percent in the feed and 80 to 90 percent in the permeate. Overall, the CMS membrane was exposed to nearly 19 hours of syngas or hydrogen-enriched syngas. Although there were some minor operational upsets and difficulties in conducting in-situ gas permeance and selectivity measurements, the permeance and selectivity results suggest that the membrane performance was stable during the test and unaffected by contaminants in syngas. MPT will complete further data analysis. This was the first time a hydrogen-selective membrane was successfully operated on untreated coal-derived syngas.

PSDF personnel provided gas analytical services and sampling support to MPT for this test. Initially, a gas chromatography (GC) instrument was modified for the analysis of the membrane permeate stream (which contained high hydrogen concentrations). After it was determined that accurate monitoring could not be achieved with a single GC, an automated laboratory GC instrument(Agilent 5890) was put into service to monitor the membrane reject stream. New sample conditioning systems were fabricated and installed when it was determined that the conditioning systems of the membrane skid were not adequate. Smaller "knock out" pots were also supplied to supplement the membrane skid's internal conditioning system. These smaller cylinders decreased the analysis response time by 80 percent. Other services and equipment provided to MPT included overall project coordination, skid installation and removal, and various interface connections.

5.10 CO_2 Capture

Preliminary CO_2 capture testing started in August 2007. Carbon dioxide capture from syngas was performed in a batch reactor at approximately 110ºF for a few hours with syngas from the fixed bed, water-gas shift reactor. The initial commissioning test with syngas was short due to problems associated with the condensate removal system in the inlet syngas line but the data showed a decrease in CO_2 concentration, meriting additional tests.

Prior to syngas testing, kinetic tests with the bench scale reactor were performed using bottled CO_2 and nitrogen. The data generated from the bench scale reactor was used as a guide for the design of a continuous pilot reactor for CO_2 capture. In addition, preliminary solvent/additive screening tests for CO_2 capture from flue gas at low pressure were performed. Initial results indicate that the amines such as piperazine were the most effective solvents for CO_2 capture from flue gas at low pressure.

In July 2008, about 40 absorption and 40 regeneration tests were performed with the bench scale Parr reactor to capture syngas CO_2. During testing, parameters such as temperature, pressure, gas flow rate, and solvent concentration were varied to determine the optimum operating conditions for the absorber and regenerator. The syngas CO_2 concentration varied from nominally 10 to 15 percent. Preliminary analysis showed promise for high CO_2 capture efficiencies.

5.11 Johnson Matthey Mercury Sorbent

A Johnson Matthey mercury sorbent composed of palladium was tested in the syngas cleanup unit to capture mercury and other trace metals present in the syngas in July 2008. Pre-treatment of the catalyst involved reduction for 2.5 hours with hydrogen (diluted with nitrogen) at a pressure of 100 psig and a space velocity of 2,120/hr. The temperature was ramped from 86 to 212°F at a rate of 3.6°F/min, followed by a one hour hold at 212°F. The temperature was then increased from 212 to 500°F (increased at a rate of 9°F/min) with a one half hour hold at 500°F.

The mercury sorbent was exposed to 500°F syngas over a period of 330 hours, 260 hours with hydrocarbon cracking and 70 hours without hydrocarbon cracking. The syngas samples were collected in the inlet and outlet of the mercury sorbent reactor for the analysis of mercury and other trace metals using a modified EPA Method 29. Depending on sample flow, sampling times ranged from 2 to 5 hours. Results indicated high capture of mercury. During the test, the pressure ranged from 150 to 200 psig, the syngas flow ranged from 25 to 50 lb/hr, and the space velocity varied from 1,500 to 3,700/hr.

6.0 INSTRUMENTATION, SAMPLING, AND CONTROLS

Because of the research nature of the PSDF and the unique process conditions, significant effort went into the development of instrumentation, solids and gas sampling systems, and process controls. Instrumentation development focused primarily on coal feed measurements, gasifier operation, and particulate monitoring. Solids and gas sampling involved development of specialized components, and PSDF sampling specialists incorporated numerous enhancements to sampling methods. Highlights of the process control development included Transport Gasifier controls and implementation of a safety interlock system (SIS).

6.1 Coal Feed Rate Measurements

An on-going area of sensor development at the PSDF has been accurate measurements of feed rates from the two dry coal feed systems. Both feed systems, the original and developmental systems, were installed with feeder weigh cells, which provided reasonable accuracy. However, since the feed rates calculated from the weigh cell measurements are averages over time and not instantaneous indications, measurements that are more responsive were needed for control of gasifier temperature and safety interlocks. For process controls, the needed measurements would supply:

- Coal/no coal indication (instantaneous indication of coal stoppage)
- Fast response (on the order of 2 seconds)
- Load change stability
- Process upset recovery

Some of the challenges experienced with accurately measuring dry coal rates include:

- Inhomogeneous solids distributions in feed lines
- Irregular velocity profiles (horizontal conveying, particle settling, etc.)
- Variable particle size and moisture content

6.1.1 Granucor Coal Rate Measurement

The Granucor coal rate measurement from Thermo Electron Corporation was installed on the developmental coal feed system. The instrument uses two sensors: the first to measure capacitance (which is correlated to density), and the second to measure velocity using a statistical process of cross-correlation.

This coal rate measurement was sensitive to coal type, and changes in coal type required changes in instrument settings. The coal moisture content also affected measurements. Most of the problems in obtaining consistent measurements were sensor failures, particularly with the velocity sensor. A positive aspect of the Granucor measurement is its sensitivity to changes in feed rates, and of the measurement methods tested at the PSDF, the Granucor proved to be best for instantaneous indications of coal stoppages.

6.1.2 Nuclear Densitometers

Tangential/Perpendicular Measurements with Original Feeder. For coal measurements with the original coal feed system, the nuclear instrument selected was the MeasureTech NDMi. This unit utilizes a 50 milli-curie source and a scintillation detector suitable for small pipe diameters. One densitometer was installed horizontally in the feed line and the other in the vertical to improve measurement accuracy and to provide saltation (settling of solids in the piping) information in addition to average density. This coal flow rate measurement incorporated an estimated velocity from conveying gas flow rate and pipe size, assuming little or no slip.

Several challenges were experienced with this coal rate measurement. Because of the small pipe size (1 inch outer diameter), the noise associated with the nuclear measurements was large in proportion to the measurements. Saltation in the line caused inconsistency in the horizontal portion of the measurement. Frequent recalibration proved necessary, and the instrument showed low accuracy for flow rates below 1,000 lb/hr. Operation showed a lengthy time delay for noise reduction and a slow instrument response.

Annular Measurement with Developmental Feeder. With the development coal feed system, the approach to nuclear instrumentation incorporated an annular measurement to reduce the signal-to-noise ratio compared to the tangential/perpendicular measurements used with the original coal feed system. The instrument measures the coal rate over a three-foot portion of pipe. Figure 6-1 is a schematic of the densitometer on the original coal feed system.

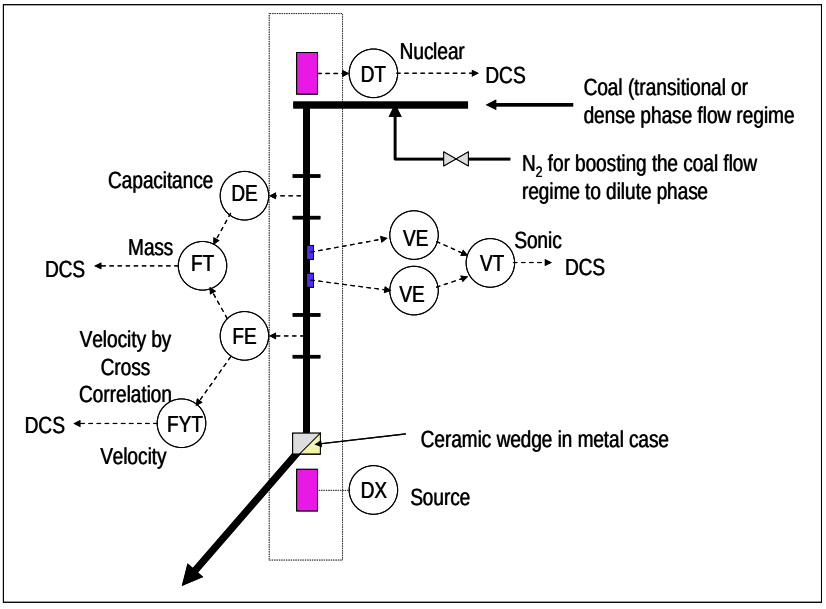

Figure 6-1. Schematic of Nuclear Densitometer Layout for Developmental Coal Feed System.

Figure 6-2 plots the coal feed rate measurement based on the weigh cell calculation and the nuclear densitometer. There was reasonable agreement with the two measurements.

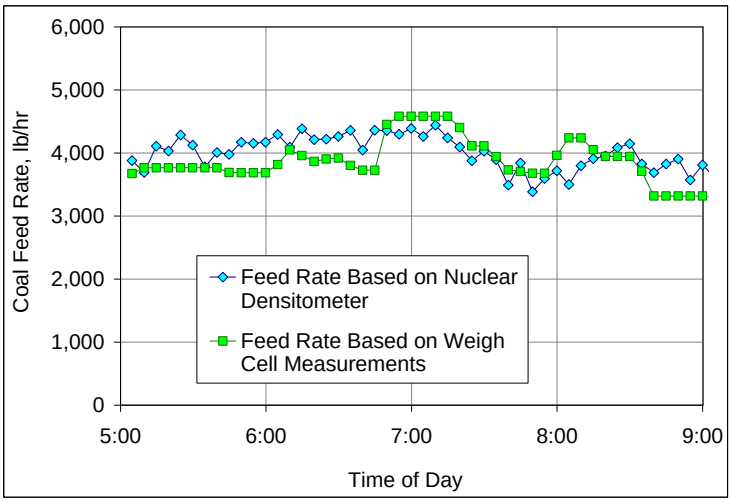

Figure 6-2. Coal Feed Rate Measurements.

6.2 Gasifier Pressure Differential Indicators

The gasifier pressure differential indicators (PDIs) are necessary for monitoring the gasifier solids inventory and solids circulation. The major challenges with these instruments include high purge flow requirements and plugging of the impulse lines.

Ceramic Inserts. To reduce instrument purge flow requirements by over 50 percent and reduce plugging problems, ceramic tips, manufactured by Foreman Instrumentation and Controls, were installed on three gasifier PDIs. Figure 6-3 provides a schematic of one of these ceramic tips.

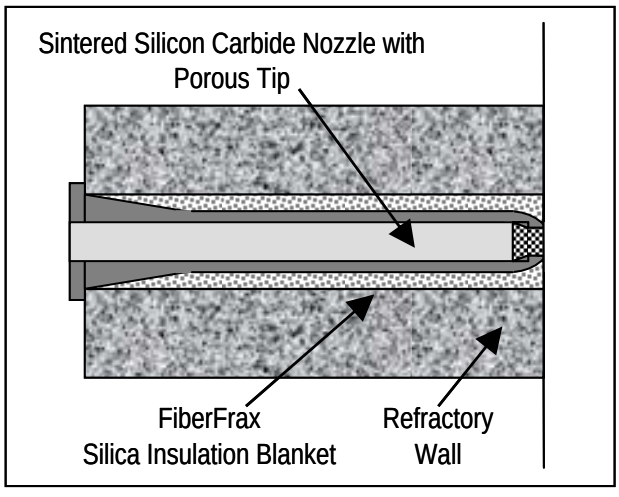

Figure 6-3. Schematic of Ceramic Tip for Pressure Differential Indicator.

Testing of the ceramic tips occurred from 2005 to 2007, with installation of two PDIs in the gasifier riser and one PDI in the solids separation unit. The ceramic tips on the riser were the SGC05 design, a high differential pressure, low purge flow design. The solids separation device PDI was fitted with MAC10 inserts, a low differential pressure, high purge flow design.

When plugging did not occur, measurements with the ceramic tipped purge ports compared well with the standard measurements, as indicated in Figure 6-4. The two SGC05 designs compared well to standard PDI measurements in similar locations. The MAC10 data in Figure 6-4 did not compare as well to the standard measurement since the purge ports were located at slightly different elevations on the seal leg. Although the distance between the ports was the same, the test ports were approximately one foot lower than the standard measurement. Variability in the density in this region caused a difference in calculations. However, the test PDI showed promise since the ports did not plug in this area of high solids concentrations.

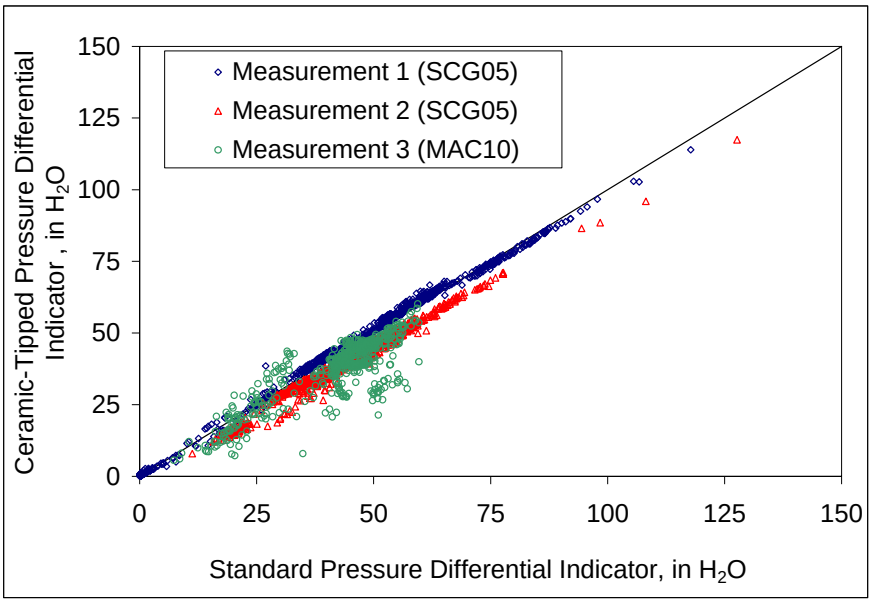

Figure 6-4. Measurements of Ceramic-Tipped Pressure Differential Indicators Compared to Standard Pressure Differential Indicators.

Overall, the low differential pressure design matched conventional measurements well, but the high differential pressure design often plugged due to nitrogen purge flow control difficulties. Installation of low nitrogen flow meters was investigated as a way to improve performance, but further testing of the ceramic tips was suspended because of the high material cost and the limited potential for commercial applications.

6.3 Gasifier Thermocouples

Gasifier thermocouples are critical for monitoring gasifier performance, for providing input for control logic, and for automation of parameters such as air flow rate and coal

feed rate. The primary concern of thermowell performance in the Transport Gasifier is excessive wear of the tip exposed in the gasifier from solids erosion and/or corrosion. Maximizing thermocouple lifetime was the focus of thermocouple testing. To improve gasifier thermocouple longevity, testing included thermocouple configurations, insertion lengths,and thermowell materials.

6.3.1 Configurations

Spoilers. A thermowell configuration utilizing a Sailon spoiler inserted at a steep angle lasted five hours more than one without a spoiler at the same location in the gasifier. The temperature deviation using the spoiler was almost 100°F at times. The Sialon spoiler did not show any noticeable signs of wear, but additional testing was not conducted due to the high temperature measurement error caused by the spoiler.

Insertion Lengths. Temperature measurements in gasifiers are traditionally made by estimating center temperature from refractory wall temperature measurements. While this is an acceptable method for slagging gasifiers, it does not provide the accuracy needed for operating non-slagging gasifiers such as the Transport Gasifier. Several insertion lengths (0, 2, 5, and 8 inches) were tested in an effort to balance accuracy and thermocouple longevity. Based on the different insertion lengths tested, it was determined that a 2-inch insertion beyond the refractory wall plane was sufficient for 0.75-inch thermowells. There was no difference in accuracy between the measurements made at insertion lengths from 2 to 8 inches.

6.3.2 Thermowell Materials

Several thermowell materials were tested in the gasifier, including ceramic, HR-160, and Stellite-coated Hastelloy-X materials. Testing with the ceramic and HR-160 materials continued for long-term testing, but testing of Hastelloy-X was discontinued after a short period due to its poor performance. In general, thermowell life and thermocouple reliability improved following the 2006 gasifier configuration modifications, which allowed operation of the gasifier at significantly lower velocities.

Ceramic Thermowells. Operation with the ceramic thermowells demonstrated high resistance to corrosion and erosion. The ceramic thermowells operated a few thousand hours and showed only minimal wear on the thermowell tips. However, failures incurred during removal of the thermowells was a concern. Figure 6-5 shows a ceramic thermowell that was broken during removal. The tip of this element did not show significant wear.

Figure 6-5. Ceramic Thermowell Damaged during Removal.

Testing of the ceramic elements continued over time, but further development of this thermowell material was not pursued because of its brittleness and high cost compared to metal materials.

HR-160 Thermowells. The most promising and extensively tested thermowell material was the HR-160 metal fiber media. During initial HR-160 testing, several types of coatings were utilized, including complex oxides, chrome carbide, tungsten carbide, zercinium oxide, alumina titania oxide, Wallex 50, and Colmonoy 88. None of these coatings markedly improved the durability of the HR-160 thermowells, so only testing of the HR-160 material alone was continued.

The HR-160 material was generally durable, and thermocouple failure was minimal. However, some significant wear was found on thermocouples during test campaigns with erratic gasifier flow patterns. For example, several elements had shown some wear when exposed to high velocities due to deposit formations in the mixing zone during two test campaigns in 2006 and 2007 (TC21 and TC23). The tip degradation was severe, with wear to the inner sheath. Figure 6-6 is a typical example of these worn thermocouples, photographed during post-TC21 and –TC23 inspections.

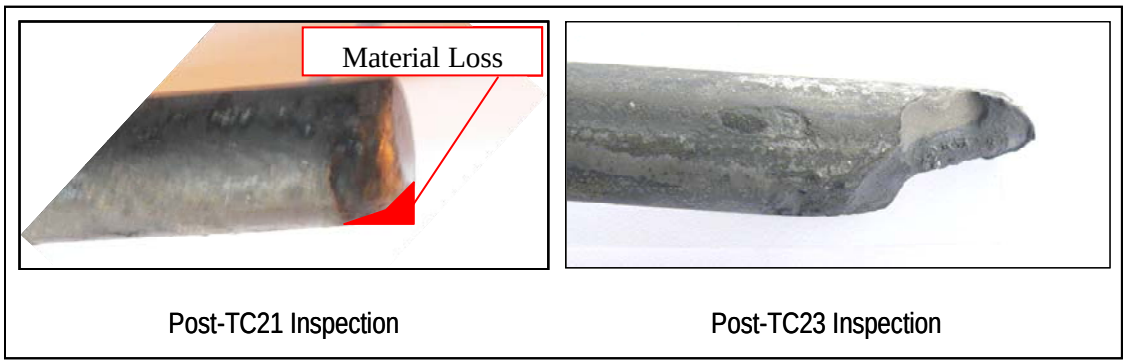

Figure 6-6. Post-TC21 and Post-TC23 Inspections of Worn HR-160 Thermowell.

Metallurgical analysis of the worn HR-160 elements indicated that sulfur species may have attacked the nickel contained in the HR-160. The increased gasifier solids particle size and hardness from kaolin sorbent addition may have accelerated the thermowell tip degradation in TC23.

During normal gasifier operations with steady solids circulation, performance of HR-160 elements proved to be reliable. Element failure was atypical, and inspections showed only minimal wear. A typical example of these elements is shown in Figure 6-7.

Figure 6-7. HR-160 Thermowell Showing Minimal Wear.

6.4 Gasifier Velocity Measurements

During two test campaigns, Promecon velocity probes were installed to procure direct measurements of the gasifier velocity. During the first of these tests, the probes gave reasonable results during the gasifier start-up period with sand circulation. However, the probes stopped functioning after a short period of on-coal operation.

During the second of these tests, six Promecon velocity probes were fitted with ceramic tips and pressure resistant seals and installed at varying lengths in the riser. The probes ceased to give output early in operation, and subsequent inspections showed that the ceramic tips had been severely damaged. Further testing was not pursued.

6.5 Real-Time Particulate Monitoring

Two real-time particulate monitors—the PCME DustAlert-90 and the Process Particle Counter (PPC) from Process Metrix—were tested extensively in the development of on-line particulate monitors for detection of very low levels of particulate at the PCD outlet.

6.5.1 PCME DustAlert-90

The PCME DustAlert-90 particulate monitor (referred to as the PCME) was used throughout gasification operation to monitor particulate concentrations by measuring the naturally occurring electrical charge on the particles. This instrument is all electronic (with only a simple metal rod in the gas stream) and proved to be reliable over many test campaigns with little maintenance required. The PCME instrument output was adaptable to a discrete alarm, which was set to alarm when the output was above 15 percent for more than 30 seconds. These alarm settings proved adequate for alerting operators while not producing nuisance alarms.

Although the PCME does not provide actual concentrations, routine calibration testing using solids injection yielded repeatable data for conversion of the PCME output to particulate concentration. Figure 6-8 provides a plot of the PCME output during a solids injection test. The background particle concentration before injection started is detectable only during the spike of particulate that occurs after a backpulse and is

indicated by a spike associated with backpulse cleaning the PCD. The average output of the PCME during the solids injection period was 3.84 percent. The average for the hour before the start of the injection test (the background level) was 0.04 percent. Comparison of these values indicates an increase of 96 times in the PCME output attributable to injection of solids.

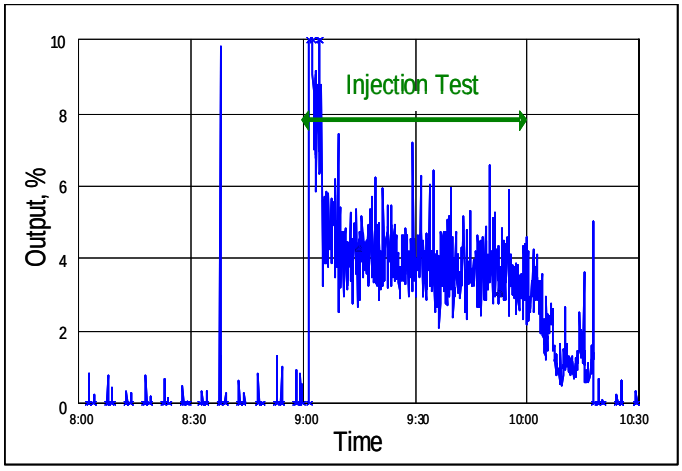

Figure 6-8. PCME Particulate Monitor Output during Solids Injection Test.

Figure 6-9 is a plot of the relationship between actual particulate concentrations (from in-situ measurements) and the PCME output for several test campaigns using PRB coal.

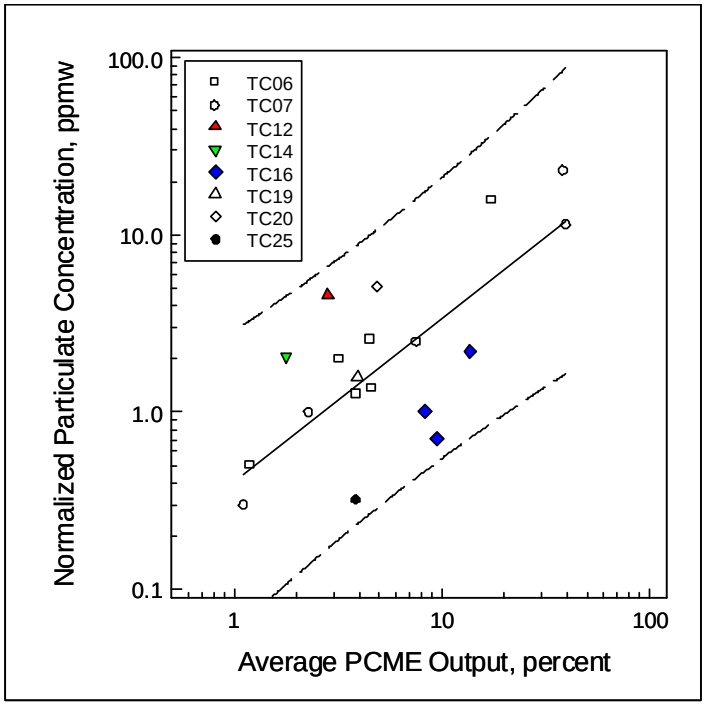

Figure 6-9. Comparison of PCME Particulate Monitor Response to Actual Mass Concentration.

Within individual test campaigns, there was generally good linear agreement, but overall the historical results are quite scattered since a differences in particle size distribution affect the PCME response. Since the instrument measures electrical charge on the particles passing nearby, other immeasurable factors may affect the sensitivity of the instrument. Calibration testing also showed that the PCME is limited to detection of particles greater than approximately 30 microns.

The PCME is a simple and effective instrument that has reliably indicated the presence of significant PCD leaks. It is not sensitive to very small leaks when there are no large particles present nor is it effective as an indicator of outlet particle concentrations. However, because of its low cost and low maintenance requirements, it is a useful instrument in appropriate applications.

6.5.2 Process Metrix Process Particle Counter

The PPC instrument system is a light-scattering single particle counter operating on an extracted syngas sample at the outlet of the PCD. The optics in the counter were optimized to the range of particle sizes from 2.5 to 75 microns, which is the range of particles resulting from PCD leaks. Though the use of a single particle counter has the potential to provide measurements at low concentration, the very low particle counts at the PCD outlet during normal operations caused inaccurate measurements.

Several critical improvements were made to this measurement system. The system optics were modified to produce a particle counting volume about 8 times larger than the original. This increased the numbers of particle counts by 8 times, but decreased the ability to measure high particle concentrations. In addition to modifying the optics to increase particle counts, the software was modified to provide an output of total particle counts to allow improved tracking of low concentrations in near real-time. The normal output of the PPC is a calculated total particle mass concentration in mg/acm. The mass calculation algorithm developed by Process Metrix requires a minimum number of counted particles in a number of size ranges during an integration period to calculate the mass concentration in the syngas. Therefore, during initial testing, long integration times were required with the loss of near real-time data, and in many cases there were not sufficient particles to conduct the calculation.

The output of the PPC during gasification testing when collection efficiency was high (low particle count) is shown in Figure 6-10. The graph shows both the particle count and the calculated mass concentration for a 20-minute period. The particle count was a continuous trace with large spikes when the PCD was backpulsed. With the 10-second integration time used during this test, the particle mass concentration was calculated for the backpulse spikes and thus is a non-continuous trace. From this graph, the particle count was high during a backpulse, indicating that particle penetration occurred during the backpulse. However, interpretation of mass concentration data is more problematic. The average concentration over the entire 20-minute period shown was 0.08 mg/acm, while the spikes are only slightly higher than this and are of short duration. This result is a function of the calculation method and the high peak to average concentration values.

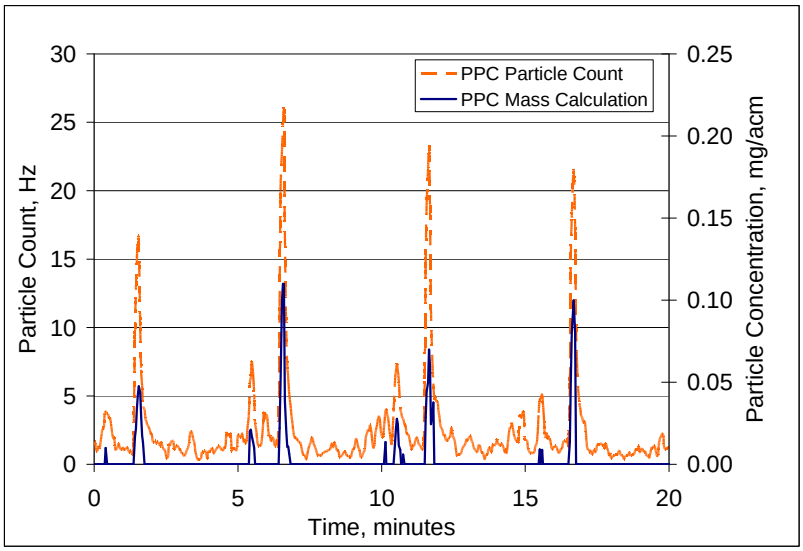

Figure 6-10. PPC Particulate Monitor Output during Low Particulate Loading.

Values of mass concentrations calculated by the PPC are compared with in-situ particle measurements in Table 6-1.

Table 6-1. Comparison of PPC and In-Situ Concentrations.

Date	Outlet Run No.	Start Time	End Time	PPC				In-Situ Loading ppmw
				Loading,		Mass > 10 microns		
				mg/acm	ppmw	% of Total	ppmw	
7/21/08	7	8:45	12:45	0.028	0.004	81.20	0.003	<0.1
7/22/08	8	8:30	12:30	0.040	0.005	88.34	0.005	<0.1
7/23/08	10	9:00	13:00	0.048	0.007	88.71	0.006	<0.1
7/24/08	11	8:45	12:45	0.040	0.005	90.23	0.005	<0.1
7/25/08	12	8:45	12:45	0.028	0.004	87.73	0.003	<0.1
7/28/08	13	9:15	10:00	2.42	0.37	82.05	0.305	0.32(1)
7/29/08	14	8:45	12:45	0.024	0.003	83.59	0.002	<0.1
7/31/08	15	8:30	12:30	0.024	0.003	86.43	0.003	<0.1
8/1/08	16	9:00	13:00	0.020	0.003	83.38	0.002	<0.1
8/4/08	17	8:45	12:45	0.016	0.002	84.11	0.002	<0.1
8/5/08	18	9:00	13:00	0.024	0.003	85.55	0.003	<0.1
8/7/08	19	9:00	13:00	0.048	0.006	81.33	0.005	<0.1
8/08/08	20	8:30	12:30	0.032	0.004	77.54	0.003	<0.1
8/11/08	21	8:30	12:30	0.020	0.003	70.78	0.002	<0.1
8/12/08	22	8:30	12:30	0.012	0.002	75.66	0.001	<0.1

Notes: 1. Dust injection for PPC calibration testing.

Except for Run 13, which was measured when the particulate concentration was relatively high because of solids injection in the PCD outlet duct, all the runs were

averaged over 4 hours. Despite the long sample time, the in-situ sampling system was not able to resolve a value below the lower concentration measurement limit of 0.1 ppmw. The concentrations measured by the PPC were comparable and ranged from 0.004 to 0.017 ppmw. Since the PPC values were below the measurement capability of the in-situ samples, the accuracy of the PPC values could not be quantified.

During the solids injection test, the in-situ sampling system indicated a particulate concentration of 0.32 ppmw compared to 0.37 ppmw calculated by the PPC. This is remarkable agreement. The average mass concentration from the PPC in the hour prior to the start of solids injection was 0.005 ppmw, suggesting an increase of 74 times resulting from the injected particulate.

Also shown in Table 6-1 are the percent of mass and the mass concentration that the PPC determined to be larger than 10 microns. These are the particles most likely to damage downstream components due to erosion. The amount of mass larger than 10 microns corresponded to 71 to 90 percent of the total mass, corresponding to 0.001 to 0.006 ppmw, well below the large particle concentration limits published by commercial turbine manufacturers.

The response of the PPC to the solids injection test is shown in Figure 6-11. The steady-state comparison period for the in-situ measurement shown in the table is indicated on the figure. Prior to the start of injection, the background concentration can be seen as discrete small spikes with mass calculation possible only after backpulse spikes. Injection of solids produced a dramatic increase in PPC output, and there was enough mass for a continuous calculation of concentration.

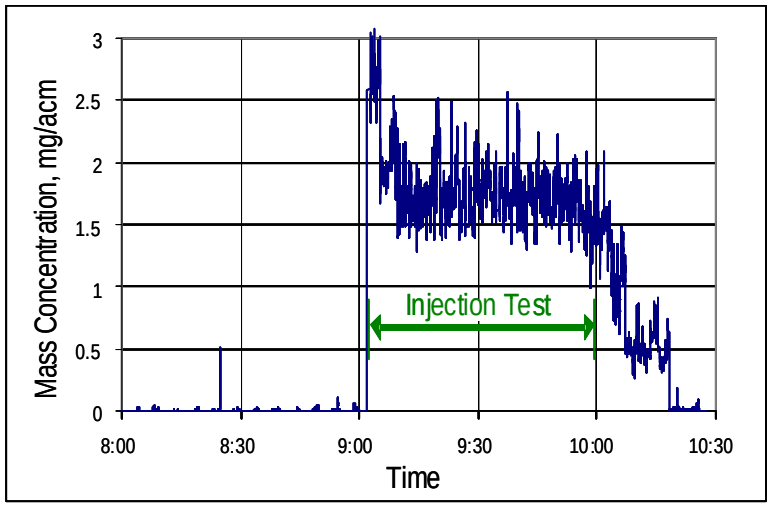

Figure 6-11. PPC Particulate Monitor Output during Solids Injection Test.

The Process Metrix PPC is a complex instrument that requires considerable maintenance to keep it operating correctly. As used at the PSDF, it is an extractive system with a considerable amount of hardware and support equipment. When the PPC is working

correctly, it has much greater sensitivity than the PCME and it is capable of monitoring particle concentrations at low levels. At its current stage of development, it is more of a research tool than a monitoring instrument.

6.6 Solids and Gas Sampling and Analyses

To assess and optimize system performance, extensive solids and gas sampling and analysis are routinely performed during gasification operation. Figure 6-12 shows the sample locations, labeled A through M, which are referenced in the following sections.

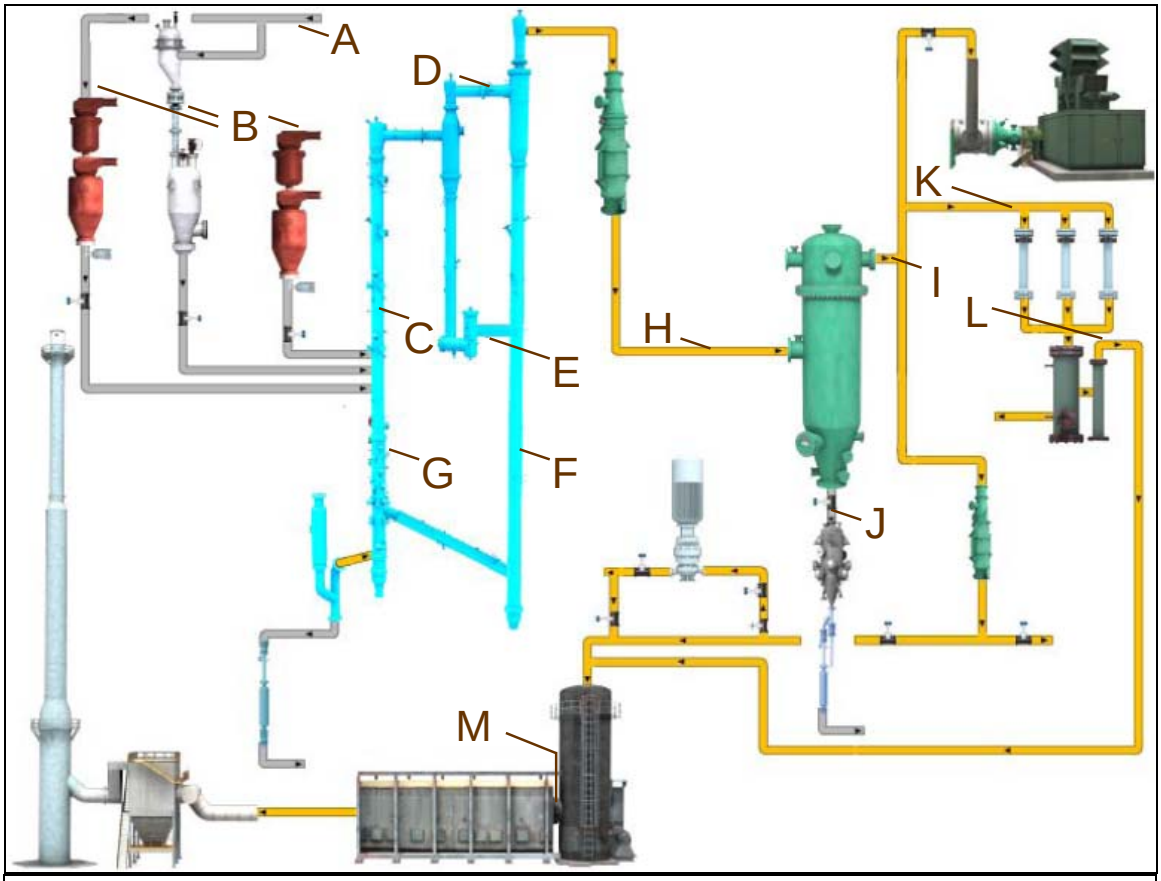

Legend			
A.	Extractive coal samples	B.	Extractive coal and sorbent samples
C.	Gasifier gas bomb and solids samples	D.	In-situ solids
E.	Gasifier solids	F.	Gasifier solids
G.	Gas bomb samples	H.	In-situ solids and continuous syngas analyzers
I.	In-situ solids and syngas moisture	J.	Extractive solids samples
K.	Syngas analyzers, including FTIR	L.	Syngas analyzers
M.	In-situ flue gas analyzers		

Figure 6-12. Sampling Locations of the PSDF Gasification Process.

6.6.1 Solids Sampling

For assessing and optimizing equipment operation, samples of coal, sorbent, and gasification ash are taken routinely. The physical properties of the samples are characterized in an on-site laboratory. Particle size analyses are performed using a Microtrac X-100 analyzer or sieve analysis; moisture values are derived using an MF-50 moisture analyzer; and LOI (loss on ignition) values of gasification ash are taken using a muffle furnace. Chemical analyses of the solids samples are obtained through an outside certified laboratory.

Coal and Sorbent (Locations A and B). Coal samples taken at various locations in the coal preparation area are used to assess coal mill operation and the extent of particle size segregation in the equipment. Samples of coal and sorbent are also taken from the surge bins of the feeders. These samples are used to develop operating envelopes for the feeders as well as to characterize the feed material. Figure 6-13 shows an example of a feeder sample system, which incorporates an auger device located on the original coal feeder surge bin.

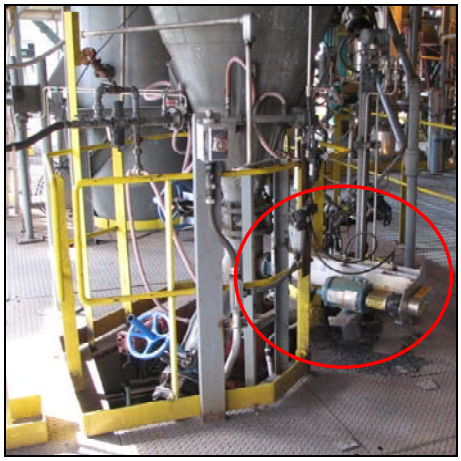

Figure 6-13. Solids Sample System at Coal Feeder Surge Bin.

Gasifier Solids (Locations C, D, E, and F). Gasifier solids are taken from the riser, seal leg, and standpipe portions of the gasifier. These samples are used to characterize gasifier performance and to identify operating conditions that could lead to agglomeration formation. Figure 6-14 is a photograph of a gasifier solids sampling system. These water-cooled systems use collection vessels that are filled by exposure to gasifier pressure.

Figure 6-14. Gasifier Solids Sampling System.

In-Situ Gasification Ash (Locations H and I). In-situ sampling at the PCD inlet is used to measure the concentration of gasification ash exiting the gasifier with the syngas. In-situ samples taken at the PCD outlet measure solids concentrations down to a resolution of about 0.1 ppmw. During outlet sampling, which takes typically four hours, the condensate from the syngas is collected and measured to provide syngas moisture concentration. The sampling systems used at the PSDF were designed (by Southern Research Institute) to collect the particulate in samplers inserted directly into the process gas stream. This in-situ approach ensures collection of the sample under actual process conditions, and that none of the sample is lost or altered during the sampling. Figure 6-15 is a photograph of an in-situ sampling system used at the PSDF.

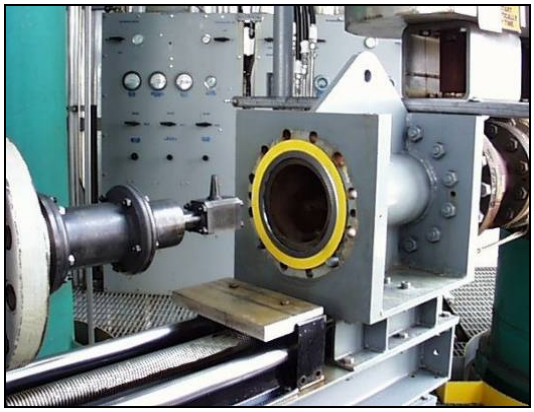

Figure 6-15. In-Situ Particulate Sampling System.

The in-situ sampling is performed routinely during gasification testing. Inlet sampling requires about 15 minutes of unfiltered syngas flow, while about four hours of gas flow at the outlet are needed due to the low particulate concentration. The outlet samples have generally indicated particulate concentrations below the sampling system lower limit of resolution (0.1 ppmw), equivalent to greater than 99.9999 percent collection efficiency of the PCD.

Extractive Gasification Ash (Location J). Bulk samples of gasification ash (PCD solids) are taken at the inlet of the CFAD system. This sample system is similar to the extractive systems on the gasifier, but does not require cooling. Solids are extracted by exposing a collection vessel to the system pressure at the CFAD inlet.

Solids Analyses Techniques. Table 6-2 lists the ASTM standard techniques used for chemical analyses of the solids samples.

Table 6-2. ASTM Standards Used in Solids Chemical Analyses.

Test Component	Standard	Standard Title
Ash Minerals	ASTM D 3682	Standard Test Method for Major and Minor Elements in Combustion Residues from Coal Utilization Processes
Carbon, Hydrogen, and Nitrogen	ASTM D 5373	Standard Test Methods for Instrumental Determination of Carbon, Hydrogen, and Nitrogen in Laboratory Samples of Coal and Coke
Carbon Dioxide	ASTM D 1756	Standard Test Method for Determination as Carbon Dioxide of Carbonate Carbon in Coal
Heating Value	ASTM D 5865	Standard Test Method for Gross Calorific Value of Coal and Coke
Moisture Content	ASTM D 5142	Standard Test Methods for Proximate Analysis of the Analysis Sample of Coal and Coke by Instrumental Procedures
Sulfur Content	ASTM D 4239	Standard Test Methods for Sulfur in the Analysis Sample of Coal and Coke Using High- Temperature Tube Furnace Combustion Methods
Volatile Content	ASTM D 5142	Standard Test Methods for Proximate Analysis of the Analysis Sample of Coal and Coke by Instrumental Procedures

6.6.2 Gas Sampling

A variety of sampling schemes are employed at the PSDF, depending on needs of individual tests. Custom built sampling/calibration panels are utilized at the PSDF. These systems, built at the PSDF, use novel configurations that allow technicians to easily switch between numerous sample and calibration streams. A fast loop bypass has been integrated into several of these systems, allowing for quick sample turnover and timely response from the analyzers. The addition of these sampling panels has reduced calibration time and increased flexibility.

Syngas Bomb Sampling (Locations C and G). Syngas composition data for difficult or non-routine samples is obtained by using bomb sampling techniques. These techniques allow for the analysis of samples that would otherwise be impossible or problematic for continuous analysis. Figure 6-16 shows bomb sample cylinders. The cylinder on the left of the figure was treated with a Sulfinert performance coating for use in sampling sulfur compounds, and the bomb sample cylinder on the right is a standard cylinder used for general syngas quality samples.

Figure 6-16. Bomb Sampler Cylinders.

Bomb samples from the gasifier riser and the upper mixing zone are captured using a sample system consisting of a 30-micron sample filter, a flow orifice, and high temperature valves. Once the samples are obtained, they are analyzed on an Applied Automation Optichrome Advance GC instrument. Measurements are taken for O_2, N_2, H_2, CO, CO_2, and CH_4.

Bomb samples are also frequently obtained at the advanced syngas cleanup unit. These samples are much easier to capture due to their lower temperature and lack of particulate. Samples from this slipstream may be analyzed for syngas quality (identical to the gasifier samples mentioned above) or for sulfur compounds. If measurements are made for sulfur compounds, specially coated bombs (collection vessels) and valves are used to minimize sample/bomb interactions. These sulfur compounds include SO_2, H_2S, COS, and carbon disulfide (CS_2). Analyses for SO_2 for specific tests are made using a Rosemount XStream analyzer; all other sulfur compounds are analyzed using an Agilent 5890 GC instrument equipped with a flame photometric detector.

Gas Analyzers (Locations H, K, L, and M). Both extractive and in-situ gas sampling systems are utilized at the PSDF. Although extractive sampling takes a longer time to gain results (at least one minute delay compared to nearly instant), the presence of particulate and the high temperature, high pressure conditions at most locations in the gasification process require that the gas be extracted and conditioned prior to analysis.

Most of the syngas quality measurements are taken at the PCD inlet, downstream of the primary gas cooler, which is the first location in the process where the temperature is suitably low. Gas is sampled here to give the earliest possible indication of process changes. GC units are used in addition to the continuous analyzers.

Figure 6-17 provides a photo of the gas conditioning system for analysis upstream of the PCD. The system uses reflux probes, which are demarked with a blue circle. The high pressure canister filter (marked with a green circle), which is shared by both probes, can be seen at the top of the photograph. The probes remove moisture and long chain

hydrocarbons from the syngas, and the filter removes any residual particulate matter. This system provides uninterrupted sample flow for all of the major syngas components.

Figure 6-17. Gas Conditioning System.

The temperature control set up for the gas conditioning system, shown in Figure 6-18, includes temperature control thermocouples (marked in blue), a control valve (outlined in yellow), and a vortex chiller (circled in red). With this control system in place, the outlet sample temperature is maintained between 70 and 100°F.

Figure 6-18. Gas Conditioning System with Temperature Control.

A disassembled reflux probe is shown in Figure 6-19. The cooling coil/fins, along with the de-mister pad are shown on the left of the figure. Cooling air/nitrogen from the vortex chiller flows through the interior of this section. The main body of a reflux probe (minus the insulation) is displayed on the right. This section houses the cooling coils and also has its own cooling jacket.

Figure 6-19. Disassembled Reflux Probe.

The reflux probes used at the PSDF are ready for commercial applications. All probes in use have a pressure rating of 500 psig, and higher ratings are available. The temperature control loops were designed and built at the PSDF, and involve only typical equipment, such as thermocouples and control valves. Most commercial gasifier analyses will employ reflux probes, and the current setup using manual steam cleaning is acceptable for commercial application. Automated steam cleaning could be added, but would involve significant safety measures to avoid analyzer damage in the event of a leak.

Figure 6-20 shows a disassembled canister filter. This type of filter is used to remove particulate from the PCD inlet prior to gas sampling. During operation, the filter is replaced once a week.

Figure 6-20. Disassembled Canister Filter.

Several Agilent 5890 GC instruments have been tailored for use on-line. These instruments allow for the low level measurement of COS, H_2S, and CS_2. The laboratory GC units also permit the use of capillary columns which are not applicable in most process GC units. The biggest advantage of these columns is the reversal of elution order

for hydrogen sulfide and carbonyl sulfide. This change makes it possible to measure low ppm levels (2 to 3 ppm) of carbonyl sulfide in the presence of 3,000 ppm of hydrogen sulfide, which is not possible with a process GC unit.

The laboratory GC units also offer greater flexibility than the process GC units. The laboratory GCs are accurate from low ppm levels up to percent levels. Minor modifications and calibration of the GC unit are required but are not complex or time consuming. This flexibility permits one instrument to support numerous and varying tests.

Figure 6-21 is a photograph of the on-line laboratory GC unit. This Agilent GC unit analyzes for varying levels of H_2S, COS, and CS_2. The analytical method and GC integration were developed at the PSDF. This instrument, and others like it, have been valuable in the successful evaluation of H_2S sorbents and COS hydrolysis catalysts.

Figure 6-21. On-Line Laboratory GC Unit for PCD Inlet Gas Analysis.

The continuous PCD inlet analyzers are shown in Figure 6-22. This analyzer cabinet houses the fast response analyzers used for gasifier monitoring. The response time for these instruments is typically less than 5 minutes. This bank of analyzers consists of four Rosemount XStream units (blue and gray) along with an oxygen analyzer (bottom of photo) which is used as a backup. The Rosemount units provide redundant analyses for O_2, CO, and CO_2. A customized sample system (built on-site) can be seen at the top of the cabinet.

Figure 6-22. Continuous Analyzer Cabinet for PCD Inlet Gas Analysis.

In-situ analyzers are located at the outlet of the atmospheric syngas combustor. Shown in Figure 6-23, the in-situ system features an infrared analyzer (marked with blue) manufactured by Procal Analytics. The system measures the flue gas at the syngas combustor outlet for percent levels of moisture and CO_2, as well as for SO_2, nitrogen oxides, and CO in the ppm range. The auto zero/calibration unit (marked with green), was designed and built at the PSDF.

Figure 6-23. In-Situ Flue Gas Analyzer.

Measurements of water vapor, ammonia, and hydrocarbons in the syngas are made by the on-line Fourier Transform Infrared (FTIR) system, which was manufactured by Temet Gasmet. This system, pictured in Figure 6-24, is located at the advanced syngas cleanup

unit. The primary enclosure (outlined in red) contains the laser and infrared sources, the measurement cell, and associated electronics (power supplies, processors, and relays). The sample interface unit (outlined in blue) on the right contains components related to temperature and valve control. The analyzer at the bottom of the photo is an SO_2 analyzer.

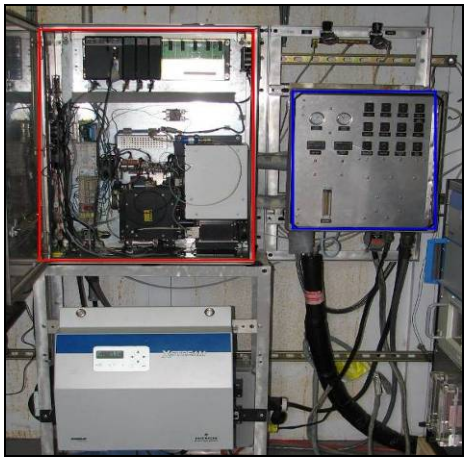

Figure 6-24. FTIR Gas Analysis System.

The PSDF utilizes a Gasmet online FTIR for numerous measurements (moisture, ammonia, hydrocarbons, etc.). Initially, the analyzer operated for only 20 minutes before it required disassembly and repair. The changes made to this instrument permit it to operate for up to 10 hours before in-depth maintenance is required.

A change to the sampling cell internals accounts for most of the improvement in FTIR measurements. A special Teflon deflector shield was added, which effectively protects the sensitive gold optics from particulate and soot build up. Several different designs have been tested, and all designs greatly increase the life span of the optics.

Several changes were made to the FTIR sample interface module. This interface controls temperature and valve functions. When maintenance is performed, this large component must be removed from the side of the main FTIR enclosure. Adding a sliding support to the interface module along with extended cables and sample lines reduced maintenance manpower requirements by over 75 percent.

In addition to these major improvements, smaller changes have also been made which add to the dependability of the instrument. These changes include new power supplies, solid state relays, valve replacement, and changes to thermal overload.

Also located at the advanced syngas cleanup unit are analyzers for assessing CO_2 separation, direct oxidation of H_2S, and water-gas shift reactions. These analyzers are shown in Figure 6-25. The Rosemount XStream analyzer at the top of this bank is the main instrument used to monitor water-gas shift reactions. The other XStream is used to monitor CO_2 separation testing. The oscilloscope at the bottom of this bank is used to set

up and test FTIR parameters. The sample system (valves and flow meters) is used to calibrate/zero both of the XStream analyzers.

Figure 6-25. CO_2 Capture and Water-Gas Shift Reaction Analyzers.

Figure 6-26 shows a process GC unit used for syngas quality measurements.

Figure 6-26. Syngas Quality Gas Chromatograph.

Sample conditioning at the syngas cleanup unit is provided by thermoelectric chillers. Essentially, these chiller units provide the same service to the cleanup unit that the reflux probes provide to the gasification process unit. Chiller units manufactured by Baldwin/Permapure are utilized, and the impinger portions of the systems were designed and built on-site to accommodate the higher pressures.

These chillers utilize typical gas cooling techniques (thermo-electric, vortex tube, etc.), but the sampling impingers are constructed of large diameter stainless steel tubing. The small volume of the impingers allows samples to be extracted without causing gasification system flow and pressure swings. High pressure valves and flasks are installed on the bottom of these impingers in a lock vessel arrangement. This design allows the condensate to be drained from the impinger without causing pressure fluctuations at the analyzer. If H_2S is to be analyzed, the impingers are treated with performance coatings supplied by Restek to prevent reaction of the H_2S with the stainless steel. Accurate, low level H_2S analyses would be nearly impossible without these coatings.

Figure 6-27 shows the components of the gas conditioning system, including a Baldwin/Permapure chiller unit and a coated impinger and drain valve assembly.

Figure 6-27. Gas Conditioning System.

6.7 Sensor Research and Development Semi-Conducting Metal Oxide Sensors

Sensor Research and Development (SRD) Corporation developed, with DOE funding, a prototype sensor system for in situ real-time detection, identification, and measurement of coal-fired combustion gases. The PSDF provided the testing site for the SRD prototype in support of the DOE sensor program. The sensor system incorporates SRD's semi-conducting metal oxide sensors and novel gas pre-filtration techniques. SRD has

previously shown optimization of the gas delivery, sensor chamber, and data acquisition and control system for the testing of simulated flue gas.

SRD performed field-testing on its chemical analyzer prototype at the PSDF during TC22. The purpose of the test was to optimize the gas sampling times; to evaluate the accuracy of the hit-detection and classification algorithms used by SRD's prototype; and to determine the accuracy of concentration estimates made by SRD.

Performance criteria for the SRD chemical analyzer included a false positive rate, consisting of incorrect classification and false alarm due to noise, and a false negative rate. The SRD analyzer performed with 97 percent accuracy in detecting and classifying post combustion gas constituents with a zero percent false negative rate. The false positives were entirely due to misclassification. In addition to evaluation of the classification and hit-detection algorithms, SRD had also developed algorithms to estimate the concentration of gases in the stream. SRD found that the concentration estimates were dependent on the magnitude of the training database used in classification and concentration estimates.

SRD will focus future efforts on augmenting the training database to increase the accuracy of the concentration estimator. In order to achieve this, SRD will collect data over longer periods of time and under differing operating conditions. Testing the sensor on syngas at the PSDF may proceed if initial development is successful.

6.8 Babcock & Wilcox High Speed Pressure Sensors

EPRI has funded the development of advanced nonlinear signal analysis techniques and their application to coal combustion. Under sponsorship of EPRI, the Oak Ridge National Laboratory (ORNL) and Babcock & Wilcox (B&W) have developed the Flame Doctor diagnostic system for assessing combustion stability. ORNL has continued to apply these techniques for monitoring and controlling fluidized bed chemical reactors for industry and DOE. In all of these applications, it has been demonstrated that strong correlations exist between fluctuations in bed differential pressure signals and acoustic signals and the onset of undesirable bed conditions such as de-fluidization, slugging, and agglomeration.

EPRI funded ORNL and B&W to re-apply these advanced nonlinear techniques to develop a suite of diagnostic tools for monitoring gasifier performance. As none of the previous work was conducted in a gasification environment, a feasibility study was needed to confirm that these techniques could be extended to gasifiers. During TC22, B&W and ORNL personnel collected high speed pressure fluctuation data on the Transport Gasifier for the purpose of confirming that changes in pressure fluctuations could be correlated to changes in gasifier operating conditions. During this feasibility test, high speed Kistler piezotron pressure sensors were mounted on existing sensing lines at three locations on the gasifier: at the lower standpipe and above and below the coal feed nozzle. Changes in operating conditions were detected by the pressure sensors. These results confirm that a larger test is justified to collect more information with the

goal of developing nonlinear techniques for predicting gasifier performance. A final report from B&W is available.

6.9 Process Controls

Effective process controls are needed to safely and reliably operate complex chemical processes such as gasification. Development of automatic controls for the Transport Gasifier required extensive effort due to the intricate chemical reactions and fluidization dynamics in the gasifier. The gasifier process control strategy included the categories of temperature, coal feed rate, standpipe level, and fluidization velocity control.

6.9.1 Gasifier Temperature Control

Control of the gasifier temperature is crucial to operations and performance of the gasifier. The ultimate goal was to control the temperature profile (i.e., to control the temperature in different sections of the gasifier). To avoid ash agglomeration in the gasifier, the temperature is maintained about 300°F below the ash fusion temperature in the LMZ due to the higher solids-to-gas ratio and low gas velocity in this region. The temperature in the UMZ can be higher but must be kept about 200°F below the ash fusion temperature. On the other hand, the temperature in the riser must be maintained sufficiently high to achieve the desired carbon conversion and targeted syngas heating value.

Control Scheme Description. Initially a simple proportional-integral-derivative (PID) control loop was utilized for a single temperature control loop. The control loop was tuned and tested but gave unsatisfactory results, as it was only able to control the temperature within a 40°F band.

Parametric tests were performed by varying the independent variables such as the air, steam and coal flow rates, standpipe level, and gasifier pressure individually by a predetermined amount while holding the other independent variables constant. These tests evaluated the response time of the dependent variables (the temperatures in different gasifier sections) to the process change induced. A specialized procedure was used to acquire higher resolution data from the plant historian to improve the process model. Based on this data, a pseudo-fuzzy control plane was developed for feed forward controls into the multi-temperature control loop.

The control strategy consisted of using the riser temperature as the primary control and the upper mixing zone as the secondary control. It included settable parameters for the acceptable temperature deviation from section to section and the temperature differential between the sections and the ash fusion temperatures. Based on the predictive model, air flows to the different sections were controlled using four flow control valves. Additional features included recognition of erroneous temperature readings and automatic corrective actions to avoid process upsets that could be caused by the erroneous measurements.

Results. Subsequent testing confirmed that the temperature profile could be effectively controlled using the pseudo-fuzzy control scheme over a wide range of operating conditions. The air/fuel forward-looking alarm notified the operators when the rate-of-change was trending out of the acceptable pre-defined range. Other observations such as the process sensitivity to higher flows through the highest level of air introduction in the upper mixing zone significantly improved the controllability. Figure 6-28 shows a comparison of the temperature control by simple PID loop and by the pseudo-fuzzy control plane, and Figure 6-29 shows the pseudo-fuzzy controller response to a change in temperature setpoint.

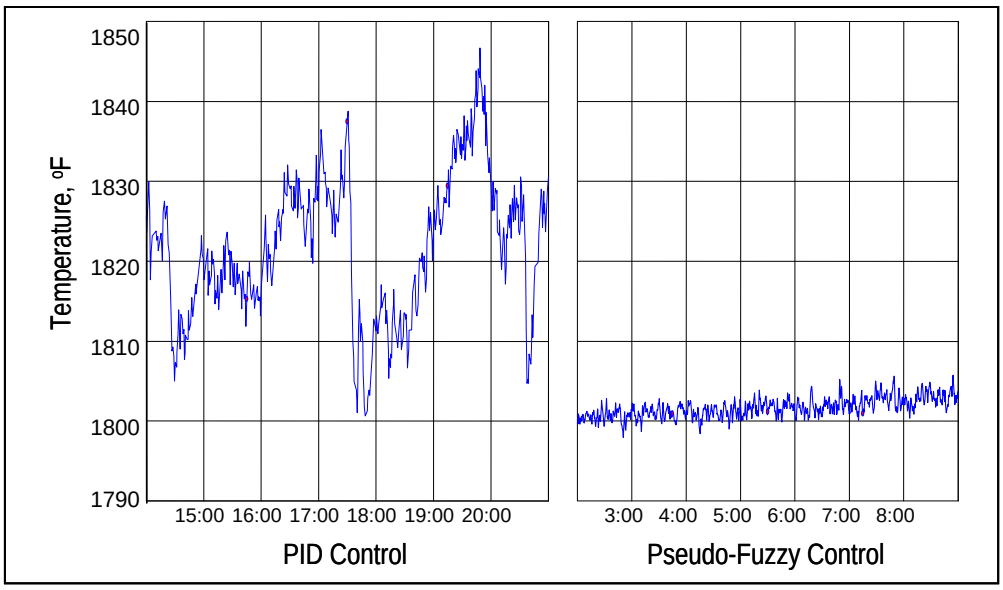

Figure 6-28. Comparison of Gasifier Temperature Control Schemes.

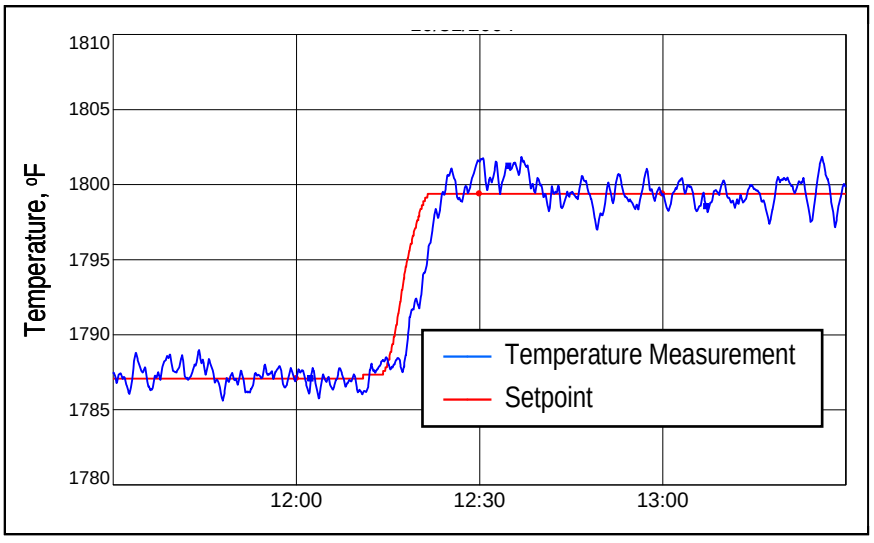

Figure 6-29. Gasifier Temperature Response to Setpoint Change using Pseudo-Fuzzy Control Plane.

6.9.2 Coal Feed Rate Control

Since the coal mass feed rate affects the gasifier operating temperature, standpipe level, carbon conversion, and syngas heating value, it is crucial to control it at the desired setpoint. The main challenge was developing an accurate and reliable instantaneous coal mass flow rate measurement. Since the feeder is a constant volume feeder, changes in the density will affect the mass flow rate. A negative feedback loop was employed to adjust the motor speed to control the mass feed rate. The controller was affective in controlling the rate. Figure 6-30 shows results of a setpoint change utilizing this control loop.

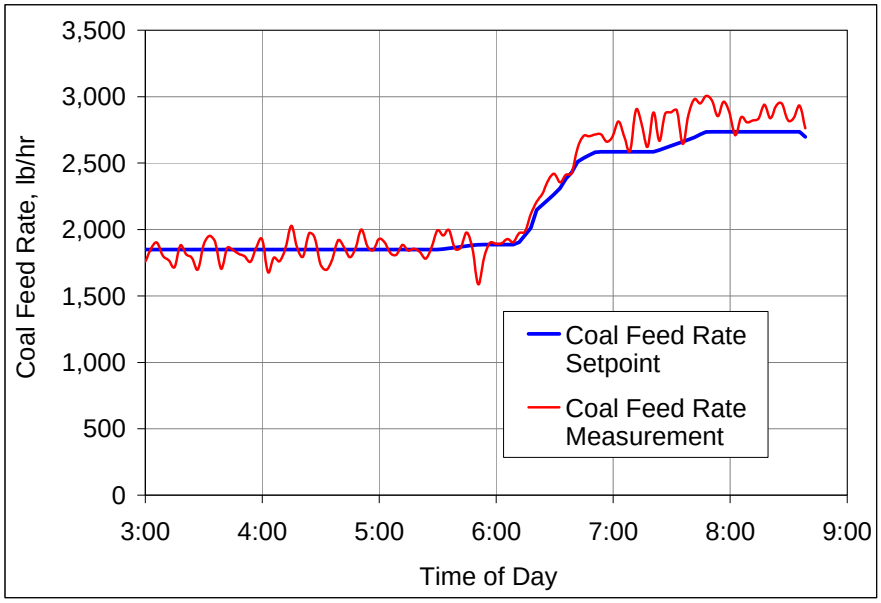

Figure 6-30. Coal Feed Rate Response to Setpoint Changes.

6.9.3 Standpipe Level Control

Standpipe level has a positive linear correlation with the solids circulation rate. The circulation rate directly affects gasifier operation and performance by controlling the solids-to-gas interaction rate and temperature profile. During normal operation, (especially during high ash yield operation) the solids level inside the standpipe measured by a pressure differential indication will increase gradually due to the accumulation of gasification ash in the gasifier. To achieve stable circulation around the gasifier loop, a constant solids level inside the standpipe must be maintained.

Description. The ash removal rate through CCAD is varied to control the standpipe solids level. When the solids level is higher than the set point, CCAD will start and discharge the ash. The discharge rate is adjusted to achieve the desired level. In the event of an erroneous reading, such as a plugged sensing line, the control logic will automatically identify the error, take corrective action, and notify operators to prevent a process upset.

The control scheme configuration also addressed changes in level due to a system trip to avoid excessive removal of material.

Results. Figure 6-31 plots the response of the standpipe level to controller setpoint changes. As shown in the figure, the level control scheme worked well and controlled the standpipe level as desired. It also successfully processed erroneous readings caused by plugged pressure sensing lines.

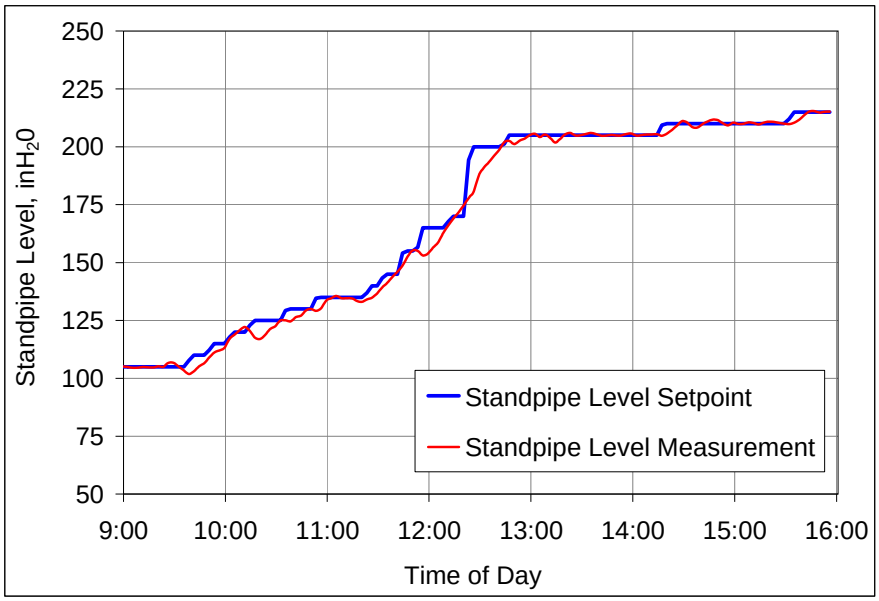

Figure 6-31. Standpipe Level Response to Setpoint Changes.

6.9.4 Fluidization Velocity Control

Description. Proper fluidization of the seal leg, J-leg, and standpipe is required to maintain stable solids circulation in the gasifier. Fluidization regimes are based on the physical characteristics of the material, which change as the unit transitions from inert bed material (i.e., sand) to gasification ash, and are controlled by the gas velocity. Due to changes in gasifier temperature and pressure, velocities vary with a constant mass flow. Since constant velocity is the control parameter, velocity control loops were employed to minimize the effect of pressure and temperature changes. Negative feedback loops were used to vary the gas mass flow to achieve the target velocity for the seal leg, J-leg and standpipe fluidization gas flows.

Results. The velocity control loops were tuned and operations demonstrated good response to changes in gasifier temperature and pressure as well as changes in setpoint. Figure 6-32 plots the setpoint and calculated value of one summand of the J-leg velocity (the total J-leg velocity is the sum of the velocity of two aeration gas flows) as the system pressure decreased. As shown in the figure, the controller maintained a narrow velocity range throughout a steep decrease in system pressure.

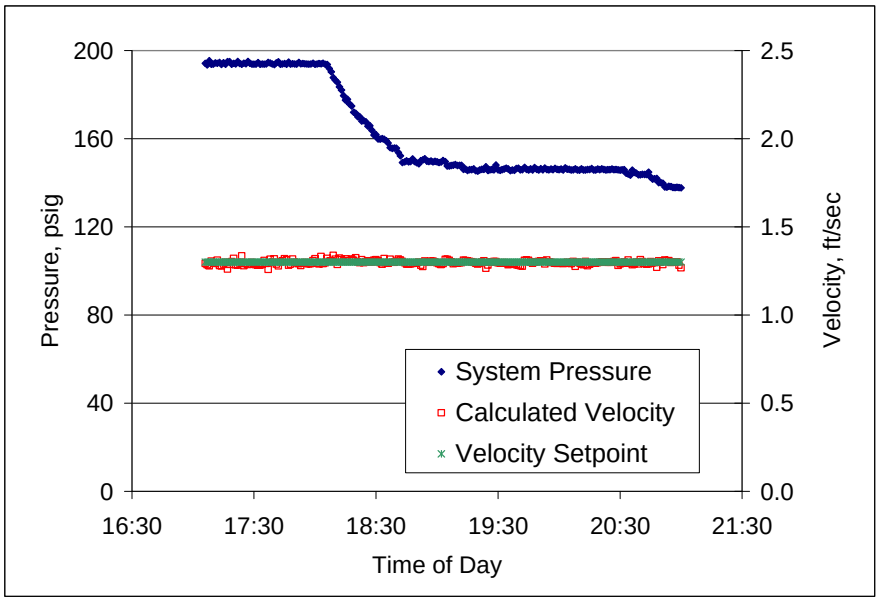

Figure 6-32. Gasifier J-Leg Velocity Control Response to Pressure Change.

6.9.5 Safety Interlock System

A critical piece of the process control system is the safety interlock system (SIS). The SIS provides automatic actions to correct abnormal plant events, and entails measures structured for the protection of equipment and personnel. The SIS organization is instrumental in assisting operations personnel in event awareness and troubleshooting.

Some of the key features of the SIS include:

- Identification of numerous equipment trip scenarios
- Categorization of trip scenarios into groups based on the severity of the event consequences
- Configuration of specific sequences of events following trips to safeguard the system
- Automatic surveillance by a series of group interlocks of gasifier and subsystems operation
- Individual trip sequences for controlled shutdowns of the gasifier and each subsystem when needed
- Permissive interlocks that insure all operational conditions are satisfied before equipment is allowed to start
- Flexible interlock configuration to accommodate a range of operating scenarios such as air- or oxygen-mode gasification and different fuel types
- Configuration of alarms to notify operators of imminent trip events

Figure 6-33 shows a distributed control system (DCS) screen that was configured with all interlock information summarized by affected equipment and trip classification to assist operations personnel in troubleshooting trip events.

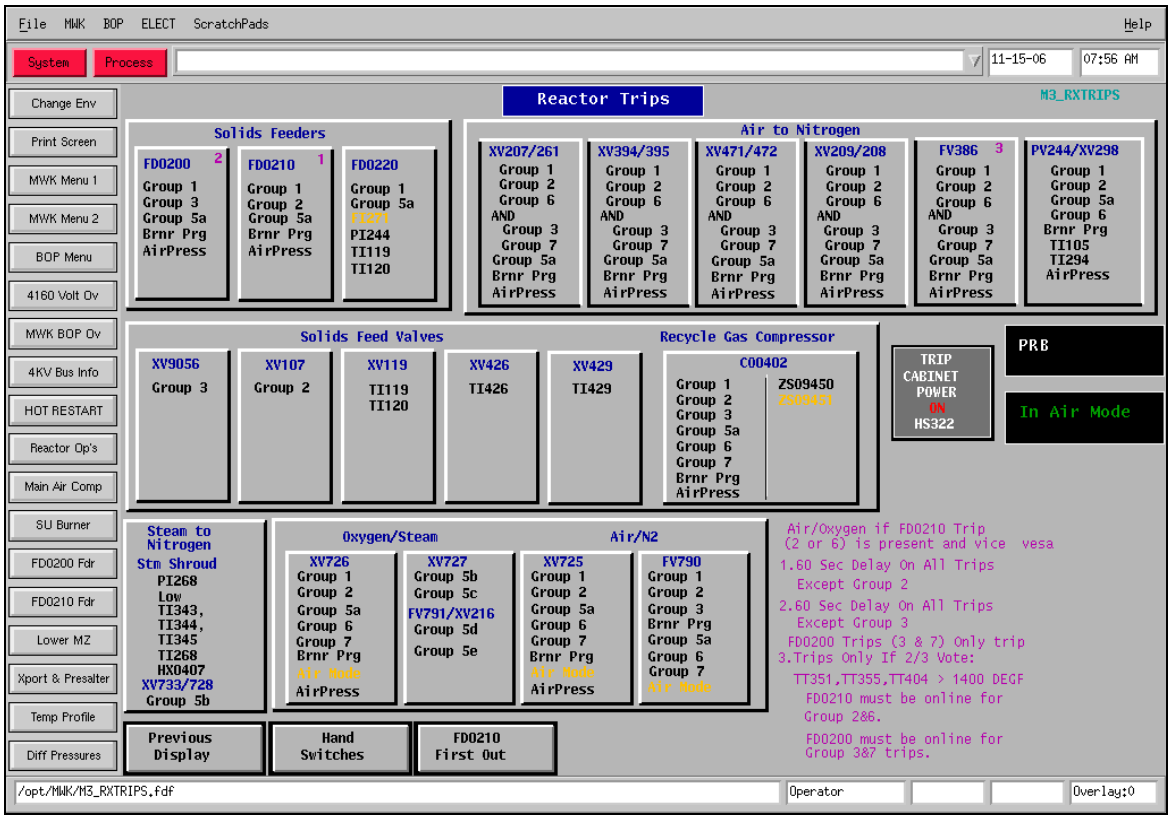

Figure 6-33. DCS Safety Interlock System.

Over time, PSDF controls specialists incorporated numerous enhancements to the SIS based on operational experience. Some of these enhancements include:

- Two out of three logic voting system for gasifier thermocouples interlocked to gasifier trips for prevention of unnecessary trips
- Identification of coal feeder stoppages and installation of fast acting valves to stop gasifier air feed for reduced occurrence and severity of oxygen breakthrough to the PCD
- First-out alarms for the groups and individual trips in each group for identification of root causes of trips and shutdowns for improved system availability

7.0 SUPPORT EQUIPMENT

7.1 Recycle Gas Compressor

To support further development and better simulate commercial operation of the Transport Gasifier, a new recycle gas compressor was installed at the PSDF in 2005. Recycled syngas is used for aeration in the J-leg, standpipe and seal leg. Using recycled syngas instead of nitrogen increases the syngas heating value and reduces plant operating cost by reducing nitrogen consumption.

Background. The original recycle gas compressor, a reciprocating compressor that operated at low temperature, did not operate reliably. Internal valve failures were the main operating issue. Valve failures were caused by liquid species that formed in the line downstream of the separator due to the low operating temperature. Figure 7-1 shows a valve that failed during testing.

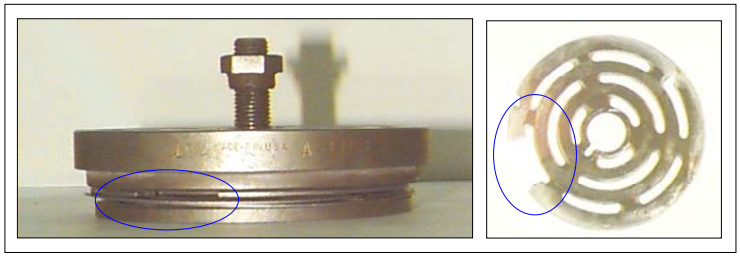

Figure 7-1. Valve Failure on Original Recycle Gas Compressor

Compressor Description. The new recycle gas compressor is a vertically mounted centrifugal compressor which operates at high temperature (nominally 500 to 600°F). The compressor was manufactured by Sundyne Corporation, and was designed to have a throughput of nominally 2,000 to 3,000 lb/hr. A schematic and photograph of the compressor is shown in Figure 7-2.

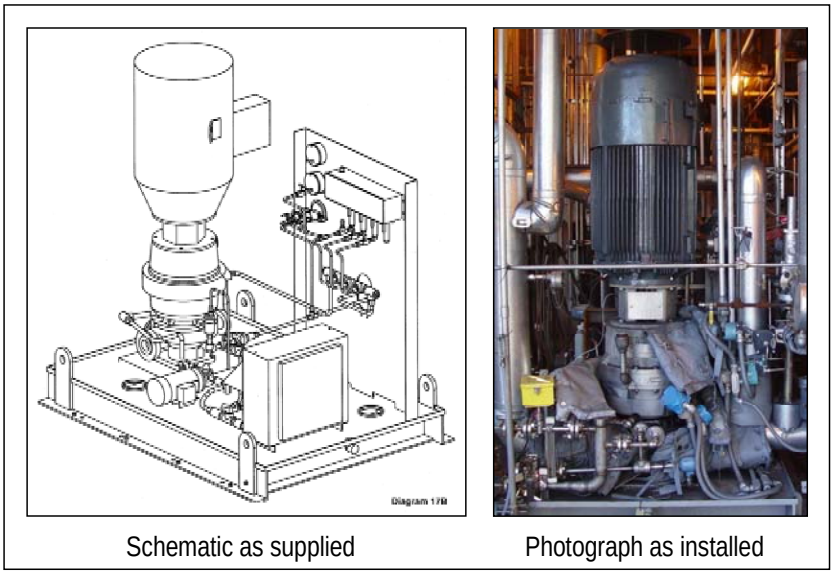

Schematic as supplied Photograph as installed

Figure 7-2. Schematic and Photograph of Recycle Gas Compressor.

Operations and Performance. The recycle gas compressor was initially commissioned on heated nitrogen and experienced excessive motor vibration. The motor was replaced, and the vibration issues were resolved. The compressor has since operated reliably supplying recycle syngas to the gasifier for 1,860 hours. The compressor operating conditions were:

- Inlet temperatures ranging from 450 to 600°F
- Syngas flow rates between 280 and 360 lb/hr
- Outlet pressure ranging from 150 to 250 psig

Recycle syngas utilization increased the raw syngas heating value about 5 to 10 percent depending on other operating conditions. In addition, the plant operating cost were decreased due to lower nitrogen consumption resulting in a total cost savings of $120,000 to date. It was instrumental in allowing continued process operations during times when vendor-supplied nitrogen was limited.

Since the compressor was experiencing several nuisance trips due interlock logic that stops the compressor under certain gasifier operating conditions, the trip logic was modified prior to the August 2007 test run (TC23) to increase the availability of the recycle gas system.

Previously, all gasifier and coal feeder trips would also trip the recycle gas compressor. Generally, coal feeder trips have a short duration, less than 5 minutes, and therefore do not impact operation of the recycle gas compressor. After completing a thorough design hazard review, the logic was changed to eliminate compressor trips due to coal feeder trips and certain gasifier trips. As a result of these modifications, the compressor availability was more than doubled, increasing from about 40 percent in recent test campaigns to over 80 percent in TC23. The higher availability increased test data available for analysis by shortening the time required to re-establish steady state conditions following coal feeder and certain gasifier trips. Based on operations in TC23, a trip condition related to the main air compressor discharge pressure was identified as another trip condition that was eliminated to further improve availability. The trip condition related to the main air compressor discharge pressure that was eliminated worked properly so that a gasifier trip caused by a low main air compressor discharge pressure did not trip the recycle syngas compressor during the subsequent test run.

7.2 Piloted Syngas Burner

Description. The piloted syngas burner (PSB) is a prototype combustor designed by Siemens Power. It has a large diameter combustor to create a favorable combustion environment while using an ultra-low heating value syngas (about 60 Btu/SCF). A schematic of the PSB and combustion turbine (CT) is shown in Figure 7-3. A model of the PSB test rig and a photograph of the PSB before installation are shown in Figure 7-4.

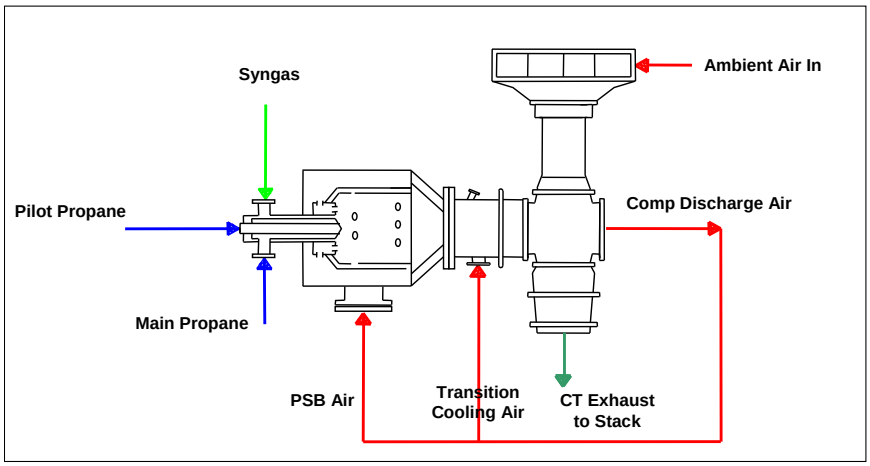

Figure 7-3. Flow Schematic of the Piloted Syngas Burner and Combustion Turbine.

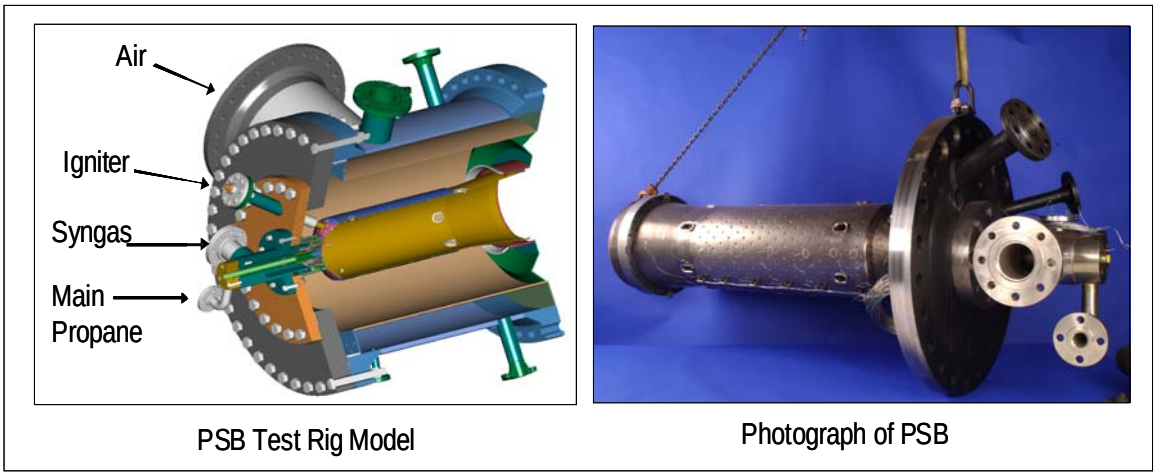

Figure 7-4. Piloted Syngas Burner Model and Photograph.

Operations. The PSB operated steadily for about 40 hours at the following operating conditions:

- Syngas heating values ranging from 59 to 76 Btu/SCF
- Syngas flow rates from 4,000 to 17,000 lb/hr
- Propane assist flow rates of 270 to 600 lb/hr
- Power output ranging from 1.0 to 1.2 MW

The PSB flame remained steady throughout testing. Process variances, such as the slight pressure swing caused by the PCD backpulse, did not affect PSB operations. To ensure safe operation of the PSB, several interlocks were configured and tested. All performed as expected during the interlock trials. When interlocks tripped the process gas to the PSB, valves diverted the flow to the flare to avoid causing gasifier pressure upsets. Once the syngas flowed to the flare, logic controls slowly restored the flow through the main pressure letdown valve to the

atmospheric syngas burner, which avoided swings in gasifier pressure. In practice, the gasifier pressure changed less than 2 psig during each trip.

A PSB flame temperature greater than 2,800°F gave a reliable indication of approaching flame instability as propane flow was decreased and syngas flow was increased. The flame temperature was maintained above 2,800°F to confirm this finding, and the PSB operated smoothly. When the propane flow decreased below 270 lb/hr, the flame blew out. Before the flame blew out, the stack CO content increased to about 200 to 300 ppm.

The PSB wall temperatures and the combustor noise both remained low throughout testing. Several improvements were made to the fuel nozzle thermocouples: increasing their size, embedding them into the nozzle, and covering them with a thermal barrier coating. These improvements reduced the frequency and intensity of the temperature spikes that occurred in the early tests. Also contributing to the reduced temperature spikes at the PSB fuel nozzle was an improved control scheme for the introducing the main propane, pilot propane, syngas, and purge flows to the PSB.

7.3 ASH REMOVAL SYSTEMS

The Transport Gasification process was originally equipped with conventional-type ash removal systems to handle the coarse gasification ash from the gasifier and the fine gasification ash filtered in the PCD. These systems proved to be incompatible with the gasification process, and they were replaced with continuous ash removal systems developed on-site.

7.3.1 Original Ash Removal Systems

The original systems consisted of screw feeders for cooling and lock hopper systems for depressurization. The lock hopper systems used Spheri valves for isolation between the lock vessels and discharge vessels. The coarse ash and fine ash removal systems had a common configuration, which is shown in Figure 7-5.

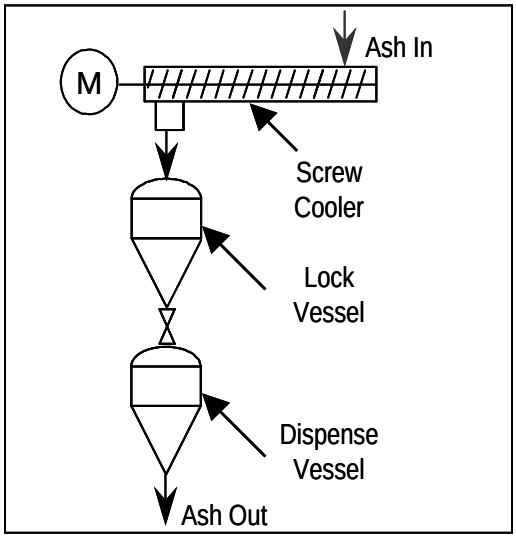

Figure 7-5. Schematic of Original Ash Cooling and Depressurization Systems.

In both applications, these ash removal systems proved to be high-maintenance and not well-suited for scale-up. To keep the systems operational, many modifications and significant maintenance activities were needed, such as:

- Logic modifications to prevent overfilling of material
- Packing gland adjustments
- Drive-end shaft-packing seal changes
- Spheri valve seal material changes

7.3.2 Continuous Ash Depressurization Systems

The original ash removal systems were replaced with proprietary continuous ash removal systems that feature:

- Reliable and continuous operation
- High capacity
- No moving parts
- No pressurizing gas
- Low vent flows of clean gas
- Solids transport using inherent gas

The CFAD system was installed in January 2004 to cool and depressurize the fine gasification ash after it is filtered from the syngas in the PCD. The system was successfully commissioned in the February 2004 test run (TC14) with inert bed material and later operated successfully on gasification ash generated from PRB coal. Following the remarkably reliable operation of the CFAD system, the CCAD system was installed in October 2005 to cool and depressurize the coarse gasification ash to control the solids level in the gasifier.

CFAD Description. The CFAD system consists of fine ash removal, cooling, and depressurization. Fine gasification ash is moved by differential pressure from the bottom of the PCD hopper, which serves as a surge volume. The ash is initially cooled by heat transfer fluid (down to below 200°F) and then is depressurized to an appropriate pressure (from about 5 to 30 psig), which is necessary to transport the ash. Details of the design and its operating principles are proprietary. A schematic of the system is shown in Figure 7-6.

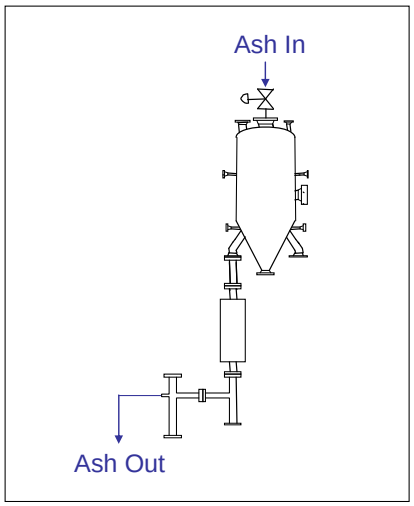

Figure 7-6. CFAD Schematic.

CCAD Description. The CCAD system consists of gasifier ash removal, cooling, depressurization and conveying equipment. Coarse ash is taken from the start-up burner leg bottom into a refractory-lined pipe, which serves as a surge volume. The ash is initially cooled by heat transfer fluid (down to below 600°F) and then depressurized to an appropriate pressure (from about 5 to 30 psig), which is necessary to transport the ash to the ash silo or to a feeder surge bin to feed to the gasifier as make-up or start-up bed material. A low pressure fluidized bed cooler, located downstream of depressurization device, further cools the gasification ash to around 200°F. When sand is first added to the gasifier for start-up bed material, the CCAD system is filled with solids. During steady state gasifier operation, the CCAD system automatically controls the gasifier standpipe level by varying the gasification ash discharge rate. Details of the design and its operating principles are proprietary.

Operations. The CFAD and CCAD systems have operated reliably over a range of flow rates, pressure, temperatures, and particle sizes. Operating conditions tested are shown in Table 7-1. Figure 7-7 provides the range of particle size distribution curves for the gasification ash handled in the two systems.

Table 7-1. CFAD and CCAD Operating Conditions.

	CFAD	CCAD
Total Operating Hours	7,950	4,300
Ash Flow Rate, lb/hr	150 to 6,000	100 to 1,500
Inlet Temperature, °F	400 to 800	600 to 1,600
Inlet Pressure, psig	150 to 250	160 to 260
Particle Size MMD, microns	6 to 20	70 to 850

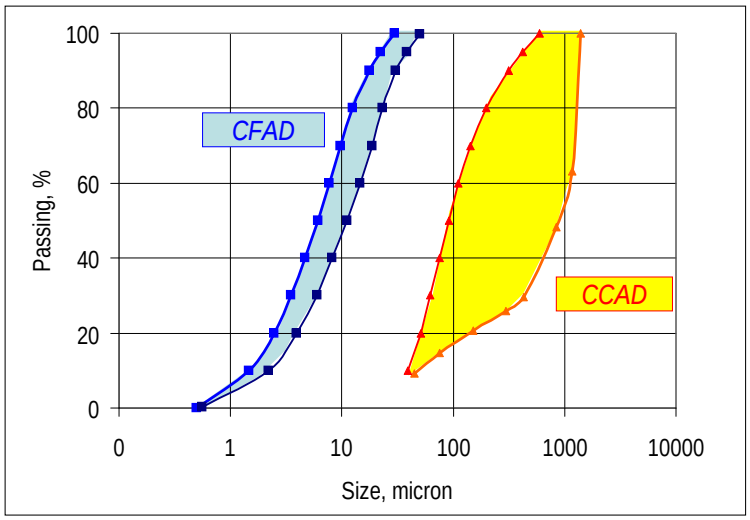

Figure 7-7. Particle Size Distributions of Gasification Ash Processed by the CFAD and CCAD Systems.

8.0 CONCLUSIONS AND LESSONS LEARNED

Work at the PSDF has included the development of several types of first-of-a-kind equipment and integration of these components into a reliable gasification process for generating data for scale-up to commercial applications. Research and development at the PSDF has advanced technology of a wide range of gasification systems and support systems. These include high pressure solids feed systems; a Transport Gasifier; the PCD hot gas filter; continuous ash depressurization systems; and various instrumentation, sampling, and controls systems. A growing area of focus at the PSDF has been advanced syngas cleanup to test emerging technologies for meeting ever-stricter environmental regulations for power generation facilities.

The PSDF's development and integration of the various systems was remarkably successful. After only eight years from the time of construction and commissioning, the Transport Gasification process was selected for commercial deployment through the DOE Clean Coal Power Initiative.

The major lessons learned for the major equipment in the PSDF gasification process follow.

8.1 Coal Preparation and Feed

- Coal silo design based on conventional coal plant experience was not ideal for the gasification process due to the differences in coal particle sizes and moisture contents (and thus flow characteristics) between the coal fed to the Transport Gasifier and coal fed at conventional plants.
- Coal silo inserts successfully addressed silo design deficiencies and prevented funnel flow and particle size segregation. The decreased particle size segregation improved coal feeder operation.
- Control of mill operation was improved by adding a V-cone flow meter with an automatic configuration to control air flow settings.
- Automatic coal mill sampling systems improved operators' ability to quickly respond to deviations in particle size and moisture content.
- A gas dehumidifier installed to remove condensate from the coal drying gas successfully reduced gas moisture content and decreased the demand for make-up nitrogen.
- The replacement of mill propane heaters with electric heaters improved mill operation since it replaced the propane heat source which was contributing to moisture saturation in the recycled gas.
- Nitrogen purges added to the mill chute improved coal flow.
- A coal particle size and moisture analyzer by Malvern did not provide useful data due to problems with the sample delivery system.
- Installing an Allen Bradley PLC to replace the original control system significantly enhanced the controls capability of the mill system.

- The fluid bed coal dryer was instrumental in expanding the PSDF fuel envelope by allowing effective drying of coals with high amounts of intrinsically bound moisture.
- Particle size attrition of the coal in the fluid bed dryer was significant, but additional pulverizing was needed.
- Operation of the fluid bed dryer with high moisture Mississippi lignite reduced coal moisture content from about 44 to 21 weight percent, allowing improved gasification operation compared with operation without the dryer.
- To improve operation of the original coal feeder, a two-inch vent valve and associated 7/64-inch flow orifice were removed and replaced with a one-inch ceramic V-ball control valve. This modification significantly reduced downtime due to vent line plugging.
- Limiting the percentage of oversize particles (greater than 1,180 microns) and the moisture content below 25 percent and modifications to eliminate low velocity regimes in the feed line have provided more stable operations, essentially eliminating occurrences of pluggages in the original coal feeder discharge line.
- Limiting the percentage of particles less than 45 microns and controlling the moisture content as well as modifying the lock vessel vent valve arrangement minimized original coal feeder vent line pluggages.
- Analysis of the original coal feeder operation has shown that reliable operation can be achieved over a wide range of MMD particle sizes (from 200 to 800 microns) and moisture contents (from 3 to 25 weight percent).
- Testing has shown that the PDAC feeder concept is promising and can increase feeder reliability. Development of the PCAC feeder will continue with improvements to feed rate control.

8.2 Transport Gasifier

- Carbon conversion is high and somewhat independent of temperature in the ranges tested when gasifier solids collection efficiency is high. For lower collection efficiency, carbon conversion is more dependent on temperature.
- Carbon conversion is a strong function of fuel type due to the short residence time in the gasifier. The higher reactivity fuels demonstrated higher carbon conversions, all other conditions being equal.
- Over the coal size range tested (200 to 700 microns, MMD) with subbituminous and lignite coals, there was no detectable affect of coal size on carbon conversion. There was also no detectable affect of residence time on carbon conversion. This was attributed to the high reactivity of these coals. With higher rank coals, operational challenges prevented parametric testing involving these variables.
- Solids circulation rate, which is dominated by standpipe level, is only a weak function of J-leg aeration rate.
- The original refractory in the gasifier standpipe showed no significant erosion or cracking after over 20,000 hours of solids circulation.
- The Atchem 85VC refractory was not suited for this application due to the high number of thermal cycles with startups and shutdowns.

- Different fuel types produce ash with characteristics that react much differently in the gasifier.
- Higher gasifier standpipe operating levels are acceptable with lower density ash.
- The optimum air flow through the LMZ is about 40 percent of the total air flow.
- The solids separation unit (consisting of two cyclones and a low density return leg into the standpipe) of the modified gasifier configuration proved more stable and higher in collection efficiency than the original configuration.
- The boundary conditions were identified with high sodium lignite operation. Adding kaolin sorbent along with the high sodium lignite feed was successful in preventing agglomeration in the gasifier.
- For the PSDF gasification process, syngas heating value is a strong linear function of coal feed rate, largely due to the fixed nitrogen input.
- Using air in the place of nitrogen for coal transport increases syngas heating value without adversely affecting temperature control.
- Using recycle gas for gasifier aeration increases syngas heating value without disturbing the gasifier temperature profile.
- Syngas methane content increases with gasifier pressure.
- Solids removal from the startup burner leg is more reliable than from the standpipe leg.
- The H_2-to-CO syngas ratio increases as the steam-to-coal ratio increases.
- Higher temperature operation with bituminous coal is needed to characterize operation. Modification to the solids separation unit are needed for further testing at higher temperatures.

8.3 Particulate Control Device

- Corrosion of the FEAL elements caused an increase in pressure drop over syngas exposure time, with sharp increases noted after about 6,000 hours of exposure. However, the elements continued to demonstrate high collection efficiency and adequate strength, and the useful life of the elements could be reasonably considered to be greater than one year. The observed rate of FEAL element corrosion may be sufficiently low to allow a two-year life in commercial operation.
- Throughout testing, all Dynalloy HR-160 elements remained intact. While the collection efficiency of the Dynalloy elements was not as high as the Pall PSS elements, it is high enough to meet turbine specifications. Testing showed that seasoning of the Dynalloy elements through syngas exposure with gasification ash improved their performance. Corrosion of the coarse fiber elements began after about 2,500 hours of syngas exposure, and corrosion of the fine fiber elements was observed after about 1,000 hours of exposure. Further testing is needed to determine the useful lifetime of the Dynalloy HR-160 elements.
- Pall iron aluminide sintered powder fuse and the CeraMem ceramic honeycomb failsafe have better particulate collection efficiencies than do the Pall Dynalloy metal fiber failsafes during the initial plugging period.

- Improvements to the Pall fuse structural integrity are needed based on the high frequency of breakage.
- During on-line failsafe testing, all of the failsafes tested (with the exception of the Specific Surface failsafe) performed satisfactorily. An elevated particle penetration occurred only during the initial plugging process for a short time period. After the failsafe plugged, the overall particulate concentration in the PCD outlet stream usually remained below the sampling system lower detection limit. Even in the initial plugging period, the particulate collection efficiencies were high enough to meet particulate concentration limits specified by gas turbine manufacturers.
- The filter element resistance probes, designed and fabricated on site, were useful in detecting ash bridging, and the probe output was successfully used to give a discrete alarm when bridging occurred.
- The addition of supported bare-wire thermocouples in the PCD hopper proved useful in providing much faster and more accurate temperature data than the original thermocouples.
- Ash bridging can be removed on-line by controlled combustion.
- The PCD size required to maintain a given allowable pressure drop is a strong function of the dustcake drag, since most of the PCD pressure drop occurs across the dustcake. Given the significant relationship between dustcake drag and PCD size requirement, the design of the PCD system must take into account the particulate characteristics that affect drag.
- The drag, and thus filter sizing requirements, of gasification ash increases with increasing carbon content.

8.4 Advanced Syngas Cleanup

- During testing of direct oxidation of H_2S, oxidation was observed only when excess SO_2 flow was used.
- The Sud-Chemie water-gas shift catalyst (T-2822) used in the PCD and the syngas cleanup unit was highly reactive with oxygen after being in a reduced environment.
- The NETL fuel cell module successfully operated with syngas for over 200 hours, and data collected through the combination of the exposure and electrochemical tests under real syngas conditions can be used for future SOFC technology development.
- Operation of the Johnson Matthey mercury sorbent showed high rates of mercury removal.
- Testing the Media and Process Technology hydrogen selective CMS membrane indicated stable operation with syngas. Performance of the membrane was not affected by syngas contaminants during the testing.

8.5 Instrumentation, Sampling and Process Automation

- The coal weigh cell measurements have provided reasonable accuracy, but since the feed rates calculated from the weigh cell measurements are averages over time and not instantaneous indications, measurements that are more responsive are needed for control of gasifier temperature and safety interlocks.

- The Granucor coal rate measurement was problematic due to sensor failures, particularly with the velocity sensor. A positive aspect of the Granucor measurement was its sensitivity to changes in feed rates, and of the measurement methods tested at the PSDF, the Granucor proved to be best for instantaneous indications of coal stoppages.
- Overall, the ceramic-tipped gasifier PDI measurements matched conventional measurements well, but plugging was an issue due to nitrogen purge flow control difficulties.
- The thermowells made of HR-160 material have shown to be the most reliable, and are resistant to wear under normal gasifier conditions.
- The PCME particulate monitor is a simple and effective instrument that has reliably indicated the presence of significant PCD leaks, and its output is easily adaptable to a discrete alarm.
- The PPC particulate monitor has much greater sensitivity than the PCME monitor and it is capable of monitoring particle concentrations at low levels, although more development is needed for reliable operation.
- Numerous modifications to sampling systems and methods have made the gas and solids sampling reliable and efficient in the unique process conditions.
- Testing confirmed that the gasifier temperature profile could be effectively controlled using a pseudo-fuzzy control scheme over a wide range of operating conditions.
- The safety interlock system is instrumental in assisting operations personnel in event awareness and troubleshooting. Key enhancements to the SIS include the addition of two-out-of-three logic voting and first-out alarms.

8.6 Support Equipment

- Operating the new recycle gas compressor at higher temperatures prevents condensation which was problematic during operation of the original recycle gas compressor.
- By using recycled syngas instead of nitrogen for gasifier aeration, plant operating cost were decreased for a total cost savings of $120,000. The recycle gas compressor has been instrumental in allowing continued process operations during times when vendor-supplied nitrogen is limited.
- As a result of logic modifications to prevent unneeded trips, the compressor availability increased to over 80 percent.
- To ensure safe operation of the PSB, several interlocks were configured and tested, and all performed as expected during interlock trials. The gasifier pressure changed less than 2 psig during each trip.
- Several improvements were made to the PSB fuel nozzle thermocouples: increasing their size, embedding them into the nozzle, and covering them with a thermal barrier coating. These improvements reduced the frequency and intensity of the temperature spikes that occurred in the early tests.
- The original gasification ash removal systems proved to be high-maintenance and not well-suited for scale-up.

- The continuous ash removal systems have operated reliably with high capacity, no moving parts, no pressurizing gas, low vent flows of clean gas, and solids transport using inherent gas.
- During steady state gasifier operation, the CCAD system can automatically control the gasifier standpipe level by varying the gasification ash discharge rate.
- Testing showed that the CFAD and CCAD systems can operated over a range of flow rates, pressures, temperatures, and particle sizes.

9.0 REFERENCES

Bush, P.V., T.R. Snyder, and R.L. Chang. Determination of Baghouse Performance from Coal and Ash Properties: Part I, *J. Air Pollution Control Association*, 39 (2), 228-237 (1989).

Dahlin, R.S. and E. C. Landham. Use of Laboratory Drag Measurements in Evaluating Hot-Gas Filtration of Char from the Transport Gasifier at the Power Systems Development Facility, Fifth International Symposium on Gas Cleaning at High Temperature, Morgantown, West Virginia (September 18-20, 2002).

Danielewski, M., S. Mrowec, and A. Stoklosa. Sulfidation of Iron at High Temperatures and Diffusion Kinetics in Ferrous Sulfide. *Oxidation of Metals*, Vol. 17, No. 1-2, 77-97. 1982.

McKamey, C. G., D. McCleary, P. F. Tortorelli, J. Sawyer, E. Lara-Curzio, and R. R. Judkins. Characterization of Field-Exposed Iron Aluminide Hot-Gas Filters. Fifth International Symposium on Gas Cleaning at High Temperature. Morgantown, West Virginia (September 18-20, 2002).

Pint, B. A., K. L. More, P. F. Tortorelli, W. D. Porter, and I. G. Wright. Optimizing the Imperfect Oxidation Performance of Iron Aluminides, *Materials Science Forum*, Vol. 369-372, 411-418 (2001).

Rogers, L.H., G.S. Boras, R.W. Breault, N. Salazar. Power Systems Development Facility Update on Six TRIG™ Studies. 23rd Annual International Pittsburgh Coal Conference. Pittsburgh, Pennsylvania (September 25-28, 2006).

APPENDIX A COAL CHARACTERISTICS

Tables A-1 through A-6 provide the characteristics of the coals tested at the PSDF for the test campaigns conducted from 2005 through 2009.

Table A-1. As-Fed PRB Subbituminous Coal Characteristics.

	Average	Minimum	Maximum	Standard Deviation
Moisture, wt %	15.9	1.1	13.0	18.0
Carbon, wt %	59.2	0.9	57.4	61.2
Hydrogen, wt %	3.7	0.2	3.2	4.0
Nitrogen, wt %	0.8	0.03	0.7	0.8
Oxygen, wt %	14.8	0.6	12.8	16.0
Sulfur, wt %	0.3	0.02	0.2	0.3
Ash, wt %	5.4	0.3	4.8	6.5
Volatiles, wt %	35.5	2.2	32.9	48.4
Fixed Carbon, wt %	43.2	2.2	30.0	46.8
Heating Value, As Received, Btu/lb	9,840	200	8,470	10,290
CaO, wt % in Ash	1.2	0.06	0.8	1.0
SiO_2, wt % in Ash	1.8	0.2	1.5	2.6
Al_2O_3, wt % in Ash	0.9	0.06	0.8	1.0
MgO, wt % in Ash	0.3	0.01	0.3	0.3
Na_2O, wt % in Ash	0.1	0.01	0.1	0.1

Table A-2. As-Fed Mississippi Lignite Coal Characteristics (TC22).

	Average	Minimum	Maximum	Standard Deviation
Moisture, wt %	28.1	25.0	30.6	1.8
Carbon, wt %	39.1	37.2	44.3	1.3
Hydrogen, wt %	5.2	4.0	6.3	0.6
Nitrogen, wt %	0.8	0.7	0.8	0.0
Oxygen, wt %	37.1	34.3	39.9	1.6
Sulfur, wt %	0.9	0.8	1.8	0.2
Ash, wt %	16.8	13.8	19.0	1.0
Volatiles, wt %	29.4	27.8	31.2	0.9
Fixed Carbon, wt %	25.6	24.0	28.6	0.9
Heating Value, As Received, Btu/lb	6,138	5,863	6,719	196
CaO, wt % in Ash	14.1	12.0	16.4	0.8
SiO_2, wt % in Ash	39.5	35.6	44.4	1.7
Al_2O_3, wt % in Ash	21.0	20.0	22.1	0.6
Fe_2O_3, wt % in Ash	7.3	6.5	9.2	0.7
MgO, wt % in Ash	3.0	2.5	3.5	0.3
Na_2O, wt % in Ash	0.3	0.0	0.7	0.3

Table A-3. As-Fed Mississippi Lignite Coal Characteristics (TC25).

	Average	Minimum	Maximum	Standard Deviation
Moisture, wt %	17.1	13.7	19.8	1.3
Carbon, wt %	46.0	40.5	50.0	1.6
Hydrogen, wt %	3.5	3.2	4.1	0.1
Nitrogen, wt %	1.0	0.9	1.0	0.04
Oxygen, wt %	17.1	13.7	21.4	1.0
Sulfur, wt %	0.6	0.4	0.8	0.1
Ash, wt %	14.8	12.0	22.0	1.7
Volatiles, wt %	37.1	33.9	40.6	1.5
Fixed Carbon, wt %	31.0	27.7	33.7	0.9
Heating Value, As Received, Btu/lb	8,000	7,230	8,380	190
CaO, wt % in Ash	15.6	11.4	19.0	2.3
SiO_2, wt % in Ash	44.2	40.2	52.3	3.6
Al_2O_3, wt % in Ash	20.2	18.0	22.8	1.1
MgO, wt % in Ash	3.2	2.6	3.8	0.3
Na_2O, wt % in Ash	0.4	0.3	0.7	0.1

Table A-4. As-Fed Utah Bituminous Coal Characteristics.

	Average	Minimum	Maximum	Standard Deviation
Moisture, wt %	2.1	1.9	2.5	0.2
Carbon, wt %	73.1	70.2	74.4	0.9
Hydrogen, wt %	5.0	4.9	5.1	0.0
Nitrogen, wt %	1.4	1.3	1.4	0.0
Oxygen, wt %	7.6	7.3	7.9	0.2
Sulfur, wt %	0.5	0.5	0.6	0.0
Ash, wt %	10.2	9.1	13.3	1.0
Volatiles, wt %	37.1	35.7	38.6	1.1
Fixed Carbon, wt %	50.5	48.3	52.1	1.2
Heating Value, As Received, Btu/lb	12,911	12,482	13,153	151
CaO, wt % in Ash	5.9	5.2	6.1	0.3
SiO_2, wt % in Ash	58.2	57.7	60.0	0.9
Al_2O_3, wt % in Ash	18.2	17.7	18.5	0.3
MgO, wt % in Ash	1.5	1.4	1.6	0.1
Na_2O, wt % in Ash	1.2	1.0	1.4	0.1

Table A-5. As-Fed North Dakota Freedom Mine Low Sodium Lignite Coal Characteristics.

	Average	Minimum	Maximum	Standard Deviation
Moisture, wt%	21.9	18.6	24.4	1.3
Carbon, wt%	48.8	47.3	51.6	1.1
Nitrogen, wt%	0.7	0.6	0.8	0.04
Oxygen, wt%	15.1	13.6	16.9	0.7
Sulfur, wt%	0.8	0.6	1.4	0.2
Ash, wt%	9.8	8.4	11.6	0.8
Volatiles, wt%	31.3	19.1	41.1	4.4
Fixed Carbon, wt%	37.0	26.9	49.5	4.5
As-Received Heating Value, Btu/lb	8,080	6,670	8,510	350
CaO, wt % in ash	19.8	17.4	22.9	1.3
SiO_2, wt % in ash	30.5	25.6	34.7	2.1
Al_2O_3, wt % in ash	11.9	10.9	13.2	0.6
MgO, wt % in ash	6.6	6.1	7.3	0.3
Na_2O, wt % in ash	1.3	1.0	1.8	0.2

Table A-6. As-Fed North Dakota Freedom Mine High Sodium Lignite Coal Characteristics.

	Average	Minimum	Maximum	Standard Deviation
Moisture, wt%	20.1	16.4	24.3	2.1
Carbon, wt%	51.7	49.0	54.5	15
Hydrogen, wt%	3.17	2.92	3.48	0.16
Nitrogen, wt%	0.94	0.88	1.01	0.03
Oxygen, wt%	15.3	14.1	16.5	0.5
Sulfur, wt%	0.73	0.66	0.95	0.06
Ash, wt%	8.0	7.2	8.9	0.4
Volatiles, wt%	32.8	31.3	34.2	0.9
Fixed Carbon, wt%	39.1	37.7	41.2	1.2
As-Received Heating Value, Btu/lb	8,147	7,635	8,628	254
CaO, wt % in ash	25.3	22.7	29.2	2.0
SiO_2, wt % in ash	19.1	16.7	21.1	1.0
Al_2O_3, wt % in ash	11.6	10.7	12.3	0.3
MgO, wt % in ash	4.6	2.5	6.0	1.5
Na_2O, wt % in ash	8.2	4.5	11.2	2.5

APPENDIX B LIST OF ACRONYMS AND ENGINEERING UNITS

Acronyms

APFBC—Advanced Pressurized Fluidized Bed Combustor
B&W—Babcock & Wilcox
Ca—Calcium
CCAD—Continuous Coarse Ash Depressurization
CFAD—Continuous Fine Ash Depressurization
CH_4—Methane
CMS—Carbon Molecular Sieve
CO—Carbon Monoxide
CO_2—Carbon Dioxide
COS—Carbonyl Sulfide
CS_2—Carbon Disulfide
CT—Combustion Turbine
DCS—Distributed Control System
DOE—Department of Energy
EDX—Energy Dispersive X-Ray Spectrometry
EPRI—Electric Power Research Institute
Fe_2O_3—Iron Oxide
FEAL—Iron Aluminide
FeS—Iron Sulfide
FTIR—Fourier Transform Infrared
GC—Gas Chromatograph
GCT—Gasification Commissioning Test
H_2—Hydrogen
H_2O—Water
H_2S—Hydrogen Sulfide
IGCC—Integrated Gasification Combined Cycle
LHV—Lower Heating Value
LMZ—Lower Mixing Zone
LOI—Loss on Ignition
MCA—Multi-Cell Array
MMD—Mass Median Diameter
MOC—Management of Change
MPT—Media and Process Technology
N_2—Nitrogen
NCC—Non-Carbonate Carbon
NETL—National Energy Technology Lab
O_2—Oxygen
OD—Outer Diameter
ORNL—Oak Ridge National Laboratory
PCD—Particulate Control Device
PDAC—Pressure Decoupled Advanced Coal
PDI—Pressure Differential Indicator
PLC—Programmable Logic Control
PI—Plant Information
PID—Proportional Integral Derivative
PPC—Process Particle Counter
PRB—Powder River Basin
PSB—Piloted Syngas Burner
PSD—Particle Size Distribution
PSDF—Power Systems Development Facility
S—Sulfur
SEM—Scanning Electron Microscope
SIS—Safety Interlock System
SMD—Sauter Mean Diameter
SO_2—Sulfur Dioxide
SOFC—Solid Oxide Fuel Cell
SRD—Sensor Research and Development
TC—Test Campaign
TRIG—Transport Integrated Gasification
UMZ—Upper Mixing Zone
WGS—Water-Gas Shift

Engineering Units

acm—actual cubic meters
Btu—British thermal units
cm—centimeters
dP or ΔP—pressure drop
^{o}F—degrees Fahrenheit
ft—feet
ft/s—feet per second
ft^3—cubic feet
g/cm^3 or g/cc—grams per cubic centimeter
hr— hours
inH_2O—inches of water
in—inches
inwc—inches of water column
kW—kilowatts
kWh—kilowatt-hours
lb—pounds
lb/ft^3—pounds per cubic feet
lb/hr—pounds per hour
mA/cm^2—milliamps per cubic centimeters
m^2/g—square meters per gram
mg/acm—milligrams per actual cubic meters
min—minutes
mm—millimeters
MMBtu—million British thermal units
mol—moles
μm—microns or micrometers
MW—megawatts
ppm—parts per million
ppmv—parts per million by volume
ppmw—parts per million by weight
psi—pounds per square inch
psid—pounds per square inch differential
psig—pounds per square inch gauge
s or sec—seconds
SCF—standard cubic feet
wt—weight